

POLITECNICO DI TORINO

Corso di Laurea Magistrale

in Ingegneria Civile

Tesi di Laurea Magistrale

Calculation of deflection in RC beams



Relatore

prof. Maurizio Taliano

Candidato

Zhao Haoye
赵浩业

A.A 2019/2020

ABSTRACT

In the field of structural engineering, while calculating the deflection and curvature of reinforced concrete beams, normally only bending moment is taken into consideration, but the fact is that with the load increasing, shear effect becomes a non-neglectable factor, especially for r.c beams with thin webs. Hence, it becomes very important to find an appropriate theoretical model for analyzing the behavior of r.c beams with thin webs.

This paper focuses on analyzing the behavior of reinforced concrete beam with double T section for short term loading. Several classic theoretical models are carried out to calculate the mean curvature and deflection, then comparing to the experimental results, verifying the accuracy of all models proposed.

In particular, the theoretical model called “simplified model” is proposed by M. Taliano, P.G. Debernardi et al., in which introduced the influence of shear effect. It simplifies the “general model” that they proposed before. In the end, the experimental data are compared to the theoretical results obtained with the simplified model, examining the influence of shear, besides the accuracy.

CONTENTS

| | |
|--|----------|
| ABSTRACT | I |
| INTRODUCTION..... | V |
| 1. EXPERIMENTATION | 1 |
| 1.1 Geometry of model | 1 |
| 1.2 Reinforcement..... | 2 |
| 1.3 Testing scheme | 3 |
| 2. CLASSIC THEORETICAL MODELS | 4 |
| 2.1 Material..... | 6 |
| 2.2 Tension-stiffening effect..... | 7 |
| 2.3 Self – weight..... | 9 |
| 2.4 Linear analysis method | 10 |
| 2.5 Non-linear analysis method | 16 |
| 2.51 Calculation of mean curvature | 17 |
| 2.52 Calculating the deflection..... | 23 |
| 2.6 Bi-linear method | 32 |
| 2.61 Calculation of mean curvature | 33 |
| 2.62 Calculation of deflection | 38 |
| 2.7 Method with coefficient η | 42 |
| 2.71 Calculation of mean curvature | 43 |
| 2.72 Calculation of deflection | 47 |
| 2.8 CEB – FIP Model Code 90..... | 50 |
| 2.81 Calculation of mean curvature | 52 |
| 2.82 Calculation of deflection | 56 |
| 2.9 Conclusion | 59 |

| | |
|---|-----------|
| 3. THEORETICAL MODEL WITH SHEAR EFFECT IN THE DEFORMATION .. | 60 |
| 3.1 Mean curvature and shear strain | 63 |
| 3.2 Calculation of the deflection..... | 73 |
| 4. CONCLUSIONS | 79 |
| NOTATION | 81 |
| LIST OF TABLES | 83 |
| REFERENCES..... | 87 |

INTRODUCTION

As we all know, the analysis of the behavior of reinforced concrete beams is always a problem because too many parameters are involved. And also, the complexity of the states of strain, stress, and deformation has increased the difficulty to find a reliable model to get a precise result.

The classical beam bending theory, which also called “Euler–Bernoulli beam theory”, offers a fundamental idea that in the elastic field the curvature is proportional to the bending moment. There are two phases in the analysis of r.c beam. Hence, based on the classical beam theory, the curvature increases linearly in state 1 and 2, only the varying of inertia moment changes the slope of the line in the diagram of bending moment and curvature. The transition from phase 1 to phase 2 is flat when the bending moment reaches cracking bending moment.

However, the real behavior of r.c beam after cracking is far from the results of the above method, which leads to the concept of “tension – stiffening”. It describes the effect of stiffening action of the uncracked concrete between two contiguous cracks. And different theoretical models can be found in literature, which differs from the law with which the tension – stiffening varies depending on the bending moment. Some standards suggest that the effect is constant, which is independent of the bending moment, while according to others, it varies linearly or hyperbolically with the bending moment varies.

Another important representative during the analysis of r.c beam behavior is the deflection, which is calculated based on the principle of virtual works. Usually, only the bending moment factor is considered. It works well in certain cases, but the shear effect is not neglectable in some cases. To solve this problem, Ritter and Morsch first proposed the solution known as lattice – like model, which assumes that the inclination of compressed struts in the web is parallel to the direction of cracks, and it is at a 45 degrees angle to the stirrup. But in the subsequent practical applications, people found that the model has often underestimated the real resistance of structural elements. Afterward, another important model called “smeared model” is proposed with modified compression field theory (MCFT) by Vecchio and Collins, which takes the variability of the angle in the web into consideration. The smeared model dealt with the cracked concrete as a new material with different mechanical properties comparing to the uncracked concrete. Then M. Taliano and P.G. Debernardi brought forward the “mixed model” based on MCFT. It can be treated as modified smeared model, which considered not only the

web but also the tensed and compressed chords. After that, in order to simplify the calculation procedure, they proposed the “simplified model”, which simplifies the iterative calculation procedure.

The thesis is divided into two parts. The first part aims to discuss the calculation of mean curvature of simply supported reinforced concrete beams with several approaches, and the calculation of deflection with the principle of virtual works, comparing the results to experimental data and verifying the accuracy of theoretical models proposed. The second part introduces the “simplified model” in detail, which explains the influence of shear effect. This part shows the effect of shear deformation to the total deflection, besides the relationship between shear and shear strain. In the end, the comparison with experimental data is carried out to examine the accuracy of the model.

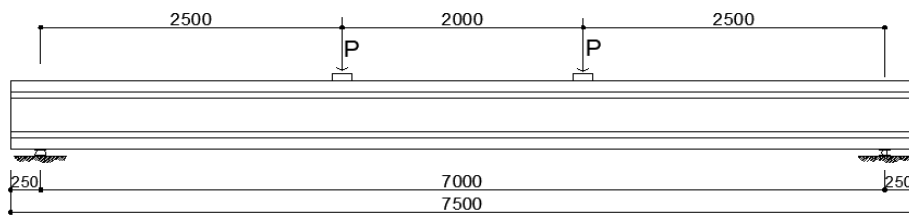
1. EXPERIMENTATION

1.1 Geometry of model

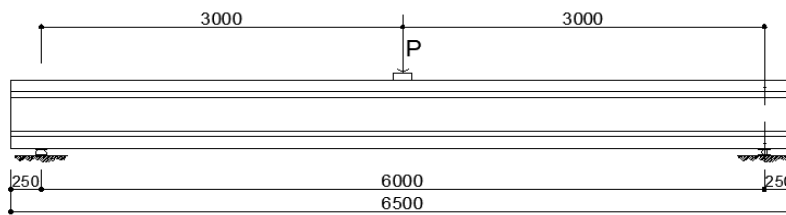
In this experimentation, there are six beams that are reinforced with ordinary reinforcement and named from Tr1 to Tr6. All beams have the same transversal section (double T section with thin web).

The general dimensions and load conditions are illustrated in the following figure. These beams are divided into 3 groups according to their length and load condition. Beam 1 and 2 have a length of 7000mm and subjected to symmetric load. And beam 3,4 are 6000mm long with a concentrated load at the midpoint, while the third group, subjected an asymmetrical concentrated load, is 7500mm including a cantilever with a length of 1050mm.

TR1, TR2 beams



TR3 beam



TR5, TR6 beams

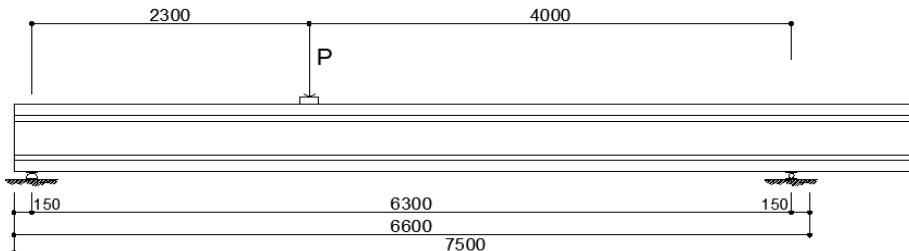


Figure 1. General dimension and static scheme in the experimentation.

1.2 Reinforcement

For total of 6 beams, the top longitudinal reinforcement is the same, which means three steel bars of 12mm diameter. And the bottom longitudinal reinforcement is made up of five bars of 16mm diameter for three beams (tr1, tr3, tr5) and nine bars with the same diameter for the other three beams (tr2, tr4, tr6). In addition, the transversal reinforcement is made up of stirrups with a diameter of 8mm, and spacing 200mm.

The following figure shows the detail of reinforcement of two types of cross section.

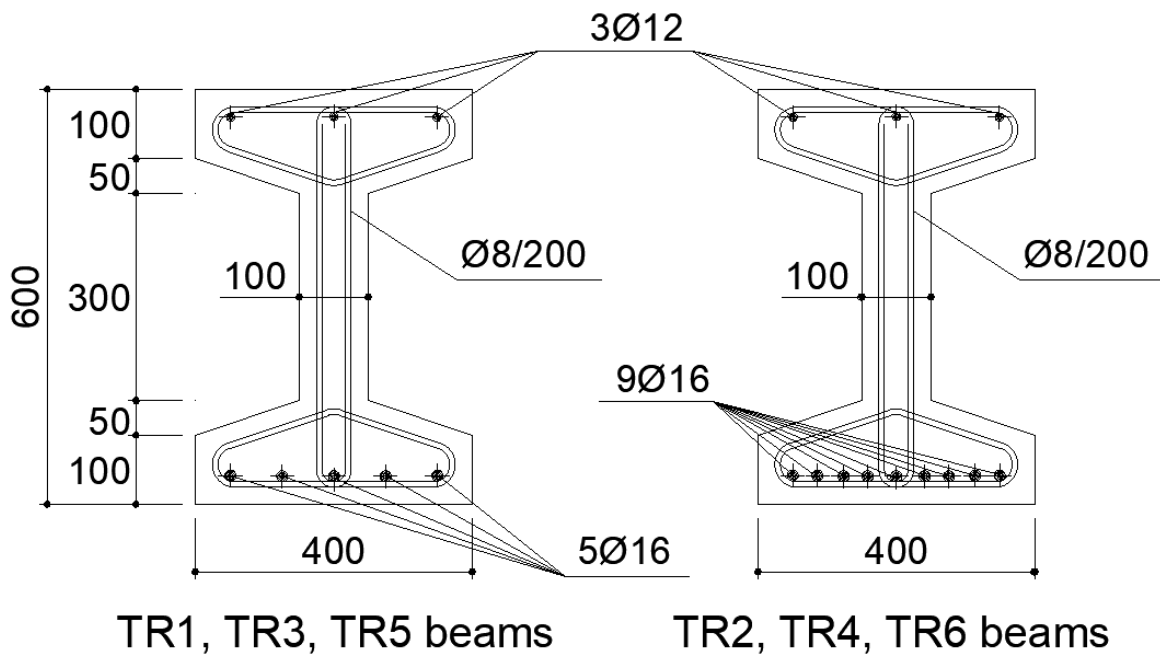


Figure 2. Detail of the cross section and reinforcement.

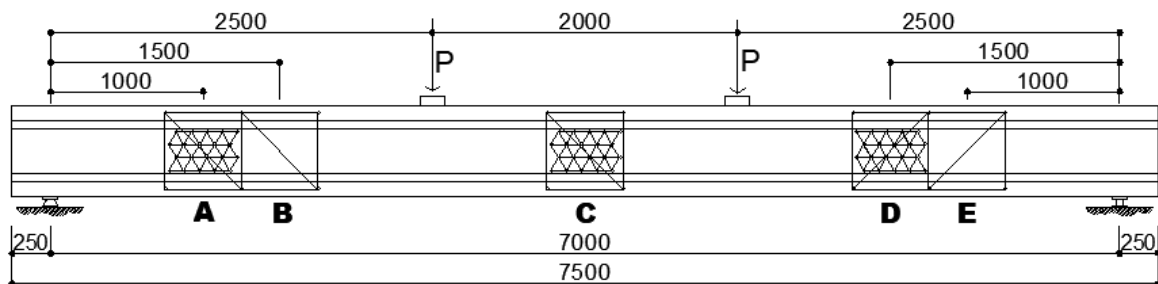
1.3 Testing scheme

The tests are executed at the laboratory of the Department of Structural, Geotechnical and Building Engineering of Politecnico di Torino.

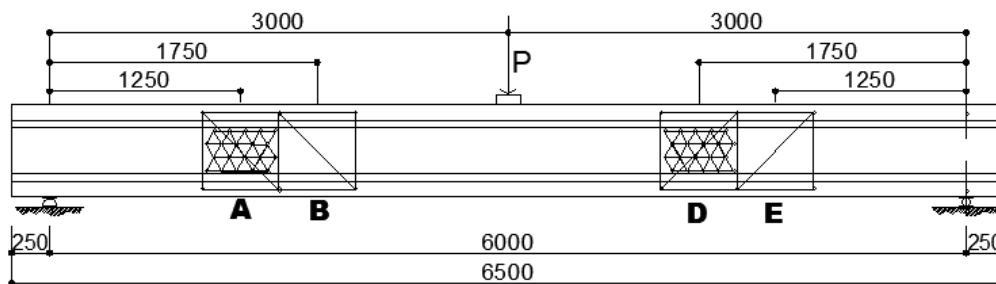
The aim is evaluating global and local strain effects by measuring instruments in different zones as shown in the following figure, square lattices are put at measuring zone in non-deformed state at the beginning, and vary their length while applying the load.

The detail of the test can be found in the paper of Guiglia (2006).

TR1, TR2 beams



TR3 beam



TR5, TR6 beams

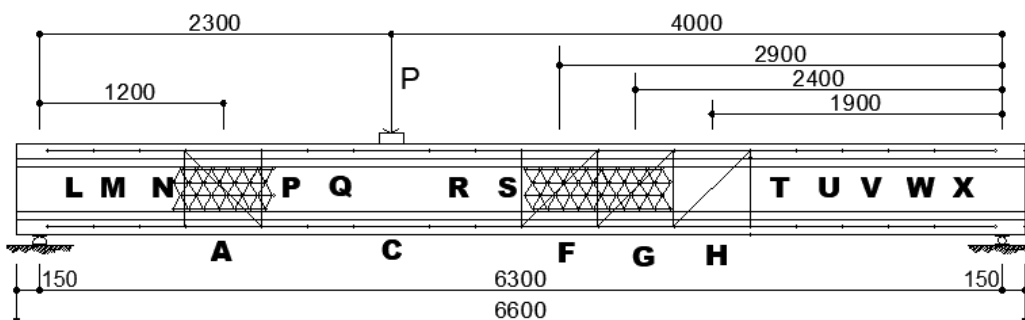


figure 3. Static scheme and struments used in the test

2. CLASSIC THEORETICAL MODELS

The mean curvature and deflection are representative deformation parameters for analyzing the behavior of reinforced concrete beams, a good calculation model is set up to evaluate the behavior of a beam, firstly, it should have an efficient result comparing to experimental data, then the calculation procedure should be as concise as possible.

This chapter is dedicated to classic calculation models. For each model, calculating the mean curvature and deflection of referencing nodes and plotting the diagram of bending moment – curvature and load – deflection. Furthermore, in the uncracked state the calculation is based on the elastic theory all the time, hence it does not enter the analysis. And also, the state after yielding of steel bars is not considered as well.

Firstly, it is introduced the analysis with linear elastic method, which is the most fundamental one. Through some assumptions, only some simple calculations are needed to find the relationship between bending moment and curvature.

Then the non – linear elastic method can be seen as optimization of the linear method, it removes the assumption of material linearity, and replacing it by parabola of Sargin. The method executes with displacement control, and its calculation subjected iterative procedure that increases the complexity.

The previous analysis takes the tension – stiffening effect as a constant, while the following models are set up based on the linear elastic method, but taking the varying of tension – stiffening effect into consideration.

According to Eurocode 2, the bi – linear method, through introducing the distribution coefficient ζ , interprets the intermediate behavior between the uncracked state and fully cracked state. The coefficient works not only in the calculation of mean curvature, but also plays a role when calculating the deflection.

Furthermore, the method of coefficient η improves the calculation of mean strain that is proposed by Model code 2010 and Eurocode 2. The coefficient η , based on the paper of M. Taliano, explains the influence of the internal secondary crack on the tension – stiffening effect which varies linearly in the cracked state as a result.

In the end, the theoretical model of Model Code1990 is performed, which shows another way to calculate the mean curvature in state 2 by introducing some parameters and the new consideration of calculation of tension – stiffening.

By calculating the mean curvature and deflection with different methods and standards, and the comparison with the experimental data obtained from laboratory tests, allowed to evaluate the precision and the reliability of the proposed models.

2.1 Material

The beam is made up of concrete and steel bars. It is assumed the mechanical properties as below.

For concrete, the characteristic compressive cube strength $f_{ck,cube}$ is 25 N/mm². Hence the characteristic compressive cylinder strength is 20.75 N/mm², calculated as

$$f_{ck,cylinder} = 0.83 * f_{ck,cube} \quad (2.1)$$

The mean compressive strength f_{cm} is 28.75 N/mm²

$$f_{cm} = f_{ck,cylinder} + 8 \text{ Mpa} \quad (2.2)$$

The mean tensile strength f_{ctm} is 2.265 N/mm²

$$f_{ctm} = 0.3 * f_{ck,cylinder}^{2/3} \quad (2.3)$$

The mean elastic modulus E_{cm} = 31282.54 N/mm²

$$E_{cm} = 22000 * \left(\frac{f_{cm}}{10}\right)^{1/3} \quad (2.4)$$

The coefficient of Poisson ν is considered as 0.15. Therefore, the shear modulus G is 13601.1 N/mm².

$$G = \frac{E_{cm}}{2 * (1 + \nu)} \quad (2.5)$$

For the reinforcement, both the longitudinal steel bars and transversal stirrups are considered as high bond bars, their elastic modulus E_s is 200 GPa.

2.2 Tension-stiffening effect

The effect indicates that the contribution of bonding force transmitted from concrete to steel bars increases the stiffness of tensile reinforcement, which means that the effect reduces the tensile deformation of steel by a certain amount. It takes the mean deformation of tension bars between two contiguous cracks into consideration.

For different standard, several models are proposed here to describe the effect.

1. Constant tension – stiffening

The model shows that the gap between mean curvature and curvature in state 2 is constant in the diagram of bending moment – curvature as shown in the following figure:

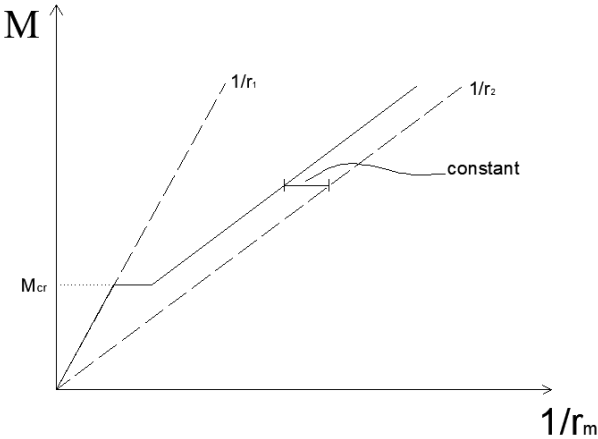


Figure 4. Relationship of bending moment and curvature with constant t.s

2. Linear tension – stiffening

When the bending moment surpasses the cracking moment, the tension – stiffening effect varies linearly in the relationship as shown below.

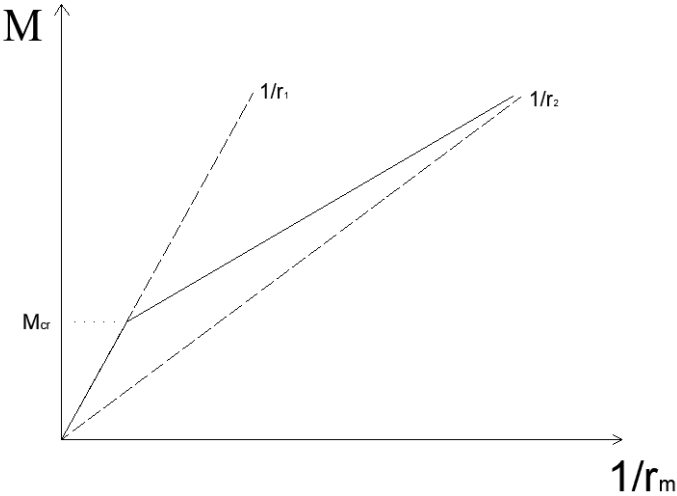


Figure 5. Relationship of bending moment and curvature with linear t.s

3. CEB model

The model has more parameters, which make the variation of tension – stiffening effect hyperbolic.

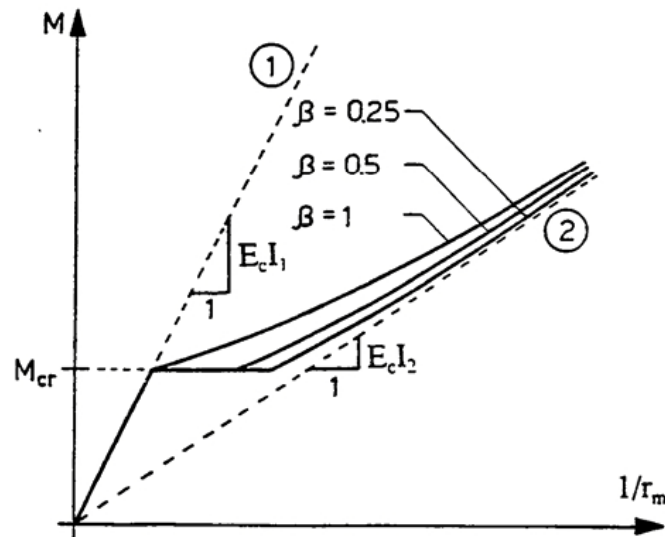


Figure 6. Relationship of bending moment and curvature in model CEB

There is also another model (ACI) utilizes the parabolic variation of tension – stiffening effect. The four models are proposed by Cosenza e Greco.

2.3 Self – weight

In the calculation, the self – weight should be taken into account which means that the deflection is not null without loading. However, experimental data shows that the initial deflection is zero, because strain gauges are installed after the deformation due to self – weight. The solution proposed here is that consider self – weight in the calculation process, but in the end, it removes the effect of self – weight.

For curvature

$$\frac{1}{r} = \left(\frac{1}{r}\right)_{tot} - \left(\frac{1}{r}\right)_{p.p} \quad (2.6)$$

Where:

$\frac{1}{r}$ is curvature due to load

$\left(\frac{1}{r}\right)_{tot}$ is curvature due to combination of load and self – weight

$\left(\frac{1}{r}\right)_{p.p}$ is curvature due to self – weight

For deflection

$$f = f_{tot} - f_{p.p} \quad (2.7)$$

Where:

f is deflection due to load

f_{tot} is deflection due to combination of load and self – weight

$f_{p.p}$ is deflection due to self – weight

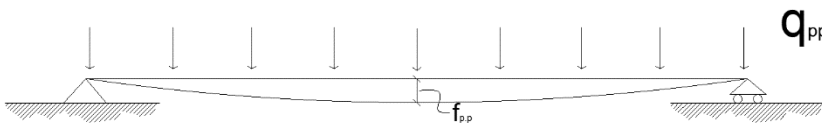


Figure 7. Dflection due to self – weight

2.4 Linear analysis method

The linear method is a basic method for analyzing the curvature of beams with the theory of elasticity, which follows assumptions below:

The cross section remains plane and will be perpendicular to the neutral axis after deformation.

Perfect bond between steel bars and concrete.

The properties of the material are linear elastic, homogeneous and isotropic.

Based on the elastic theory, calculating the curvature and plotting the relationship between the bending moment and curvature.

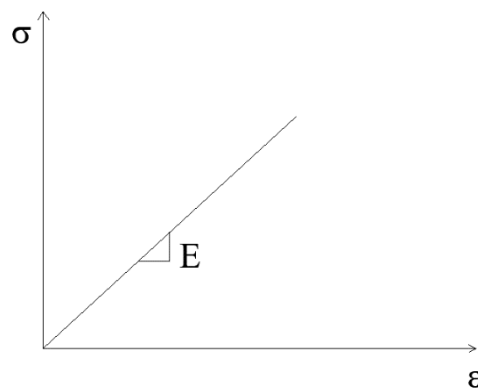


figure 8. Linear relationship of stress - strain.

In state 1, the cross section is uncracked and subjects to a bending moment which is lower than the cracking bending moment, that also means the maximum tensile stress of concrete does not exceed the mean tensile strength f_{ctm} at tension chord.

Calculating the cracking bending moment

$$M_{cr} = f_{ctm} \frac{I_{om,1}}{y} \quad (2.8)$$

Calculating the curvature corresponding to the cracking bending moment in state 1

$$\frac{1}{r_{1r}} = \frac{M_{cr}}{E_{cm} I_{om,1}} \quad (2.9)$$

State 2 corresponds to the state when partial transversal section cracked. First of all, calculating the distance between the upper surface and neutral axis x_c with the equation $S_{om,2} = 0$, it is necessary to do three attempts here to obtain the right position of neutral axis. They are $x_c > 150\text{mm}$, $100\text{mm} < x_c < 150\text{mm}$ and $x_c < 100\text{mm}$ respectively.

The curvature corresponding to the cracking bending moment in state 2 is

$$\frac{1}{r_{2r}} = \frac{M_{cr}}{E_{cm}I_{om,2}} \quad (2.10)$$

Curvature of bending moment at yielding point of bars in tension chord

$$\frac{1}{r_y} = \frac{M_{yd}}{E_{cm}I_{om,2}} \quad (2.11)$$

Taking the tension – stiffening effect into account, whose contribution is constant based on Eurocode 2

$$\varepsilon_{sm} = \varepsilon_{s2} - k_t \frac{f_{ctm}}{\rho_{p,eff} E_s} \quad (2.12)$$

k_t is the coefficient of loading duration

$k_t=0.6$ for short term loading

$k_t=0.4$ for long term loading

$\rho_{p,eff}$ is the density of longitudinal reinforcement in the effective area

Therefore, the mean curvature is

$$\left(\frac{1}{r}\right)_m = \frac{\varepsilon_{sm} - \varepsilon_c}{d} \quad (2.13)$$

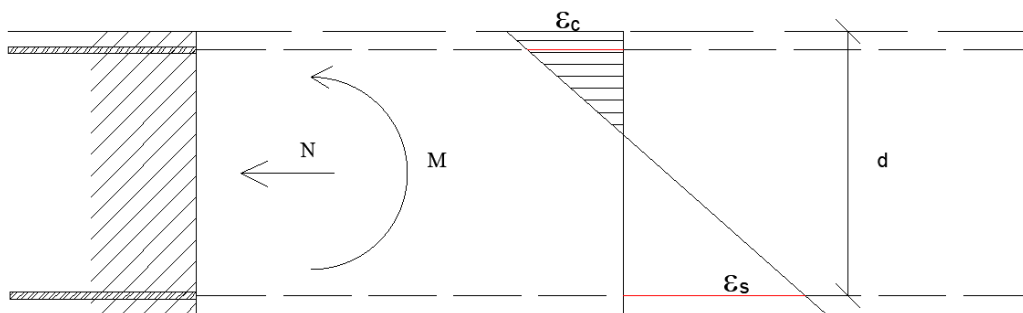


figure 9. Strain and stress in the cross section for linear analysis

Figure 10 and 11 show the generic section of the diagram of bending moment – curvature with and without the effect of tension-stiffening for the two groups of beams. It is can be seen the constant tension – stiffening and the flat transition from state 1 to state 2.

Notice that the cracking bending moment here, in fact, is produced by the sum of load and self – weight.

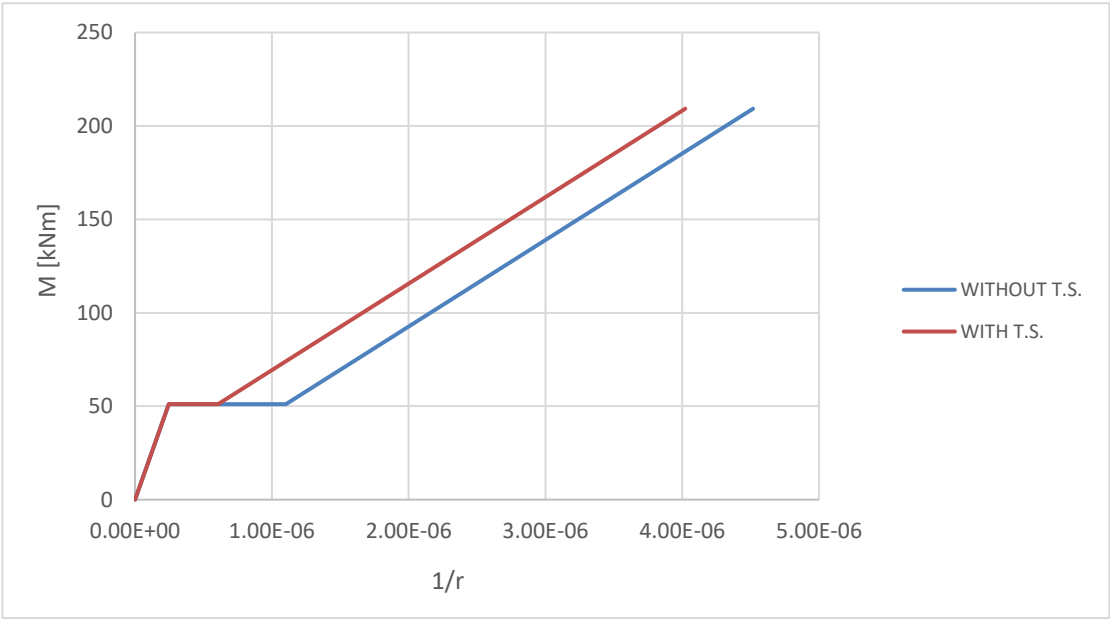


Figure 10 Diagram bending moment - curvature of Beam Tr1, Tr3, Tr5.

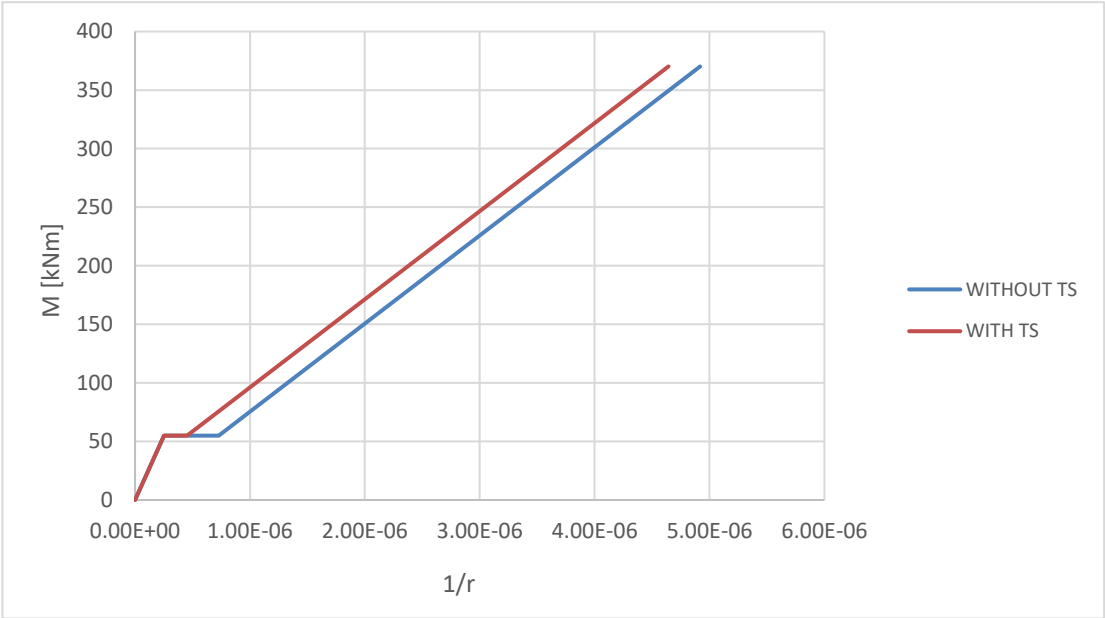


Figure 11 Diagram bending moment - curvature of Beam Tr2, Tr4, Tr6

Comparing the calculated results with the experimental data, the theoretical value under the cracked state is always small in the symmetrical load condition, and the error becomes larger as the load increases. However, comparing figure 12 and 13, it can be seen that the error is smaller with the beam of more steel bars.

The figure 14 shows the comparison of the theoretical model and experimental data of beam 3 in node A, the result is similar with beam 1 and 2, the theoretical model tends to underestimate the real behavior of the beam after cracking.

While in the condition of asymmetric concentrated load, as shown in figure 15 and 16, the theoretical curves are consistent roughly with the experiment.

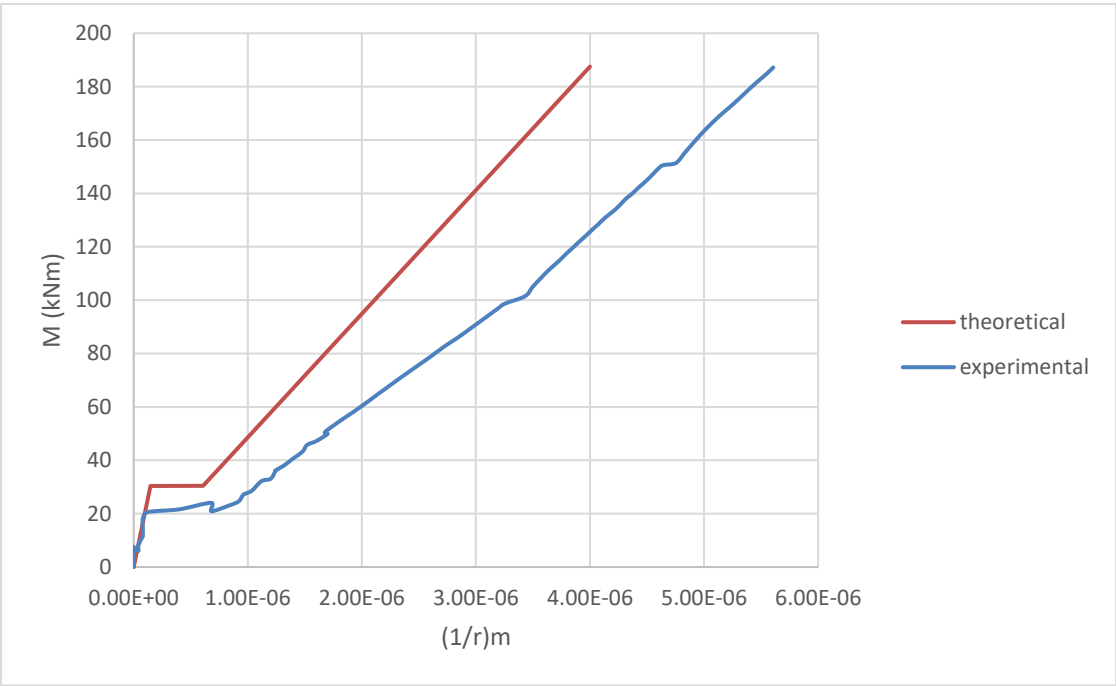


Figure 12. Diagram of bending moment – mean curvature of beam 1, node C

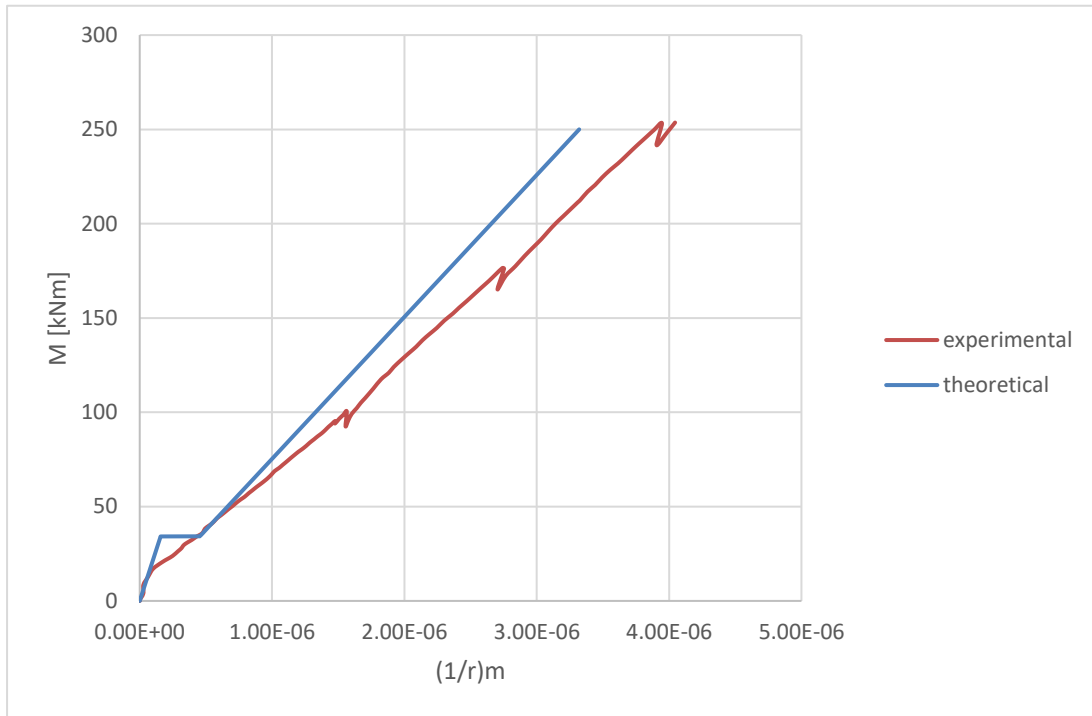


Figure 13. Diagram of bending moment - mean curvature of beam 2, node C

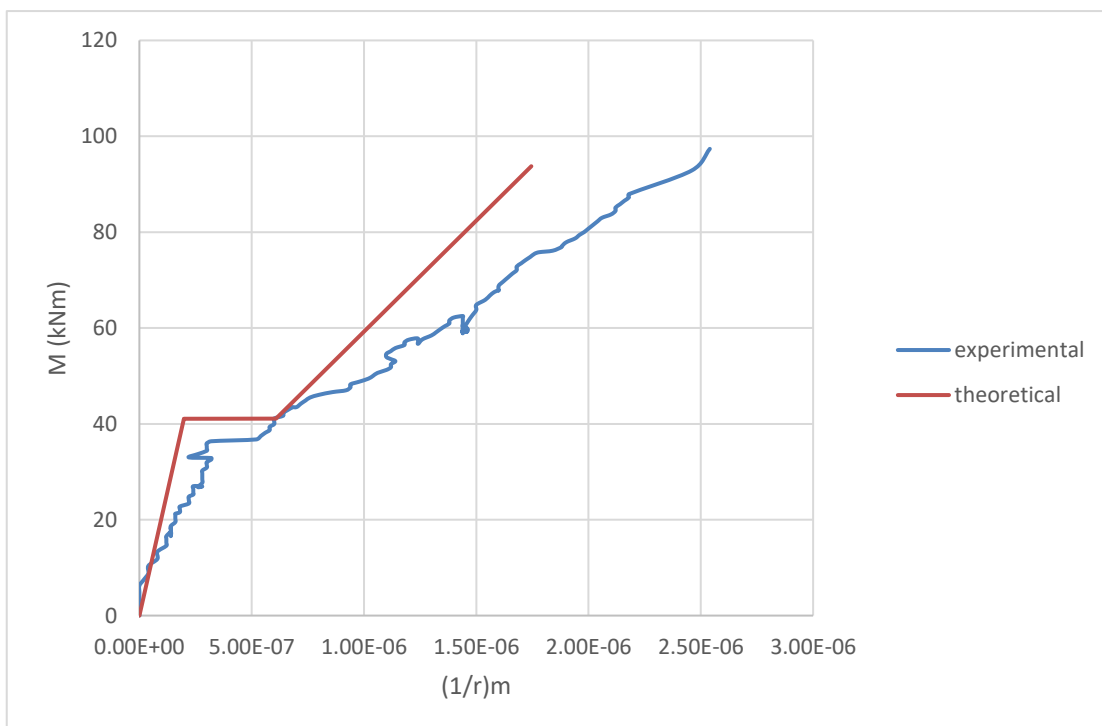


Figure 14. Diagram of bending moment - mean curvature beam 3, node A

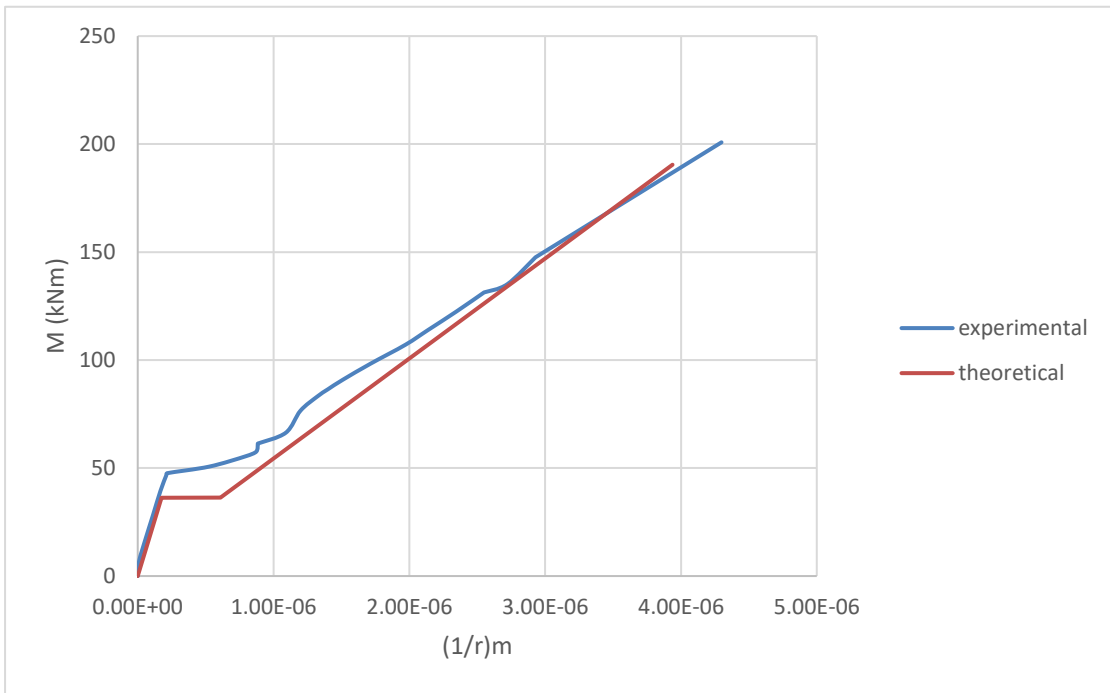


Figure 15. Diagram of bending moment - mean curvature of beam 5, node C

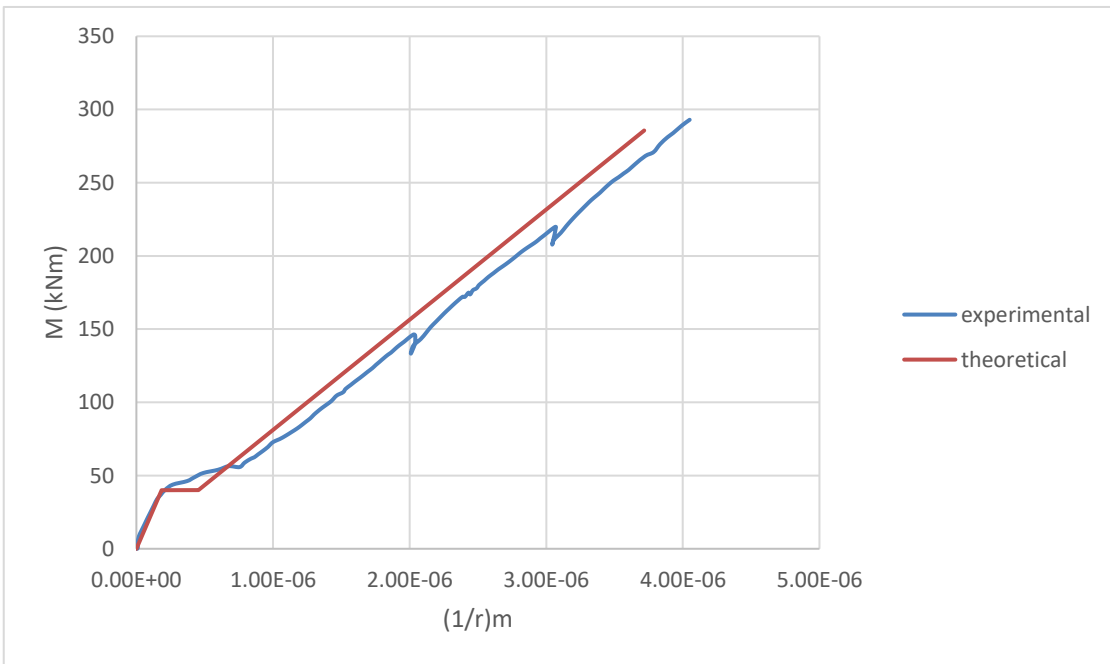


Figure 16. Diagram of bending moment - mean curvature of beam 6, node C

2.5 Non-linear analysis method

Considering the non-linear behavior of the material, equilibrium and compatibility still should be satisfied, the non-linear analysis method removes the assumption of linear relation of stress-strain and takes parabola of Sargin into account. In this condition, the elastic modulus is no longer a constant, but decreases as the stress increases. The stress-strain relation is shown below:

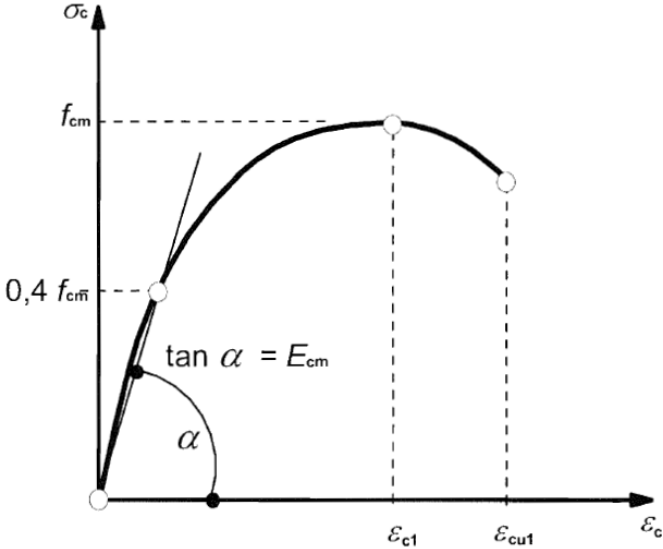


figure 17. Schematic representation of the stress-strain relation for structural analysis. From Eurocode 2

As shown in the following figure, it is can be seen the acting force and bending moment on the cross section and the distribution of compressed and tensed strain. The compressed strain is parabolic.

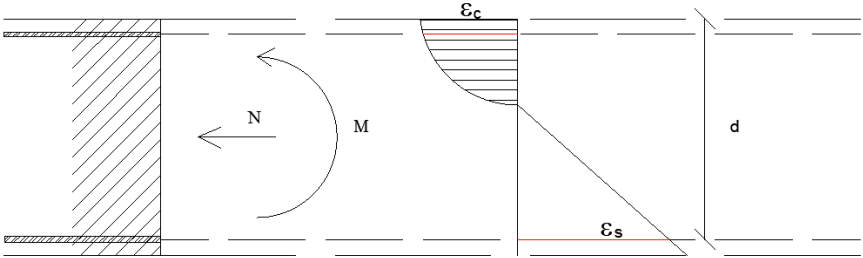


figure 18. Strain and stress in the cross section for non-linear analysis

2.51 Calculation of mean curvature

Dividing the cross section into 601 strips, each strip has thickness 1mm, thickness of the top and bottom slice is 0.5mm, the total height is 600mm. And the reference point for every strip on y axis is in middle, except that the starting and ending point are in the edge, therefore, the spacing is always 1mm for reference point on coordinate. For calculating of curvature, with a discrete way, calculating the compression strain and bending moment for each element, and making sure that every strip satisfies the equilibrium and congruence condition.

As shows in the following figure the half cross section as it is symmetric geometrically:

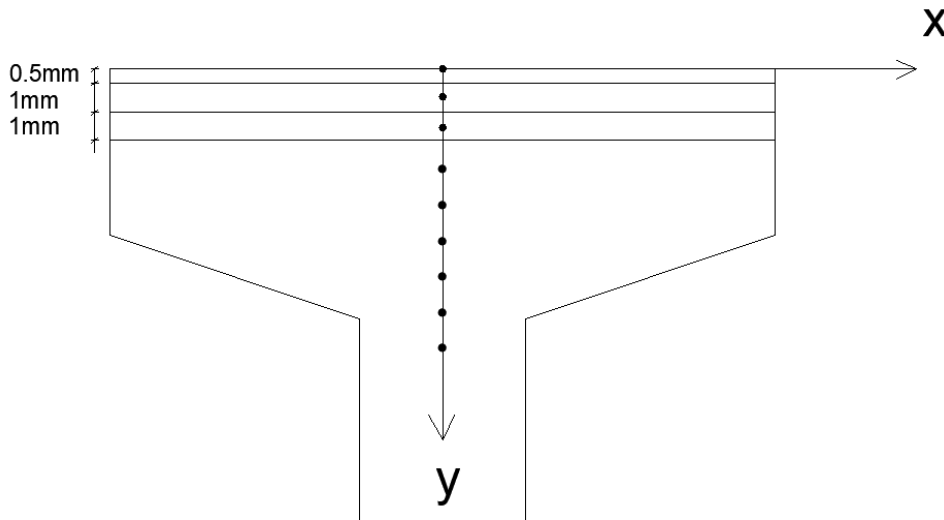


figure 19. Strips and referencing point in the cross section

1. Assuming the value of μ_x ($1/r$) and λ . Notice that the value of μ_x should be positive while λ is always negative. Calculating the compressed strain of concrete:

$$\varepsilon_c = \lambda + \mu_x y \quad (2.14)$$

λ is the compressed strain of concrete at the top chord in the section

2. Calculating the coefficient η with the relation below proposed by Eurocode2:

$$\eta = \frac{\varepsilon_c}{\varepsilon_{c1}} \quad (2.15)$$

where

$$\varepsilon_{c1} (\text{‰}) = 0.7 * f_{cm}^{0.31} \quad (2.16)$$

3. Then obtain the compression of concrete σ_c by the following formula

$$\frac{\sigma_c}{f_{cm}} = \frac{k\eta - \eta^2}{1 + (k - 2)\eta} \quad (2.17a)$$

Where

$$k = 1.05 * E_{cm} * \frac{|\varepsilon_{c1}|}{f_{cm}} \quad (2.17b)$$

Here, it is necessary to set its value by condition

if $\varepsilon_c < 0$, using the expression (2.17a).

else, considering the relationship ($\sigma_c - \varepsilon_c$) is linear, as it is in tension state.

$$\sigma_c = \varepsilon_c * E_{cm} \quad (2.18)$$

And if $\sigma_c < f_{ctm}$, $\sigma_c = \sigma_c$

else $\sigma_c = 0$.

4. Calculating the compression force F_c of concrete, the tension force F_s of bottom bars.

$$F_{ci} = \sigma_c * A_{ci} \quad (2.19a)$$

$$F_s = \sigma_s * A_s \quad (2.19b)$$

Where

$$\sigma_s = E_s * \varepsilon_s \quad (2.20)$$

$$\varepsilon_s = \lambda + \mu_x \gamma_s \quad (2.21)$$

And the same way to calculate the force F_s' of upper bars.

5. With changing the λ value, verifying the equilibrium condition.

$$\sum F_c + \sum F_s = 0 \quad (2.22)$$

6. Calculation of the sum of bending moment for every strip and bars

$$M_{tot} = \sum M_c + \sum M_s \quad (2.23)$$

7. At the end, plotting the relationship moment – curvature with and without taking the tension – stiffening effect into consideration.

The relationship of bending moment and curvature with constant tension – stiffening effect is shown below. In addition, the change due to varying elastic modulus is not distinct. Therefore, the non – linear analysis method is not necessary, at least in some cases, because the accuracy of the theoretical result does not improve much while the calculation is a lot more complicated.

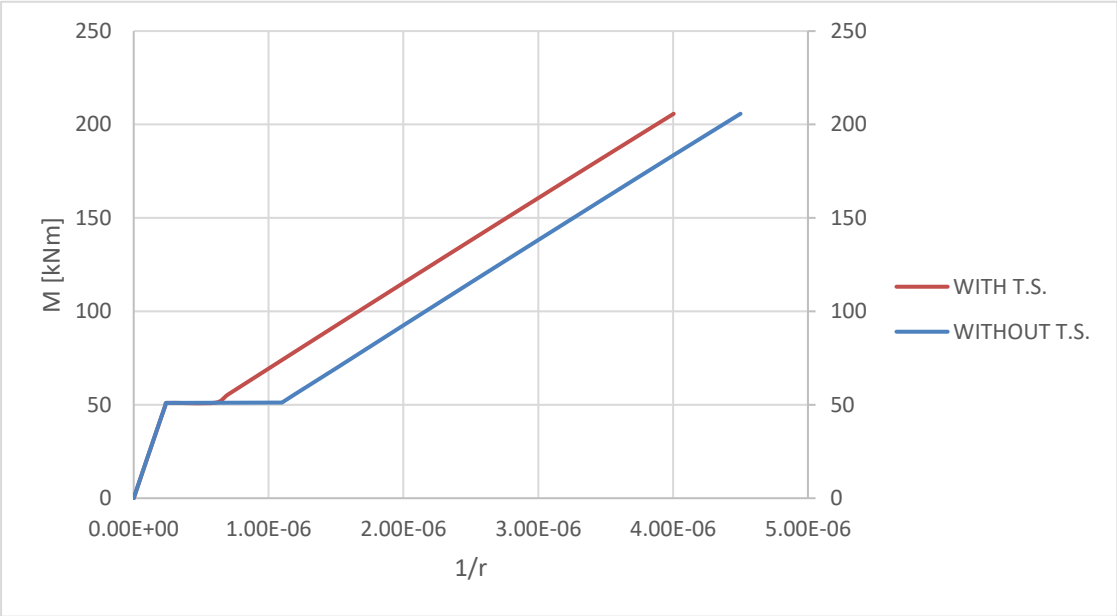


Figure 20. Diagram bending moment – curvature of Beam Tr1, Tr3, Tr5.

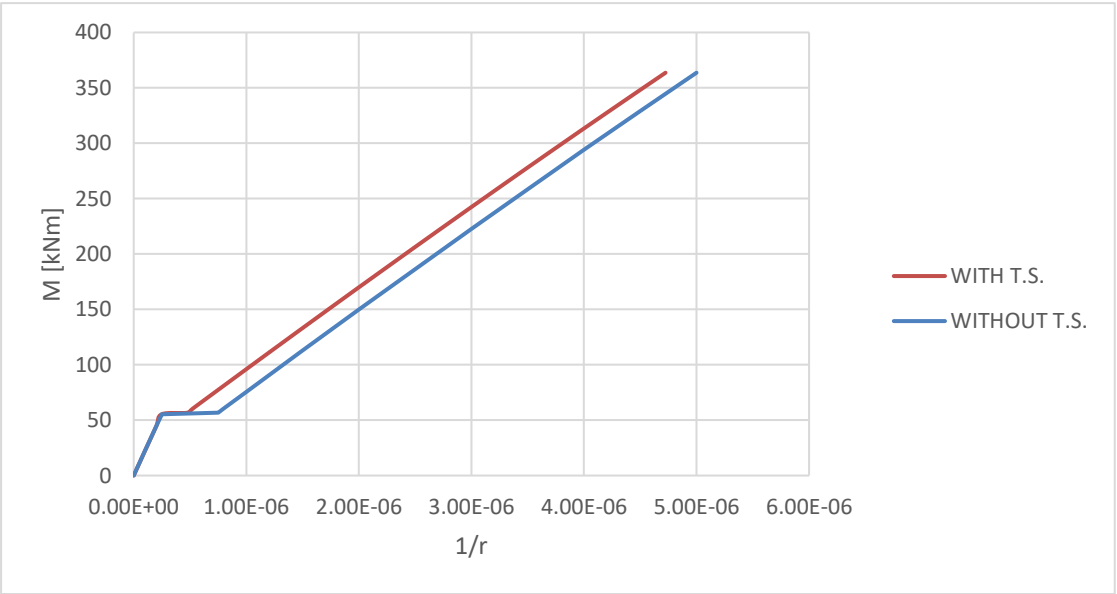


Figure 21. Diagram bending moment – curvature of Beam Tr2, Tr4, Tr6

The comparison between the theoretical values and experimental data is similar to the analysis of linear elastic method. As shown in the following figures, for beam 1, 2 and 3, the calculation becomes less precise as the load increases comparing to the real behavior. Analogously, the theoretical model can describe the performance in cases of beam 5 and 6 relatively well.

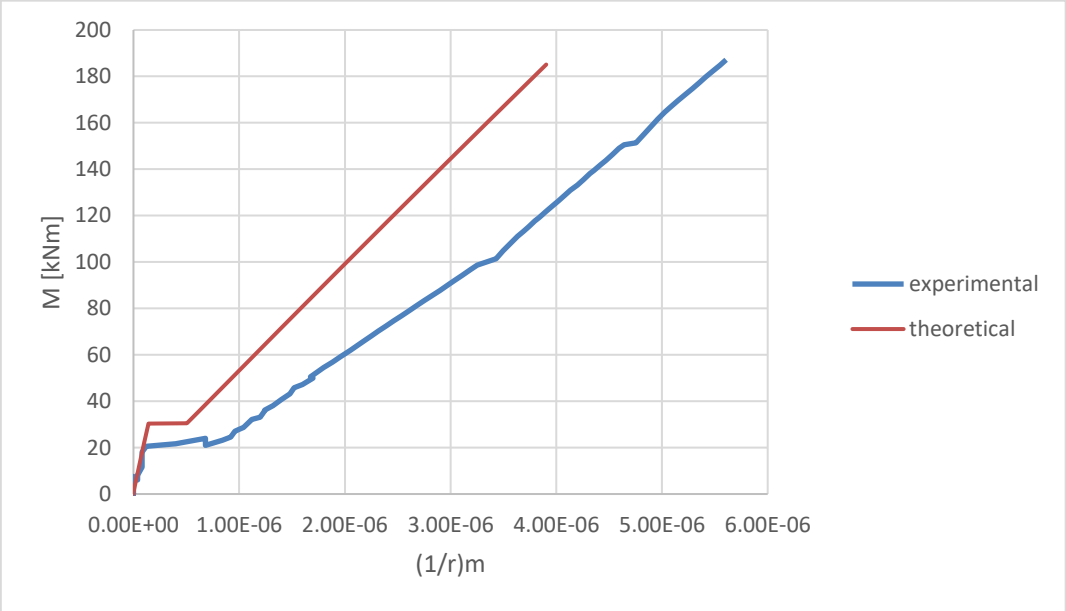


Figure 22. Diagram of bending moment - mean curvature of Beam 1, node C

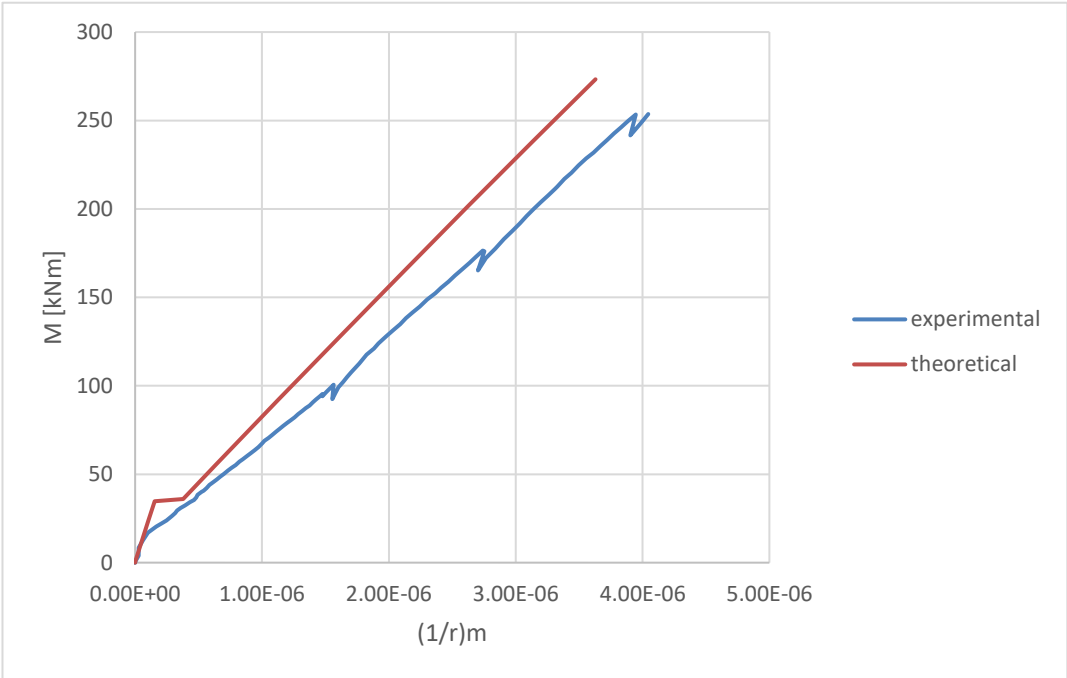


Figure 23. Diagram of bending moment - mean curvature of Beam 2, node C

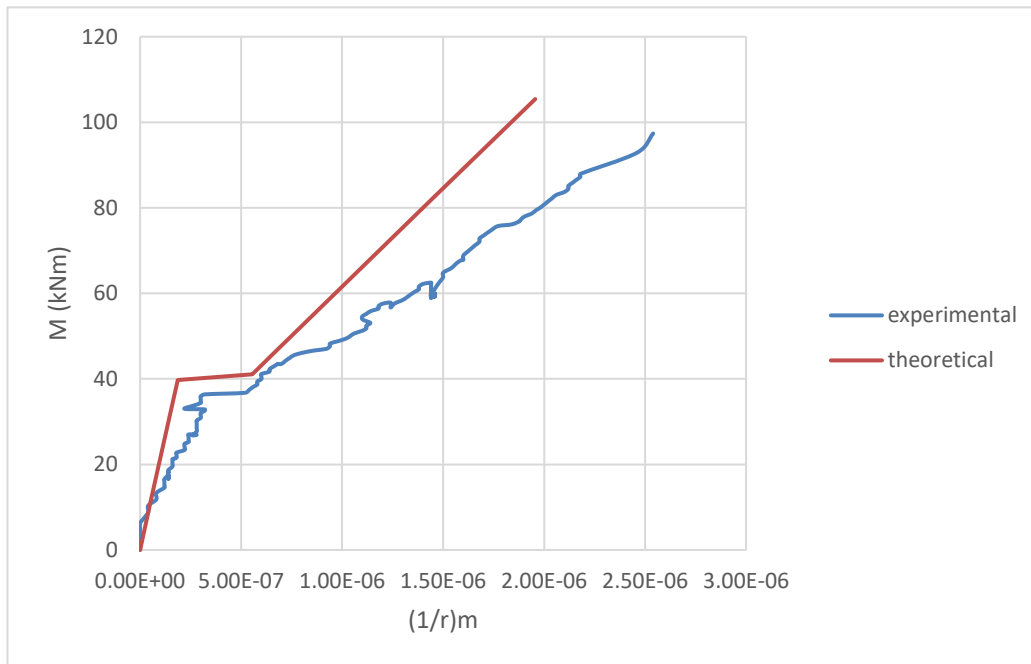


Figure 24. Diagram of bending moment - mean curvature of Beam 3, node A

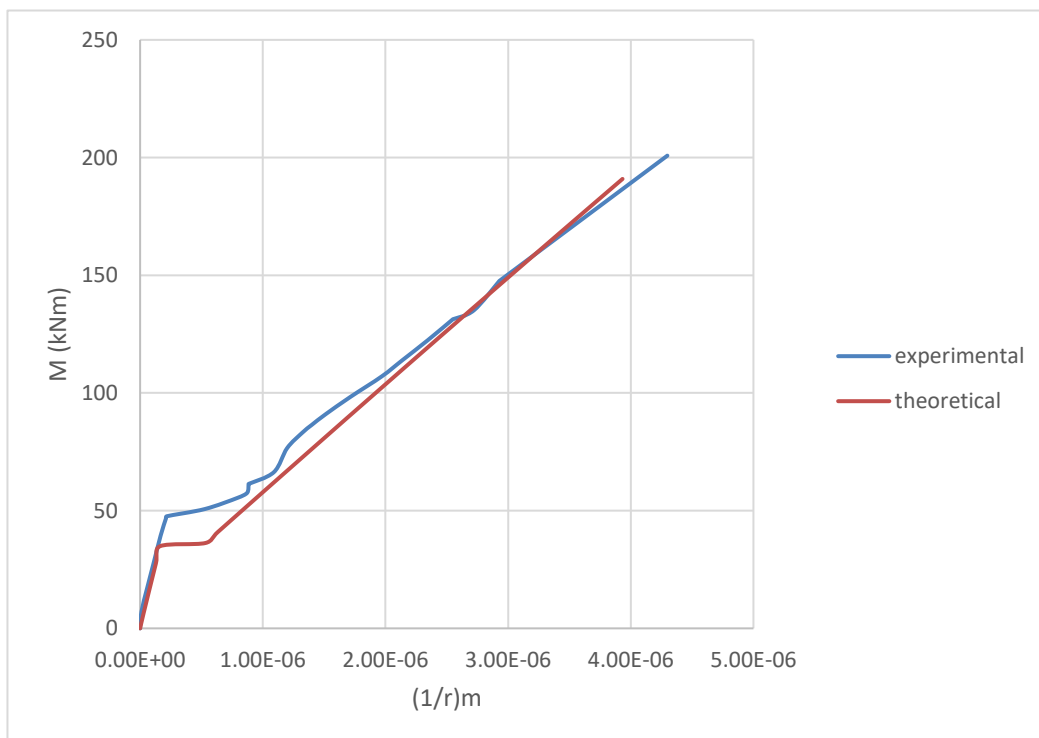


Figure 25. Diagram of bending moment - mean curvature of Beam 5, node C

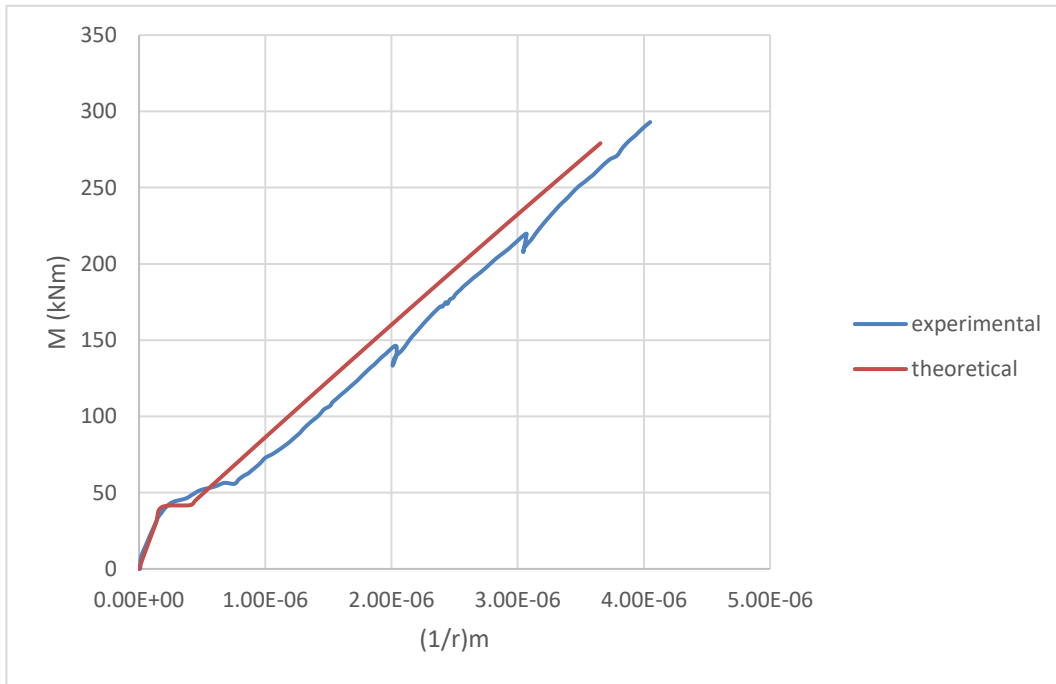


Figure 26. Diagram of bending moment - mean curvature of Beam 6, node C

2.52 Calculating the deflection

Dividing the beam into hundreds of sections, with each slice has a thickness of 10 mm except the first and last sections which are 5mm thick. The reference point on each section of the z axis is starting from 0 with spacing 10mm.

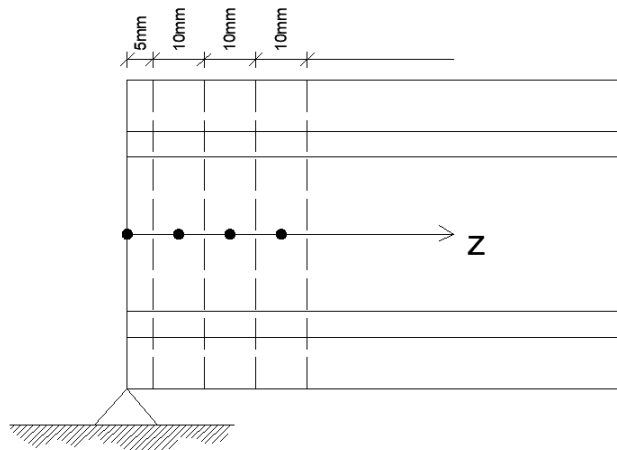


figure 27. Slices and referencing points in the front view of beam

The model also needs to specify the load condition. Real concentrated load does not exist. Therefore, it is necessary to set up the load model in an appropriate way, which shows at following two figures that equally distributes the concentrated force on the neutral axis.

TR1, TR2 beams

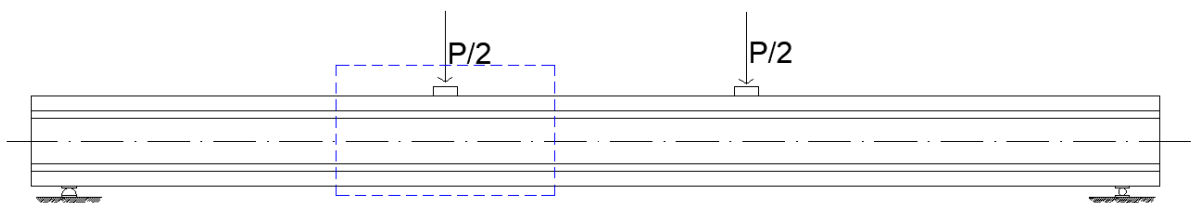


figure 28.a Example of distributing concentrated load of beam 1 and 2

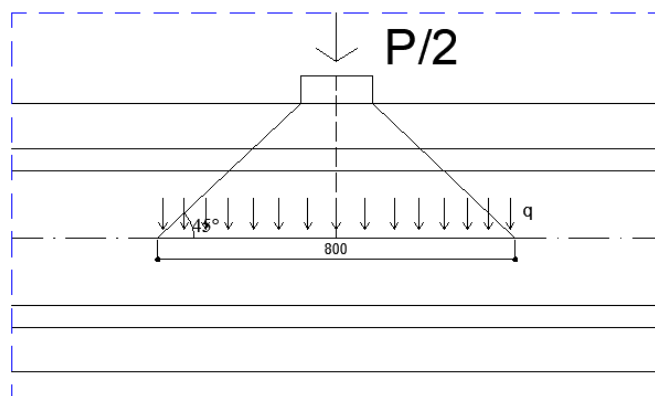


Figure 28.b The distributed load

The calculation of deflection is performed on the basis of virtual work method which affirms that the external virtual work corresponding to the load equals the internal virtual work which corresponds to the stress. Calculating the bending moment and curvature of every element, getting the displacement of measuring node produced by the intern stress of elements and then sum them up. It should be noted that the calculation proceeds discretely, hence the calculation should be done respectively based on if the cross section is cracked or not. The procedure is the same with all beams. Here, only performed once with beam 1 as an example.

1. Calculating the bending moment, of which calculation is divided into three segments. Because of symmetric model and distribution of load, only need to consider half of the beam, then multiply two when calculating the deflection.

Real system

for $z < 2100\text{mm}$

$$M_b = \frac{1}{2} * P * z_i \tag{2.24a}$$

for $2100 < z < 2900\text{mm}$

$$M_b = \frac{1}{2} * P * z_i - q * \frac{z^2}{2} \tag{2.24b}$$

for $2900\text{mm} < z < 3500 \text{ mm}$

$$M_b = \frac{1}{2} * P * z_i - \frac{1}{2} * P * (z_i - 2500) \tag{2.24c}$$

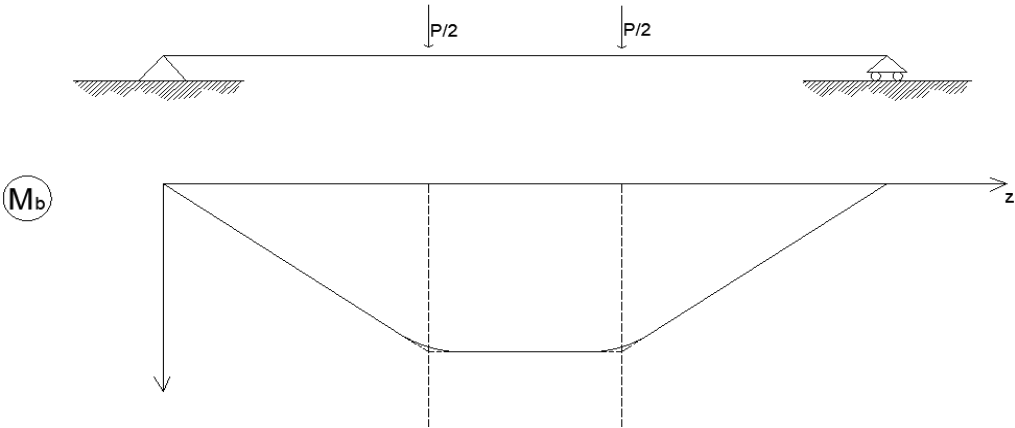


Figure 29. Bending moment in real system of beam 1

Virtual system

$$M_a = \frac{1}{2} * z \quad (2.25)$$

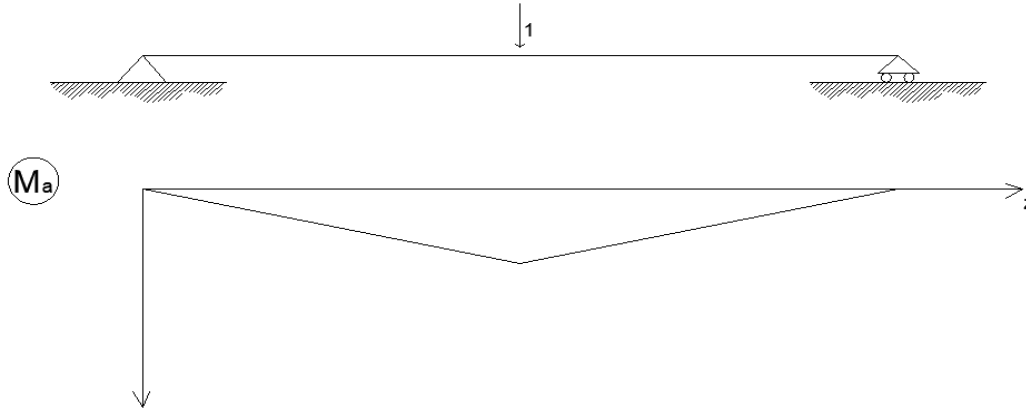


Figure 30. Bending moment in virtual system of beam 1

$$M_{b,pp} = \frac{1}{2} * q_{pp} * l_{tot} * z - q_{pp} * \frac{z^2}{2} \quad (2.26)$$

$$M_{tot} = M_b + M_{b,pp} \quad (2.27)$$

2. Calculation of curvature.

if $M_{tot} < M_{cr}$

$$\left(\frac{1}{r}\right)_{tot} = \frac{M_{tot}}{E_{cm} I_{om,1}} \quad (2.28a)$$

if $M_{tot} > M_{cr}$

$$\left(\frac{1}{r}\right)_{tot} = \frac{M_{tot}}{E_{cm} I_{om,2}} \quad (2.28b)$$

3. Calculating the deflection.

$$1 * f = \int_0^L M_a * \frac{1}{r} dx \quad (2.29a)$$

$$1 * f = \sum M_{ai} * \frac{1}{r} * L_i \quad (2.29b)$$

4. Removing the effect produced by self – weight, and plotting the diagram of relation load – deflection.

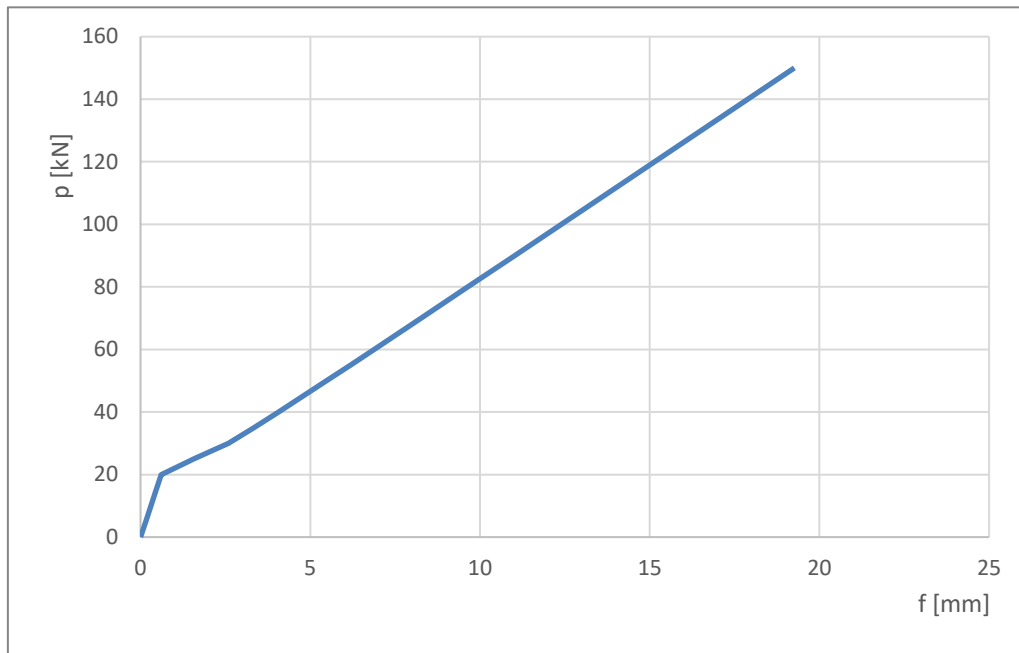


Figure 31. Diagram load – deflection of beam 1

In the end, comparing the calculation with experimental data. It can be seen that the theoretical curve is very close to the real behavior in uncracked state, even at the initial of state 2. But as the load increases, the error gets bigger and bigger. when P reaches 200 kN, the error even closes to 50% in the case of beam 1. Analogously, figure 30 shows the comparison of calculated deflection and experimental one of beam 2, the error is relatively small but still, it cannot be ignored.

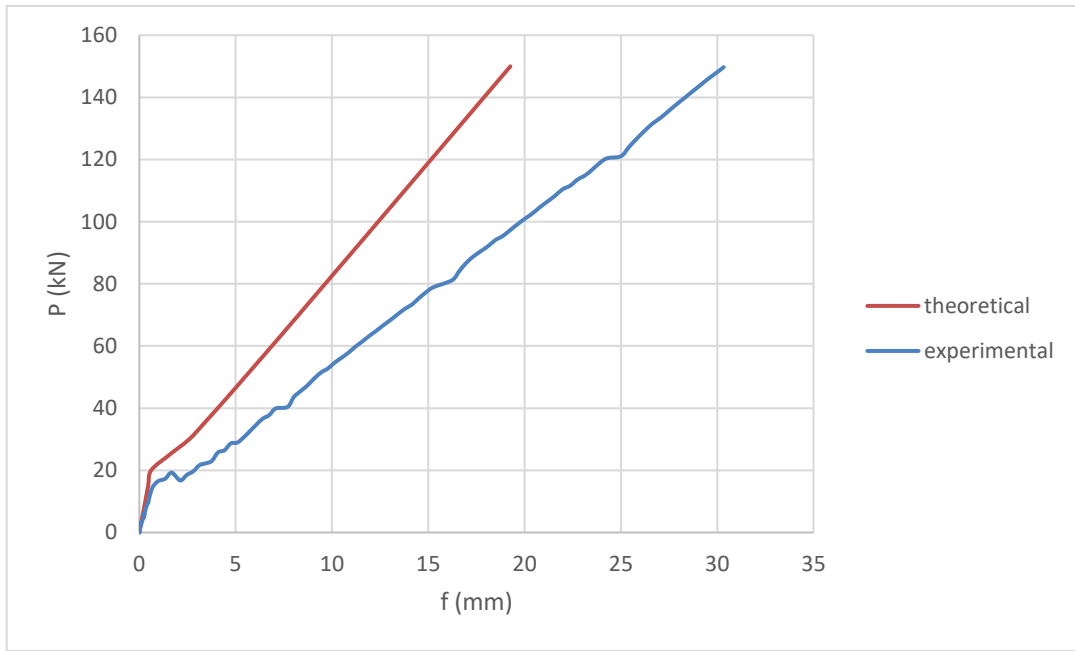


Figure 32. Diagram load - deflection with experimental data of beam 1

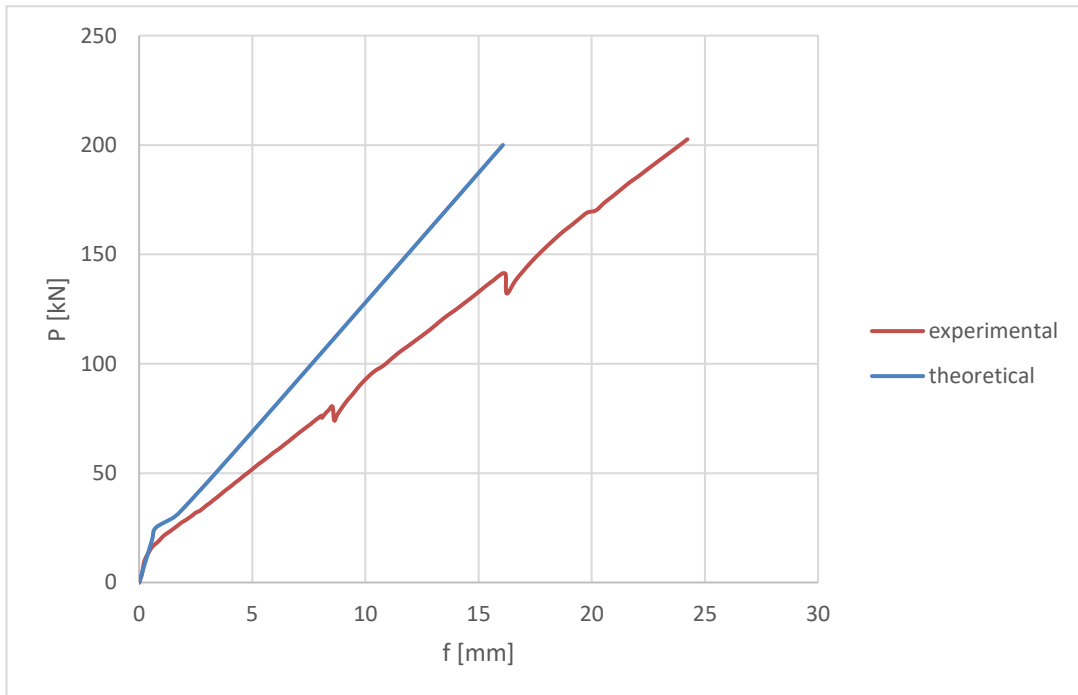


Figure 33. Diagram load - deflection with experimental data of beam 2

The following figures show the bending moment in real and virtual system for beam 3, and comparison of deflection with experimental data of beam 3. The calculation procedure is same with beam 1.

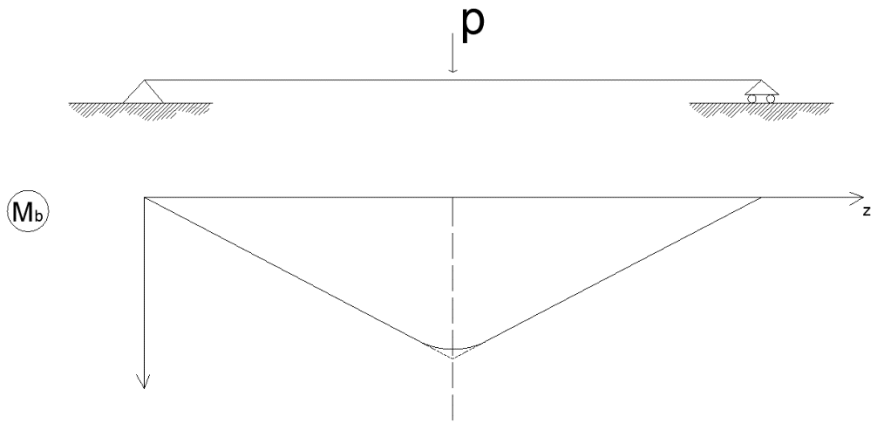


Figure 34. Bending moment in real system of beam 3

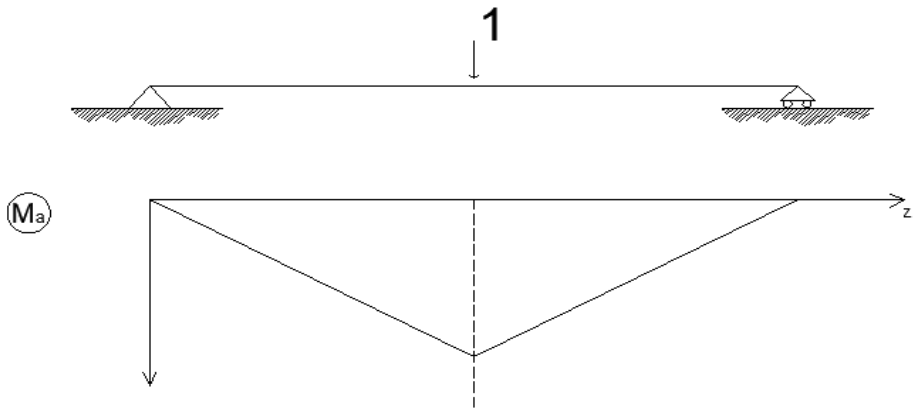


Figure 35. Bending moment in virtual system of beam 3

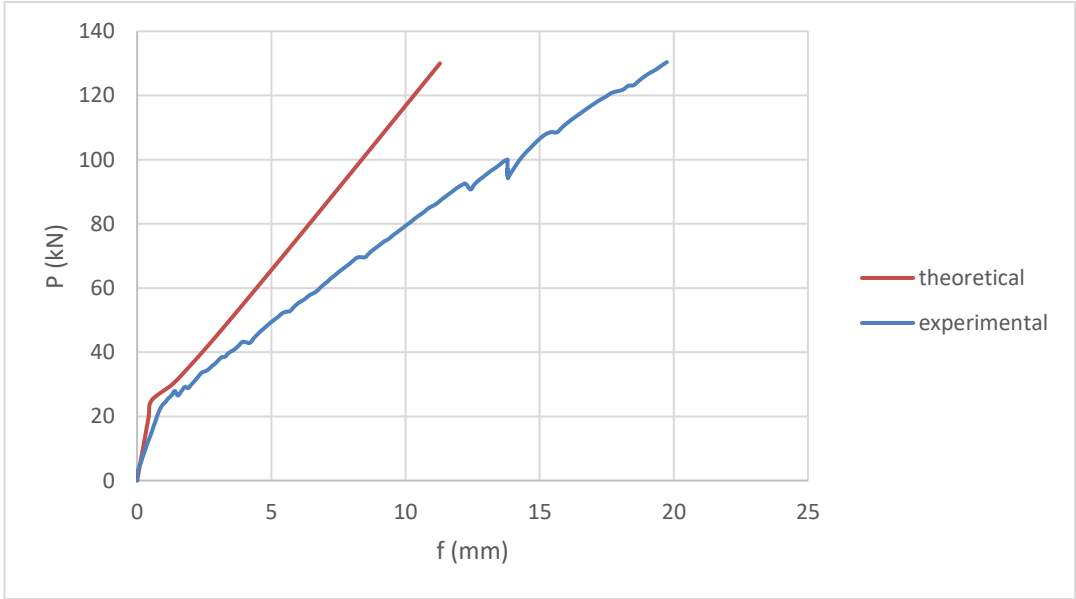


Figure 36. Diagram load - deflection with experimental data of beam 3

For beam 5 and 6, the model is no longer symmetric and it changes to a beam with cantilever subjected an asymmetric concentrated load. By the influence of self – weight, the max deflection is not at the node where applies the load, but with load increasing, it will slip to the node. Considering that the influence is not big, it is neglected in the discussion.

As the following two figures illustrate the calculation of bending moment in real and virtual system.

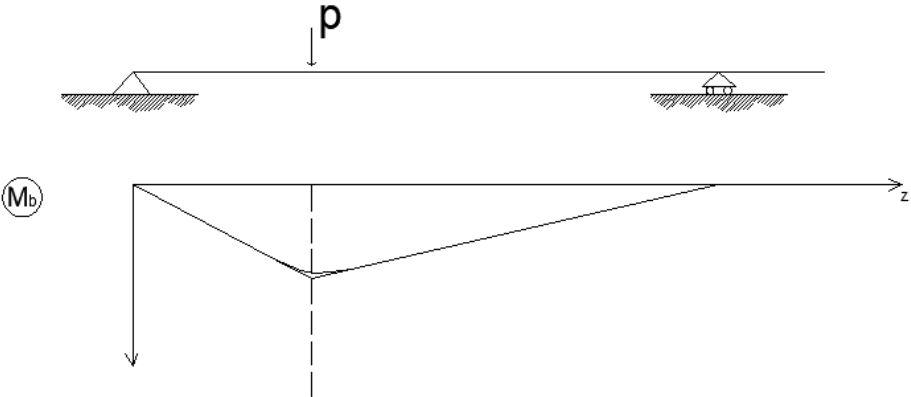


Figure 37. Bending moment in real system of beam 5

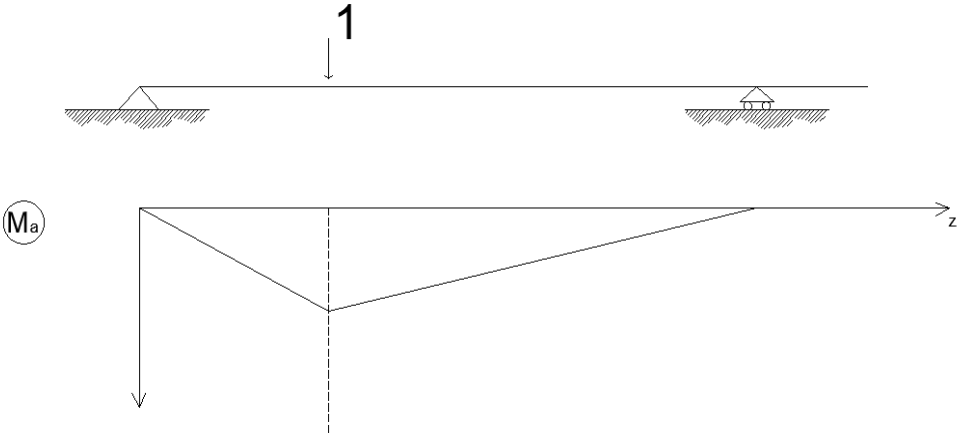


Figure 38. Bending moment in virtual system of beam 5

Comparison of theoretical deflection and experimental data of beam 5 and 6, as shown in the following figures.

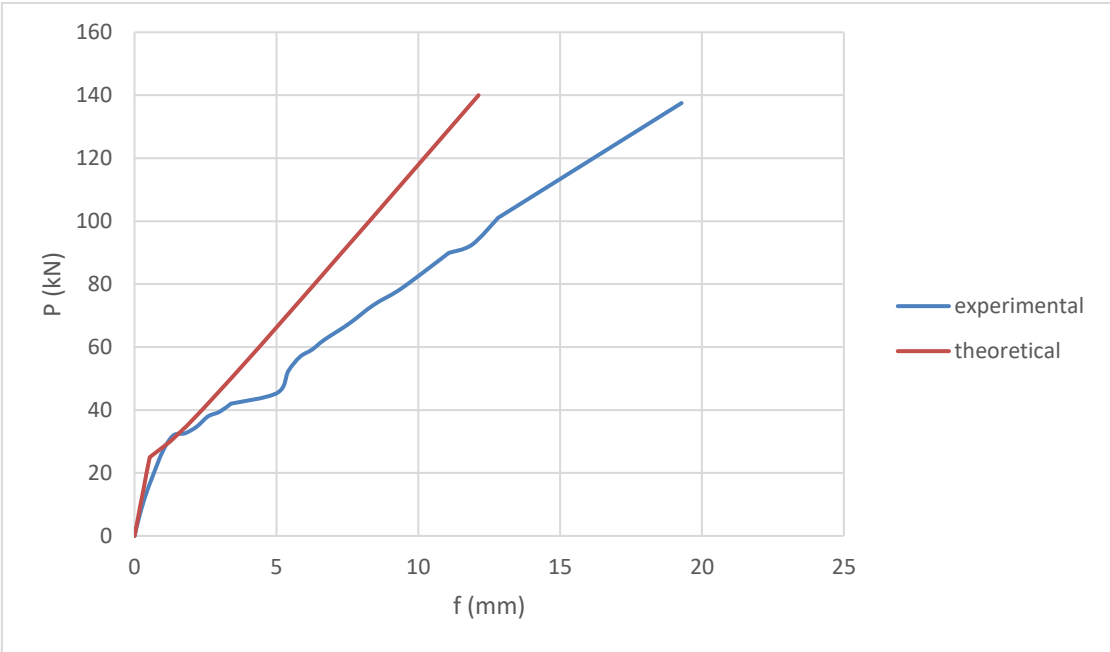


Figure 39. Diagram load - deflection with experimental data of beam 5

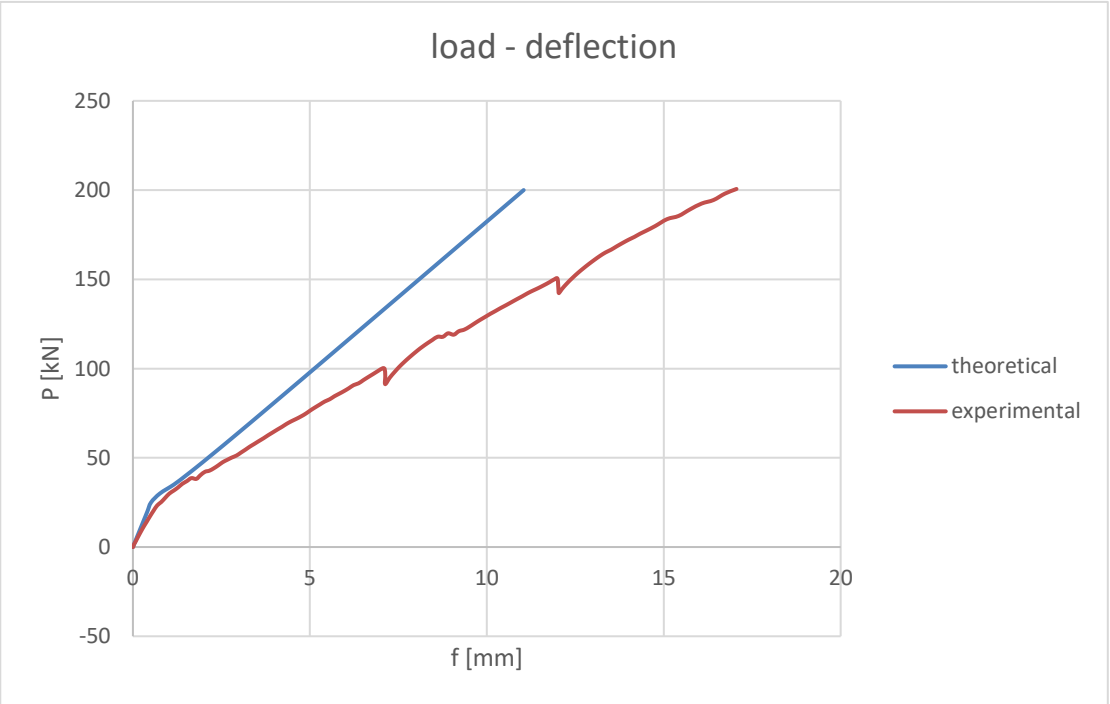


Figure 40. Diagram load - deflection with experimental data of beam 6

From the comparison of theoretical results of deflection and experimental data, it can be seen that for all beams with any load conditions, the deflection calculated is consistent roughly with the experiment when the load under a certain value, the value will be affected by the amount of longitudinal reinforcement, but then with the load increases, the gap between the theoretical value and experimental becomes larger and larger.

2.6 Bi-linear method

According to the EC2, there is an intermediate state between uncracked and fully cracked condition of the cross section, it can be described that the mean curvature or deformation is a combination of it in state 1 and 2:

$$\alpha = (1 - \zeta)\alpha_1 + \zeta\alpha_2 \quad (2.30)$$

Where

α is deformation parameter and it can be deflection or curvature.

α_1 is the value of the parameter in uncracked state

α_2 is the value of the parameter in fully cracked state

As it for curvature

$$\left(\frac{1}{r}\right)_m = \frac{1}{r_1}(1 - \zeta) + \frac{1}{r_2}\zeta \quad (2.31)$$

For deflection

$$f = f_1(1 - \zeta) + f_2\zeta \quad (2.32)$$

$$\zeta = 1 - \beta \left(\frac{\sigma_{cr}}{\sigma}\right)^2 \quad (2.33)$$

ζ is a distributing coefficient with the consideration of tension-stiffening effect, and obviously it is zero for un-cracked section.

β is loading duration factor

$\beta=1$ for short term loading

$\beta=0.5$ for long term loading

Pay attention that the ratio of cracking stress and stress in calculation of coefficient ζ , it can be replaced by terms of bending moment or tension. Therefore, it can be expressed as:

$$\zeta = 1 - \beta \left(\frac{M_{cr}}{M}\right)^2 \quad (2.34)$$

2.61 Calculation of mean curvature

1. Calculating the curvature corresponding to the cross section uncracked and fully cracked.

$$\left(\frac{1}{r_1}\right)_{tot} = \frac{M_{tot}}{E_{cm}I_{om,1}} \quad (2.35a)$$

$$\left(\frac{1}{r_2}\right)_{tot} = \frac{M_{tot}}{E_{cm}I_{om,2}} \quad (2.35b)$$

2. Removing the influence of self – weight

$$\frac{1}{r_1} = \left(\frac{1}{r_1}\right)_{tot} - \left(\frac{1}{r}\right)_{p.p} \quad (2.36a)$$

$$\frac{1}{r_2} = \left(\frac{1}{r_2}\right)_{tot} - \left(\frac{1}{r}\right)_{p.p} \quad (2.36b)$$

The curvature produced by self – weight is calculating in uncracked state.

$$\left(\frac{1}{r}\right)_{p.p} = \frac{M_{p.p}}{E_{cm}I_{om,1}} \quad (2.37)$$

3. Calculating the coefficient ζ with the formula (3.34), and obtain the mean curvature with calculation (3.31a).
4. Plotting the relationship of the bending moment and mean curvature, comparing with experimental data.

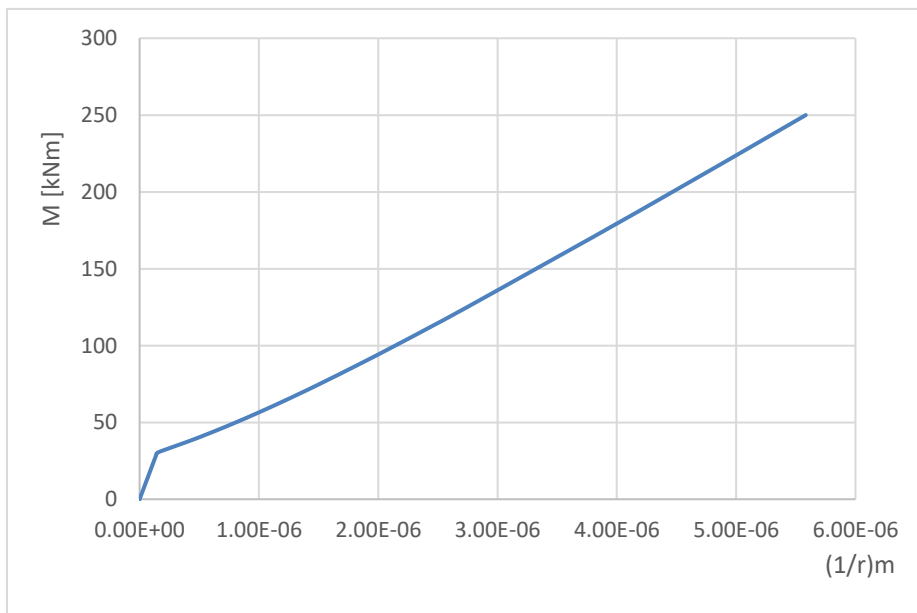


Figure 41. Diagram bending moment - mean curvature of beam 1 node C

For beam 1, the following two figures illustrate the comparison between calculation and experimental data in node C and A, where node C is in the midpoint which represent point of max bending moment, and node A is a random point except max bending moment points. It can be seen that the error is much bigger in node C than it in node A, which indicates that for a same theoretical model, the accuracy varies as the changing of section.

Comparing figure 42 and 44, increasing the number of reinforcing bars reduces the error between the calculation results and the experiment.

In the condition of concentrated load at midpoint, the accuracy is poor in state 2 and the gap between theoretical curve and experiment is approximately changeless.

The theoretical model performs well under the condition of an asymmetric concentrated load while measuring the node C subjected to the concentrated load. As they are shown in figure 46 and 47.

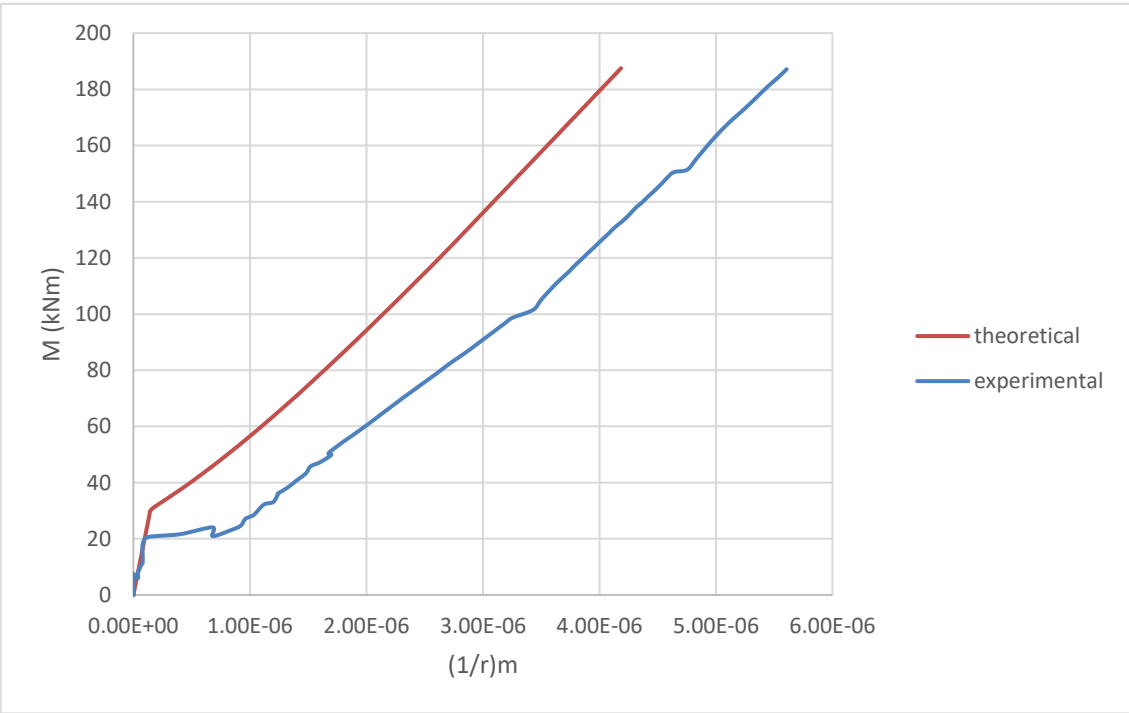


Figure 42. Diagram of bending moment - mean curvature of beam 1, node C

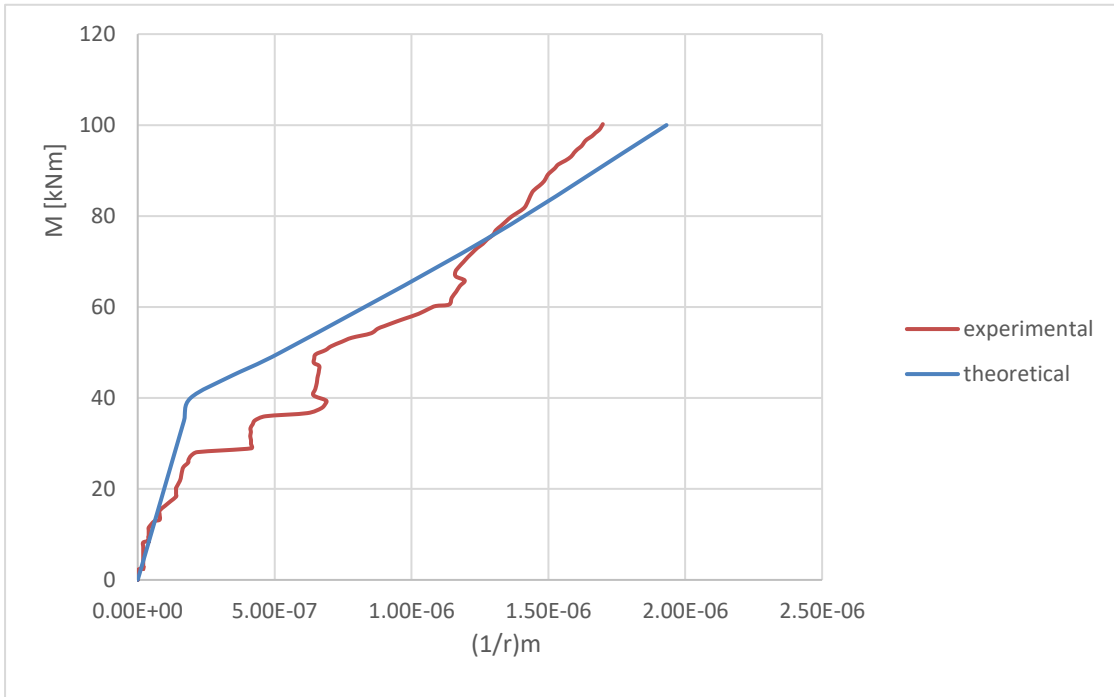


Figure 43. Diagram of bending moment - mean curvature of beam 1, node A

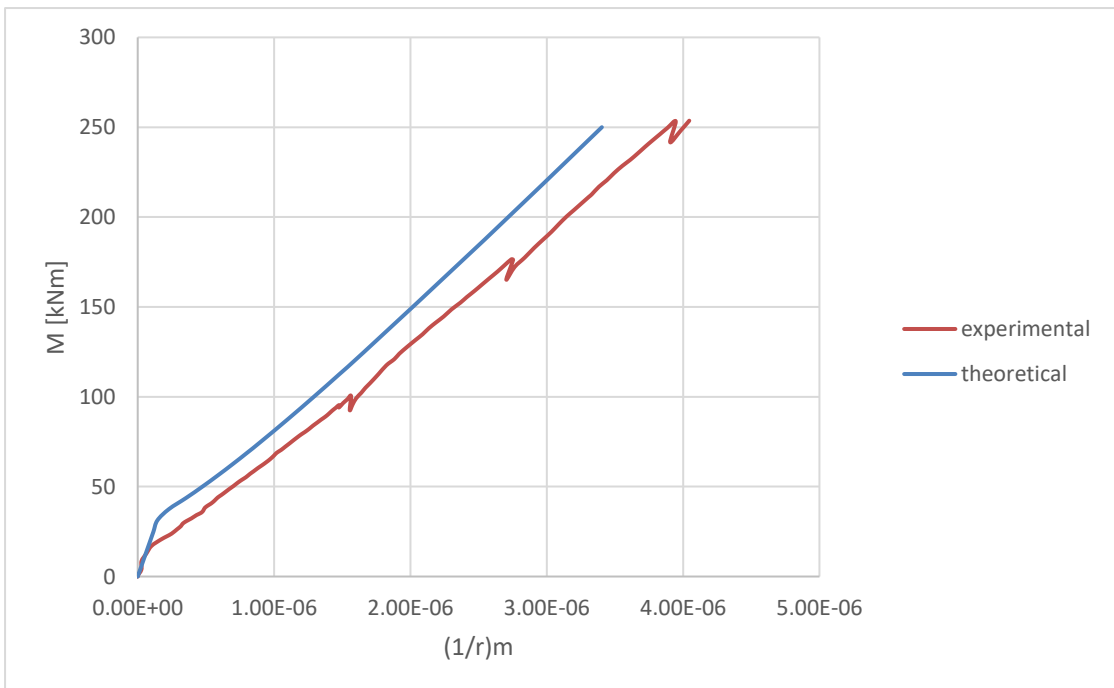


Figure 44. Diagram of bending moment - mean curvature of beam 2, node C

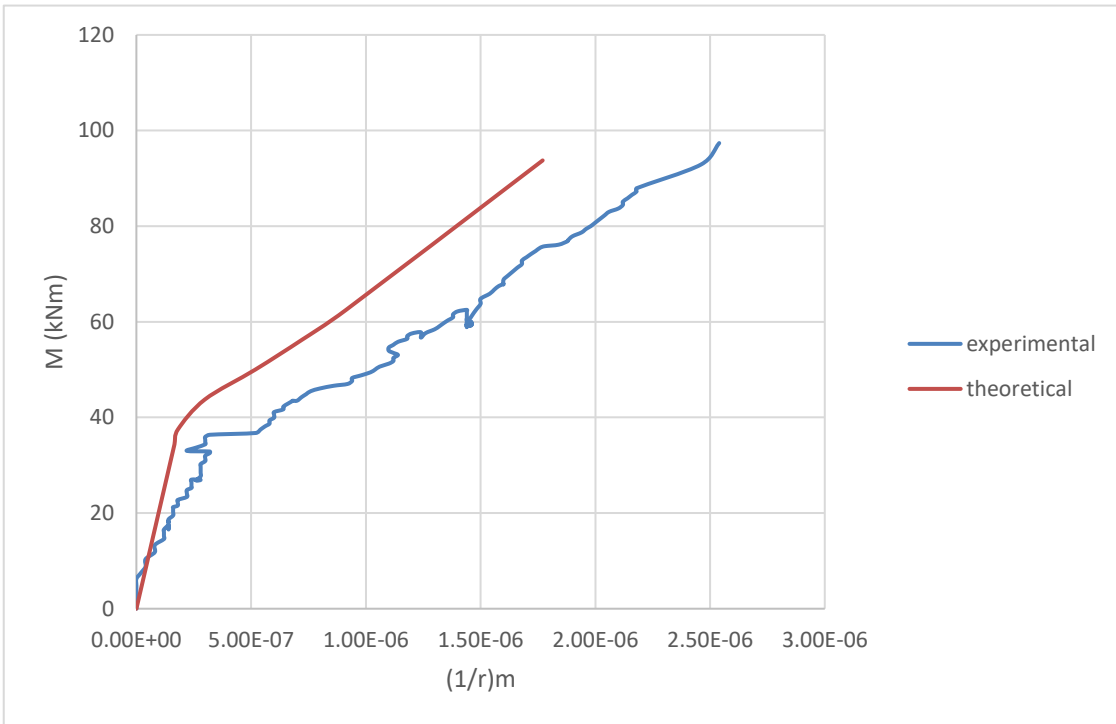


Figure 45. Diagram of bending moment - mean curvature of beam 3, node A

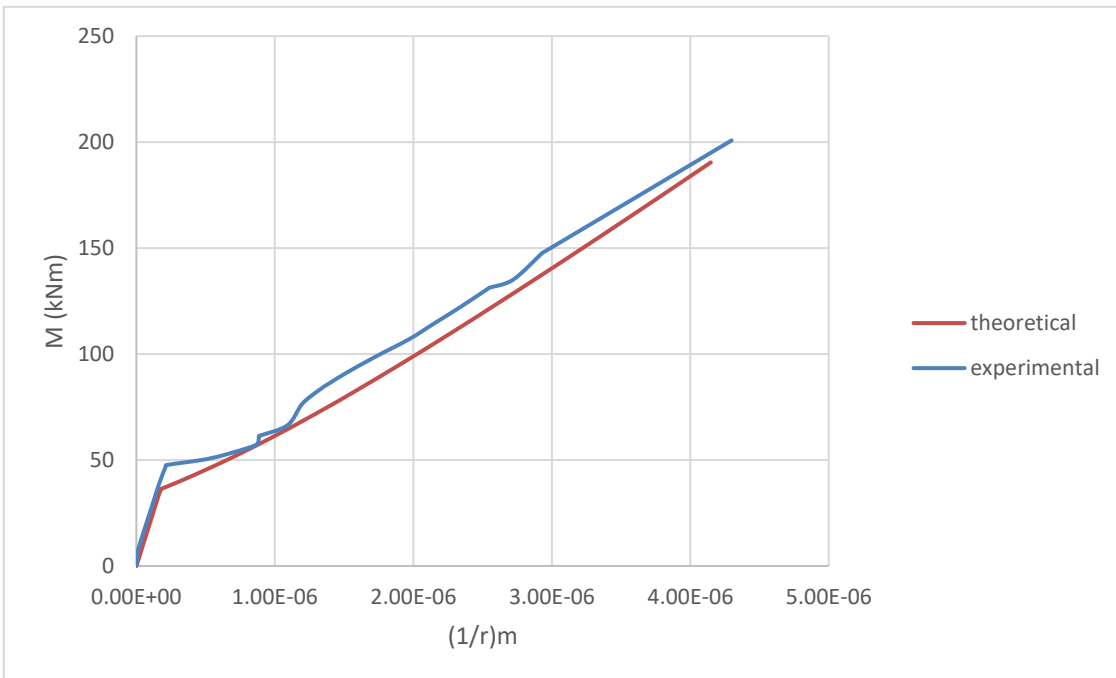


Figure 46. Diagram of bending moment - mean curvature of beam 5, node C

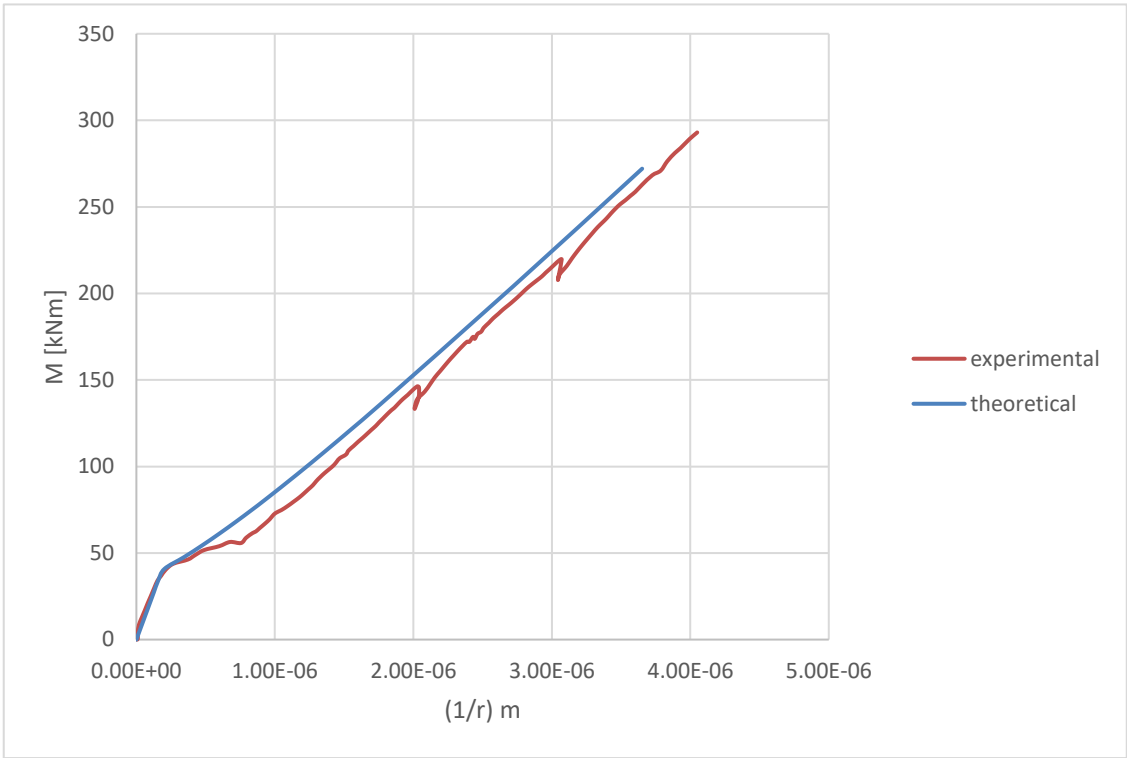


Figure 47. Diagram of bending moment – mean curvature of beam 6, node C

2.62 Calculation of deflection

As described before, the calculation of deflection is based on the principle of virtual work. With the linear analysis method, the deflection is calculated in a discrete way that means dividing the beam into hundreds of elements, here it uses the integration way instead.

As in the case of the calculation of mean curvature, calculating the deflection that corresponding to the curvature in state 1 and 2 as expressed in the previous calculations. Then obtain the deflection with the formula (2.32).

For example, with beam 1, the real system and virtual system are shown in following figures.

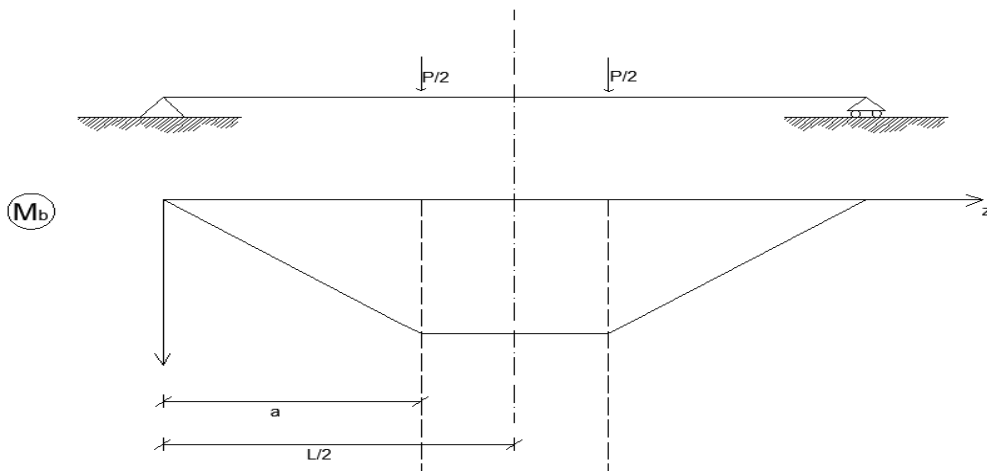


Figure 48. The bending moment in real system of beam 1

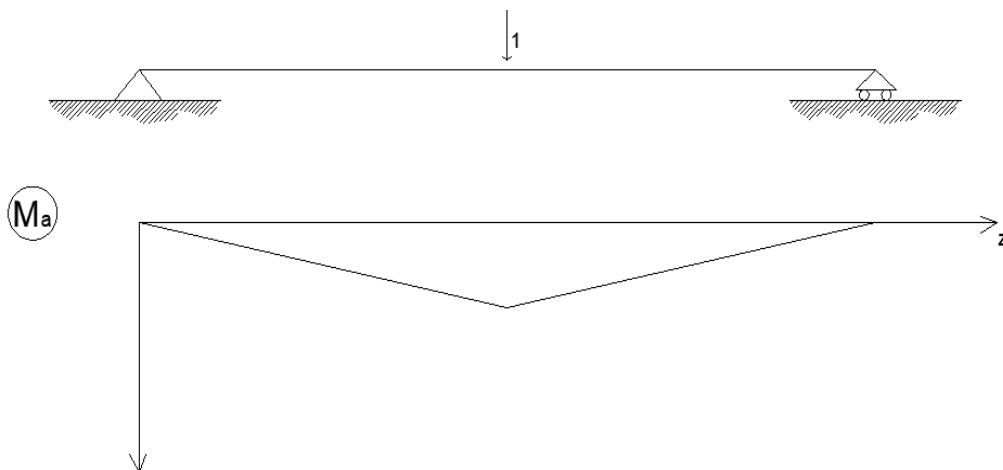


Figure 49. The bending moment in virtual system of beam 1

The deflection in uncracked state:

$$f_1 = \int_0^L M_a * \frac{1}{r_1} dz \quad (2.38a)$$

$$f_1 = 2 * \int_0^a M_a * \frac{M_b}{E_{cm}I_{om,1}} dz + 2 * \int_a^{L/2} M_a * \frac{M_b}{E_{cm}I_{om,1}} dz \quad (2.38b)$$

The deflection in fully cracked state:

$$f_2 = \int_0^L M_a * \frac{1}{r_2} dz \quad (2.39a)$$

$$f_2 = 2 * \int_0^a M_a * \frac{M_b}{E_{cm}I_{om,2}} dz + 2 * \int_a^{L/2} M_a * \frac{M_b}{E_{cm}I_{om,2}} dz \quad (2.39b)$$

The calculation procedure of other beams is mainly the same, only the distribution of bending moment needs to change with varying load conditions. The following figures illustrate the comparison between the theoretical deflection and experimental data. The result is similar to previous calculation, as the load increases, the theoretical values are smaller and smaller comparing to the experiment.

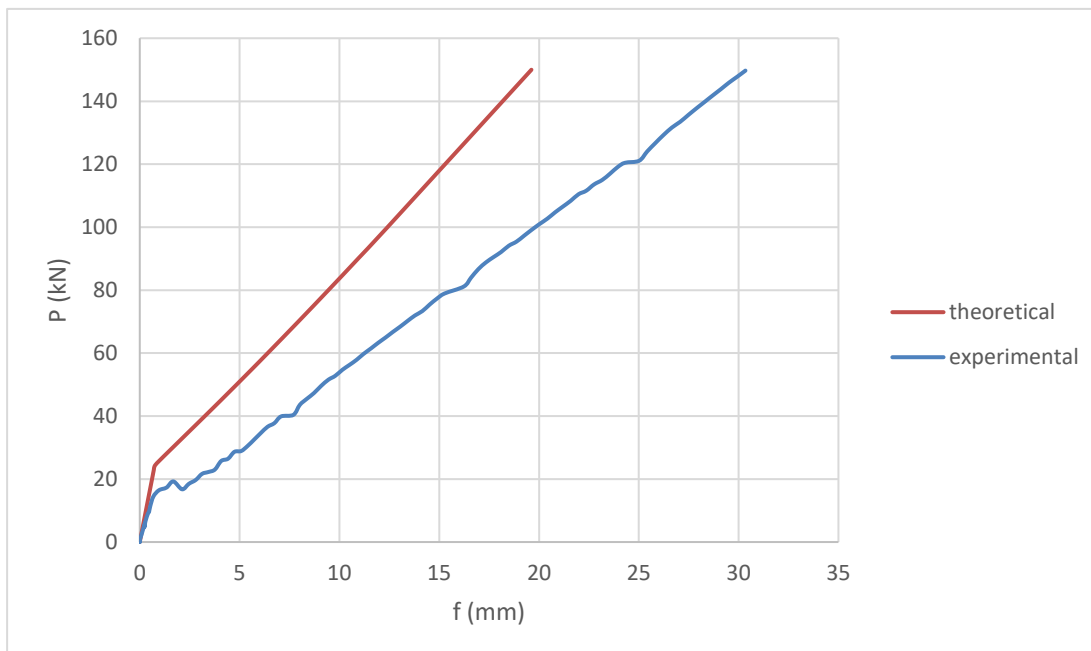


Figure 50. Diagram of load - deflection of beam 1

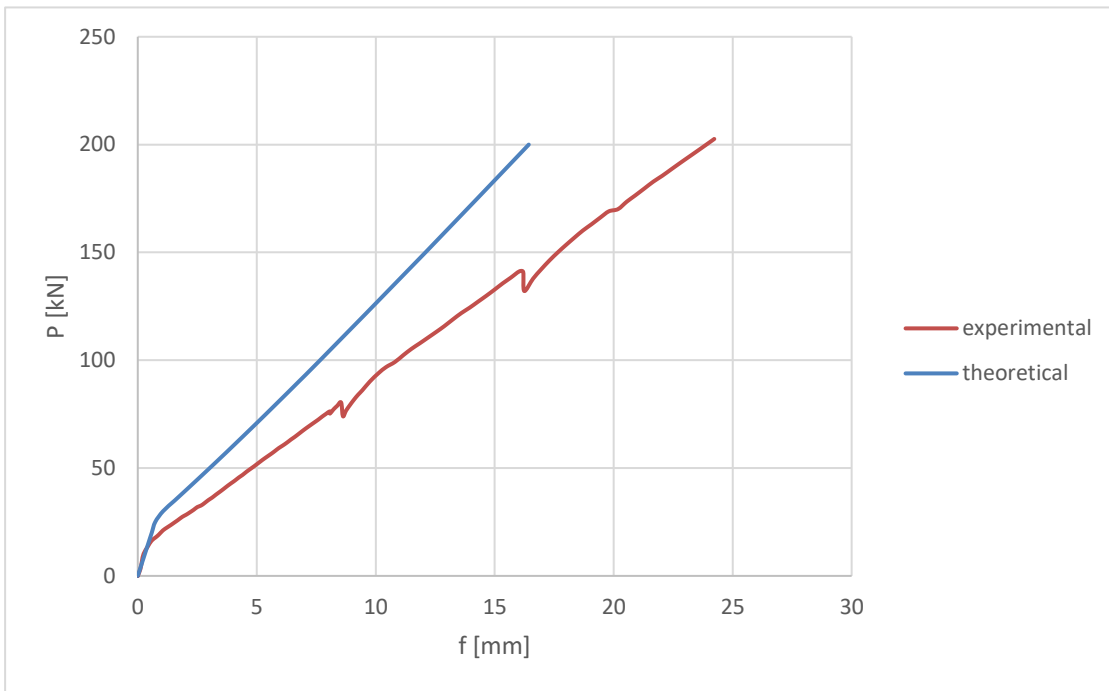


Figure 51. Diagram of load - deflection of beam 2

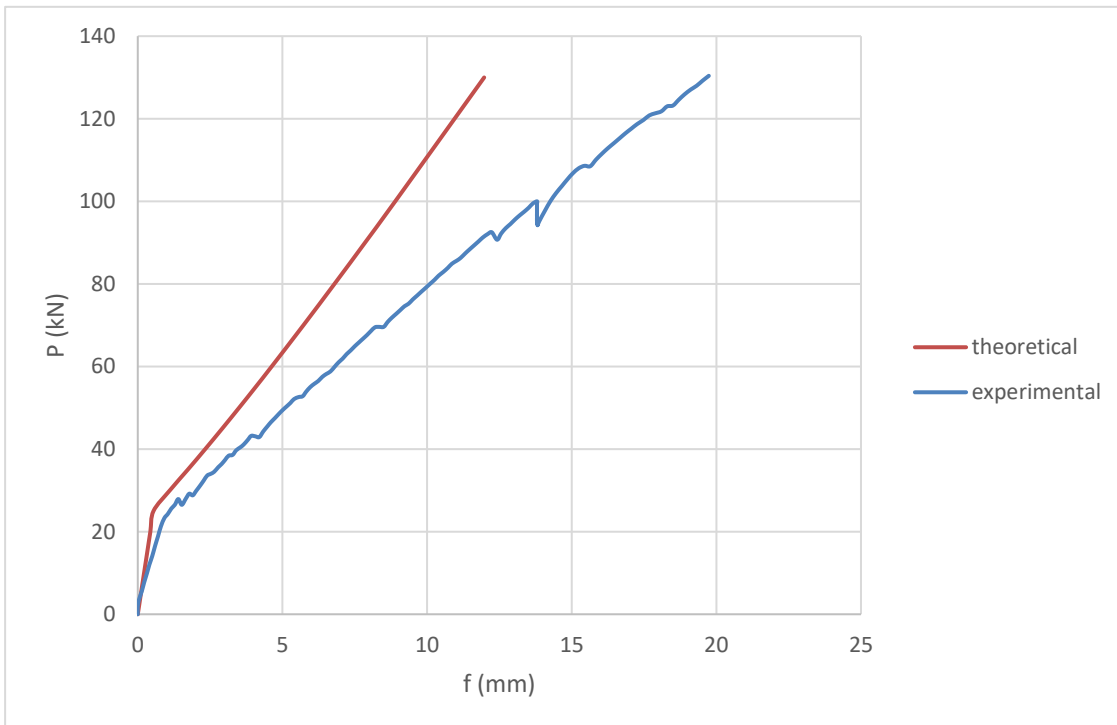


Figure 52. Diagram of load - deflection of beam 3

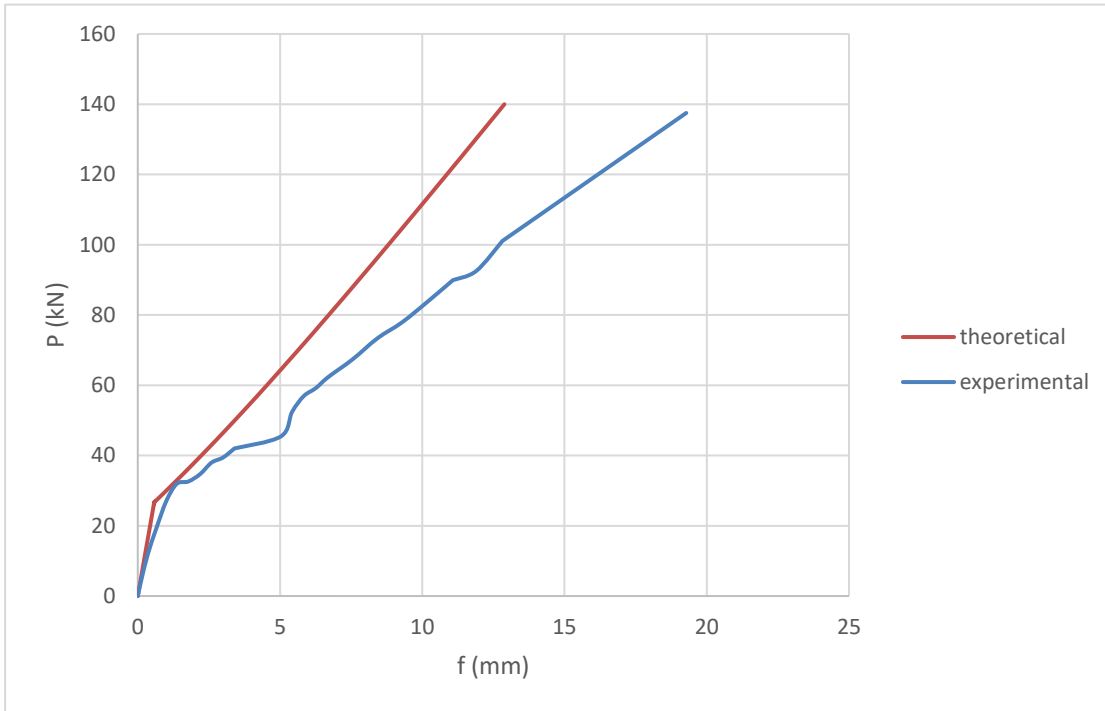


Figure 53. Diagram of load - deflection of beam 5

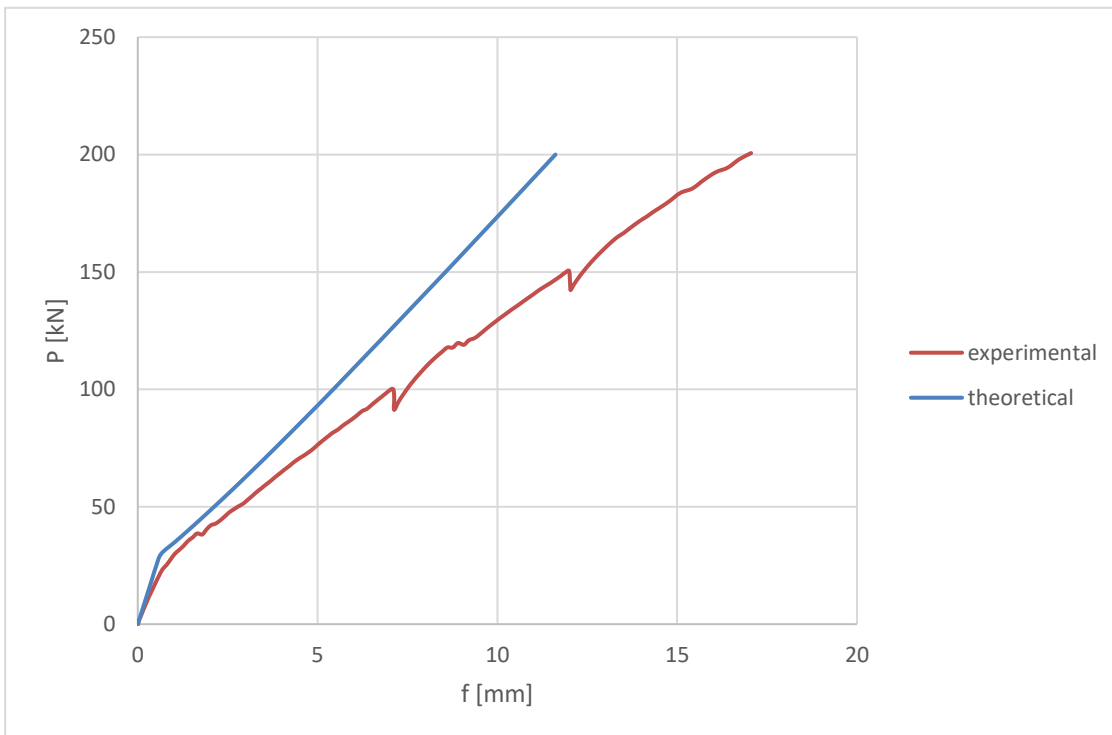


Figure 54. Diagram of load - deflection of beam 6

2.7 Method with coefficient η

The method introduces a coefficient η to improve the calculation of relative mean strain proposed by Model code 2010 and Euro code 2. On the base of assumption of linear distributed bond stress along the transmission length, the coefficient is only a function of acting axial force – to – cracking force ratio, which indicates the influence of internal secondary crack on tension – stiffening effect.

This method can be seen as the combination of the linear analysis method and bi – linear analysis method, and at the same time, it covered the characteristics of these two methods which are the flat transition from state 1 to state 2 and linear variation of tension – stiffening effect.

The coefficient η is actually the ratio of length of reduced bond l_{sc} and transmission length L_s . As shown in the following formula, it can be expressed as a function of the ratio of acting axial force-to-cracking force, or the ratio of steel stress and cracking steel stress which calculated in the cracking moment on the cross section.

$$\eta = \frac{l_{sc}}{L_s} = \left[\frac{3}{2} * \frac{F_s}{F_{cr}} - \frac{1}{2} \right] - \sqrt{\frac{9}{4} * \left(\frac{F_s}{F_{cr}} - 1 \right)^2 + 1} \quad (2.40a)$$

$$\eta = \frac{l_{sc}}{L_s} = \left[\frac{3}{2} * \frac{\sigma_{s2}}{\sigma_{sr2}} - \frac{1}{2} \right] - \sqrt{\frac{9}{4} * \left(\frac{\sigma_{s2}}{\sigma_{sr2}} - 1 \right)^2 + 1} \quad (2.40b)$$

For the second expression, if it can be considered linear relation between bending moment and steel stress as following:

$$\sigma = \frac{M}{I} * y \quad (2.41)$$

Therefore, it is equivalent to:

$$\eta = \frac{l_{sc}}{L_s} = \left[\frac{3}{2} * \frac{M}{M_{cr}} - \frac{1}{2} \right] - \sqrt{\frac{9}{4} * \left(\frac{M}{M_{cr}} - 1 \right)^2 + 1} \quad (2.42)$$

The coefficient discusses behavior of concrete reinforcement beam in the cracking state, which equals to zero at the moment of the crack formed. With the action increases, it will be infinitely close to 1.

2.71 Calculation of mean curvature

The two formulae mentioned before are both used here for calculating coefficient η , to compare advantages and disadvantages to each other.

The calculation of cracking force is

$$F_{cr} = \alpha_e * \frac{M_{cr}}{I_{om,1}} * y_s * A_{s,inf} \quad (2.43)$$

Meanwhile, the cracking bending moment has been obtained from the formula (1.1).

The compression and tension strain calculate as:

If $M_{tot} < M_{cr}$

$$\varepsilon_s = \alpha_e \frac{M}{I_{om,1} E_{cm}} * y_{s1} \quad (2.44a)$$

$$\varepsilon_c = \frac{M}{I_{om,1} E_{cm}} * y_{c1} \quad (2.44b)$$

If $M_{tot} > M_{cr}$

$$\varepsilon_s = \alpha_e \frac{M}{I_{om,2} E_{cm}} * y_{s2} \quad (2.45a)$$

$$\varepsilon_c = \frac{M}{I_{om,2} E_{cm}} * y_{c2} \quad (2.45b)$$

The method is a linear elastic analysis with considering the coefficient η . Therefore, the distribution of stress on the cross section is like figure 9, and the mean curvature is calculated in the same way:

$$\left(\frac{1}{r}\right)_m = \frac{\varepsilon_{sm} - \varepsilon_c}{d} \quad (2.46)$$

However, due to the varying of tension – stiffening effect which is now a function of coefficient η , the mean strain of steel bars in tension chord is changed.

$$\varepsilon_{sm} = \varepsilon_{s2} - k_t \frac{f_{ctm}}{\rho_{p,eff} E_s} * (1 - \eta) \quad (2.47)$$

In addition, the effect of self – weight should be removed. As the require of highlighting the transition from state 1 to state 2, it is necessary to thicken the calculating point in the interval.

The following figures illustrate the bending moment – mean curvature relationship of theoretical and experimental data.

Firstly, by comparing the results of calculation, obviously, it can be seen that calculation with the coefficient η corresponding to the bending moment, the transition part is shorter and then rises faster than it with coefficient η corresponding to the force. And with increasing of the bending moment, they tend to coincident with each other in the diagram of bending moment – curvature.

Comparing with the experimental data, with the bending moment rises, the gap between calculation and experiment for beam 1 and 2 becomes larger.

For beam 1 and 2, the node calculated is in the midpoint, they have the same loading condition with different amount reinforcement, the result of beam with more reinforcement is more precise.

While the theoretical model performs well in the condition of beam 3, 5 and 6. But as figure 58 shows, the theoretical calculation overestimates the real behavior of beam 5.

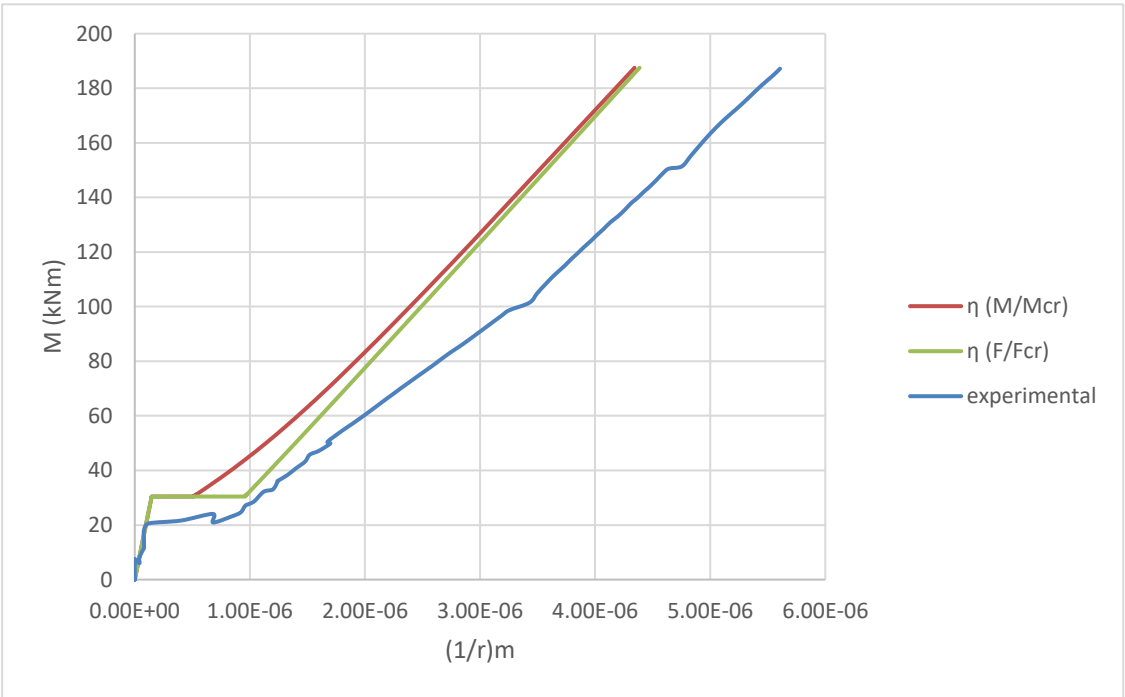


Figure 55. Diagram of bending moment and mean curvature of beam 1, node C

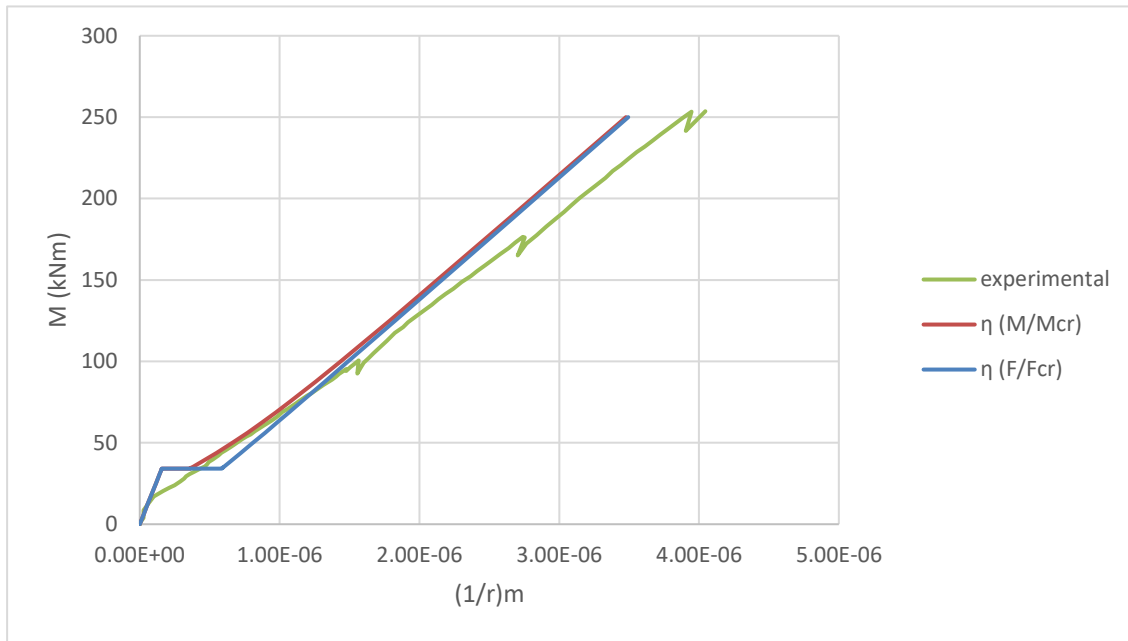


Figure 56. Diagram of bending moment and mean curvature of beam 2, node C

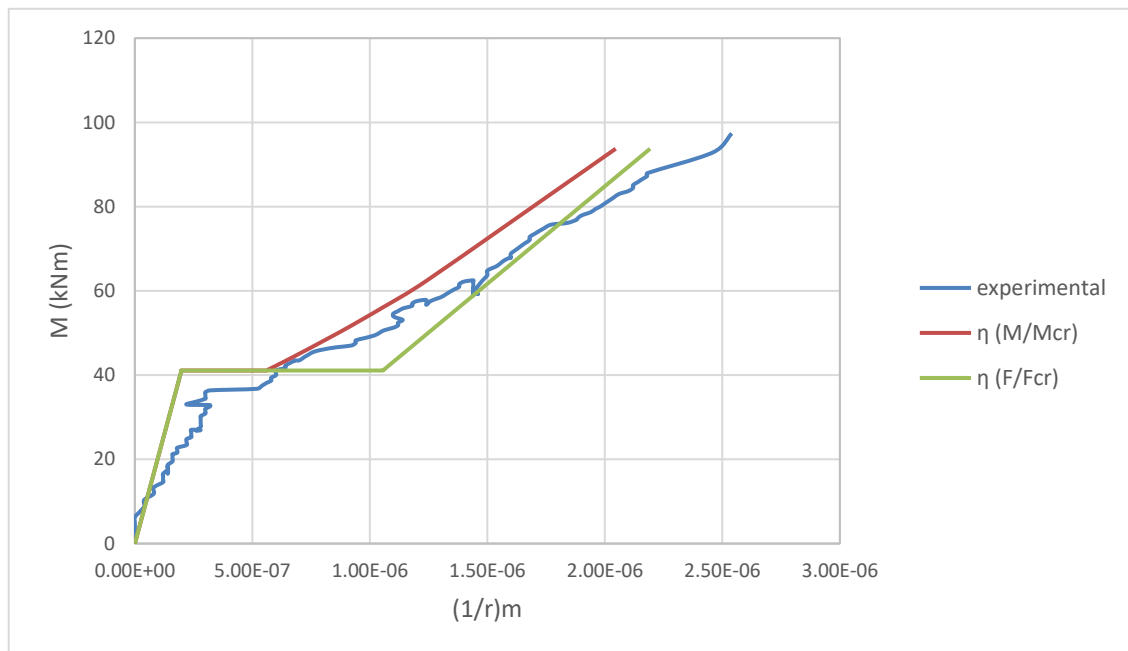


Figure 57. Diagram of bending moment and mean curvature of beam 3, node A

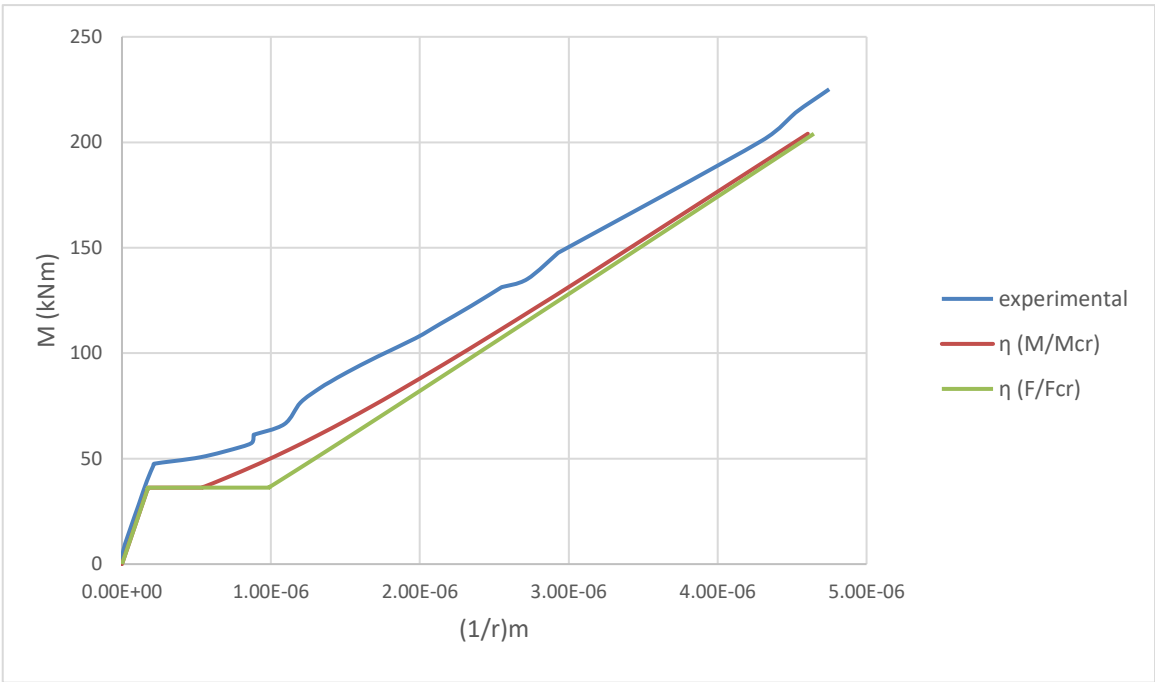


Figure 58. Diagram of bending moment and mean curvature of beam 5, node C

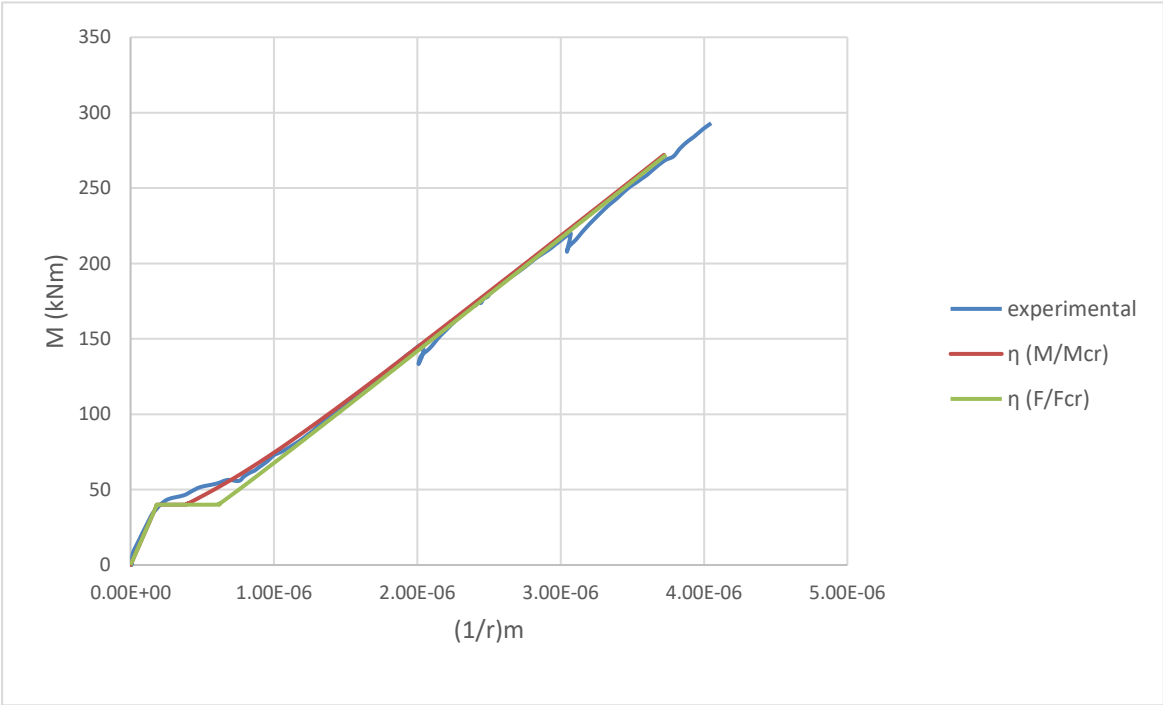


Figure 59. Diagram of bending moment and mean curvature of beam 6, node C

2.72 Calculation of deflection

As in the case of the deflection calculation in non – linear method, except that the mean curvature changed due to introducing of coefficient η in state 2, in state 1 the deflection remains the same as always.

Here the two curves that correspond to the two calculations of coefficient η are both plotted in the diagram of load – deflection. Comparing to each other, it can be seen that as same as in the calculation of curvature, there is a small gap at the transition, but as the increasing of load, it tends to disappear.

Comparing the calculation with the experiment, the theoretical model performs good accuracy when the cross section is uncracked. While at the beginning of state 2, the calculation corresponding to the coefficient $\eta(F/F_{cr})$ is bigger than the experimental value. But after that, the theoretical deflection for both becomes smaller than it in the experimentation, and the difference gets bigger and bigger with the load increasing. The theoretical model, compared to the models mentioned above, has not changed much.

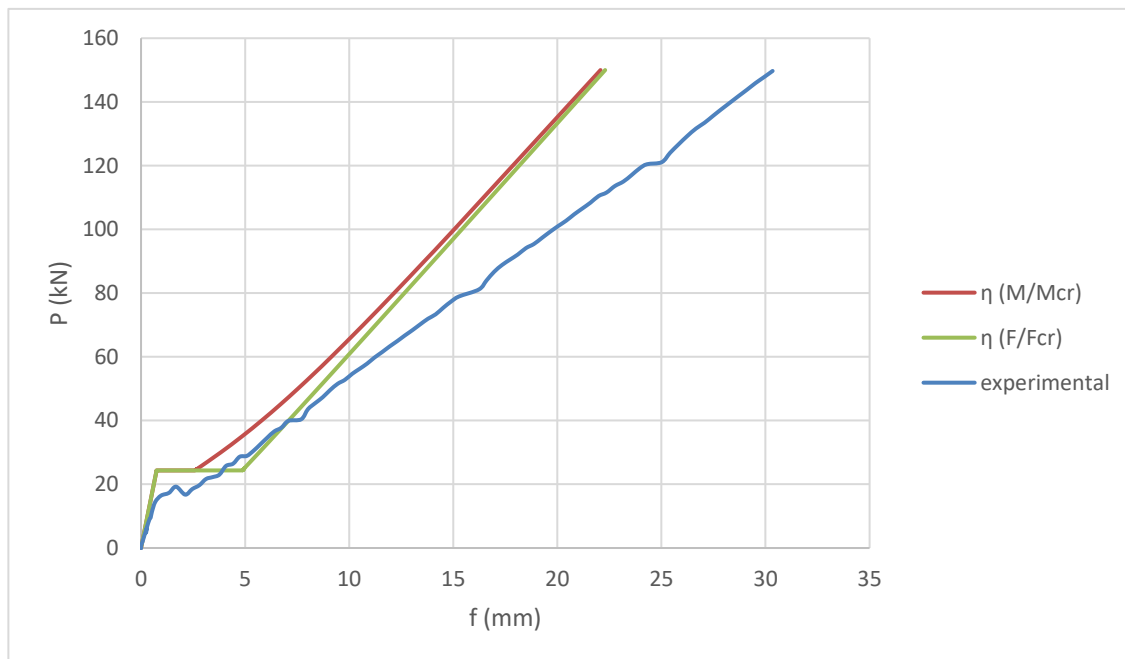


Figure 60. diagram of load – deflection of beam 1

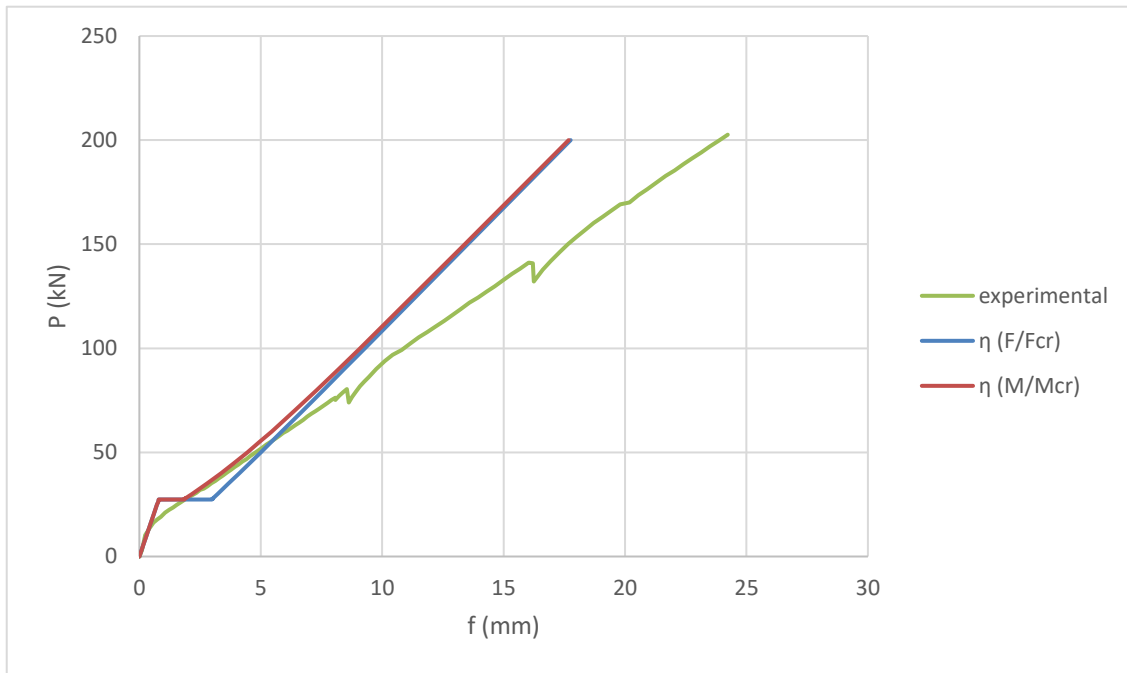


Figure 61. Diagram of load - deflection of beam 2

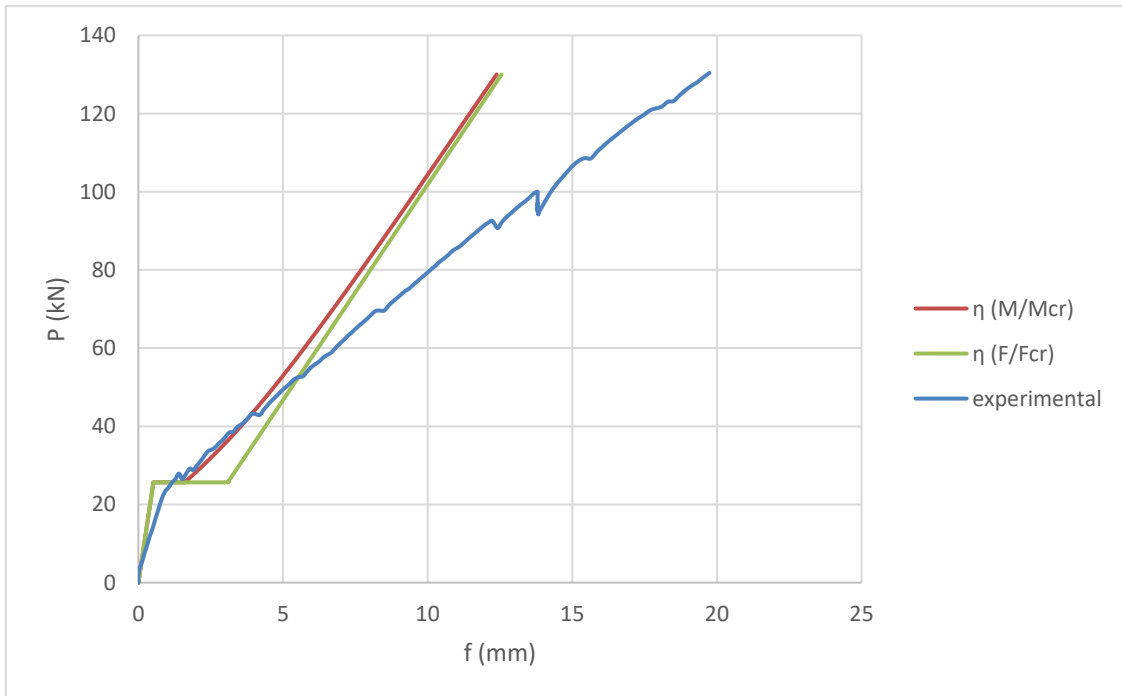


Figure 62. Diagram of load - deflection of beam 3

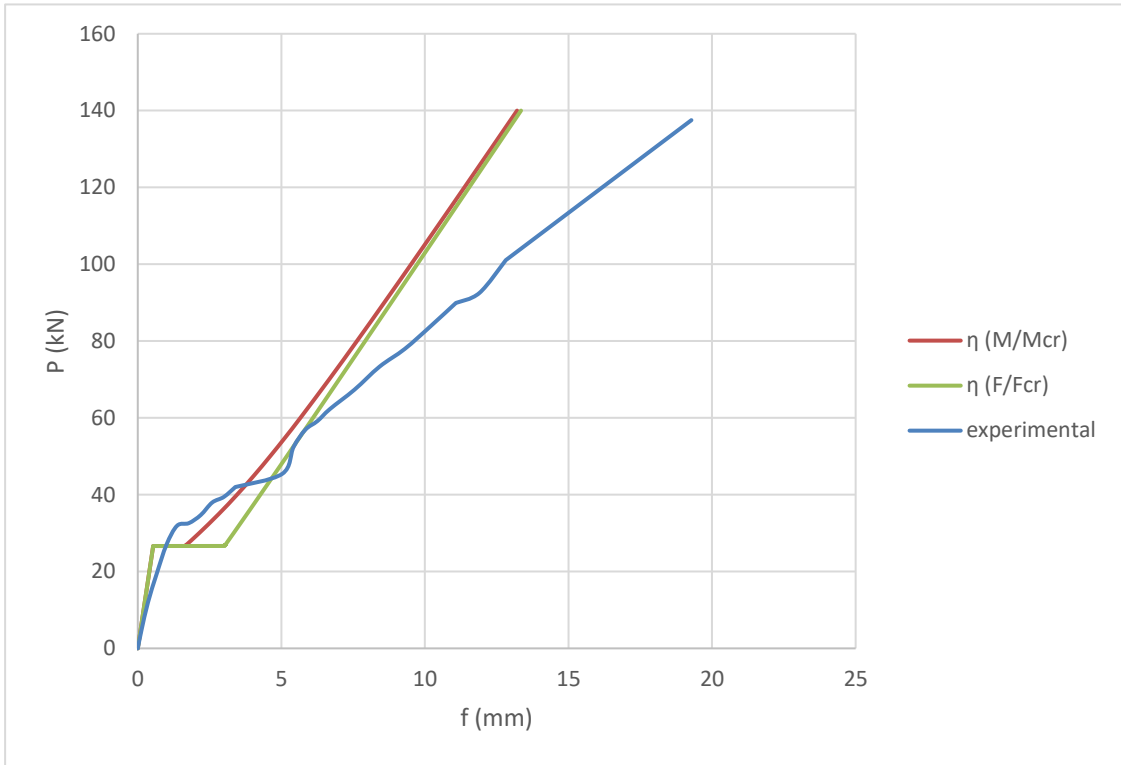


Figure 63. Diagram of load - deflection of beam 5

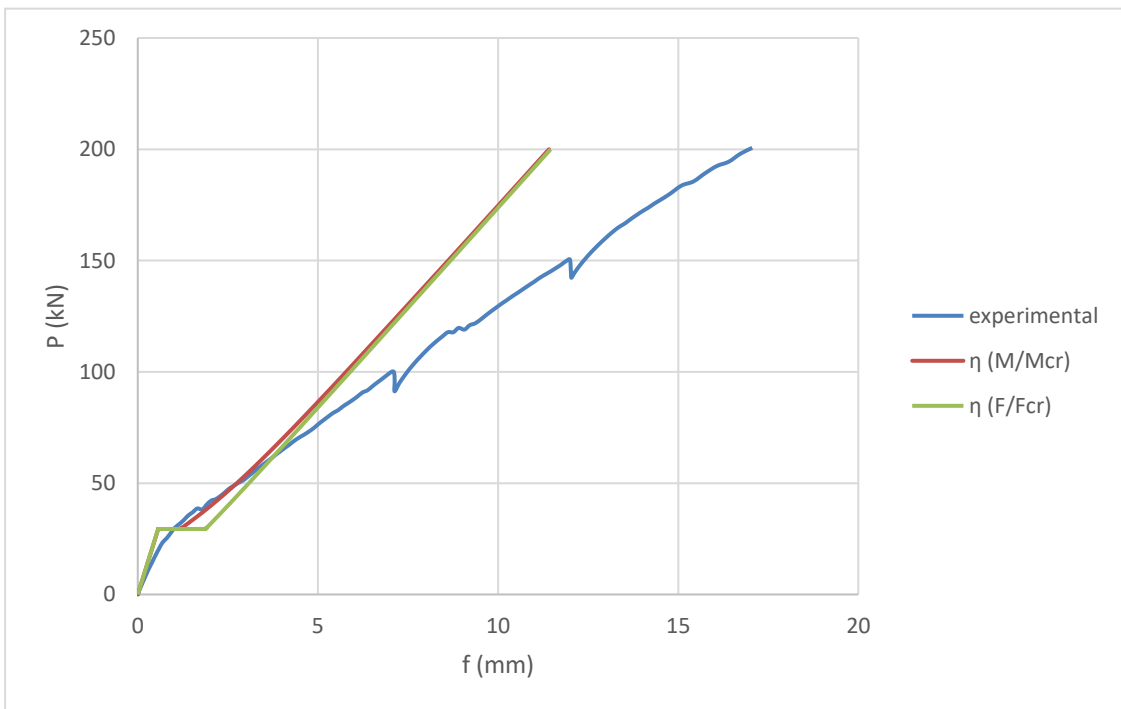


Figure 64. Diagram of load - deflection of beam 6

2.8 CEB – FIP Model Code 90

The theoretical model proposed by MC1990 gives another idea of calculation of mean curvature. As shown in the following two figures, which the first one shows the relation between mean curvature and simple bending and the other figure illustrates the relationship of mean curvature and bending moment combined with compression. For both, there are three curves which corresponding to state 1, state 2 and state after yielding of steel bars.

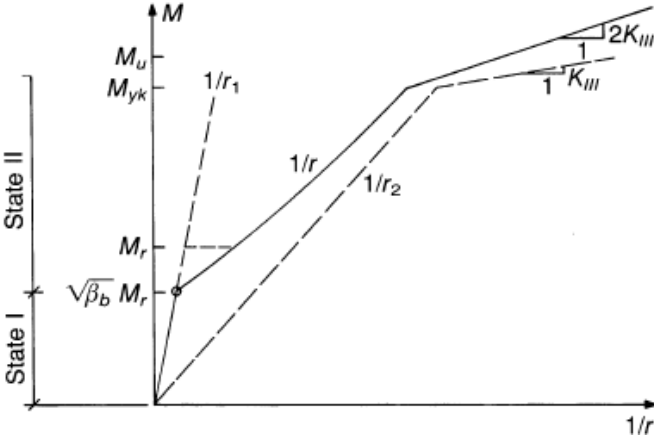


Figure 65. Diagram of mean curvature - simple bending

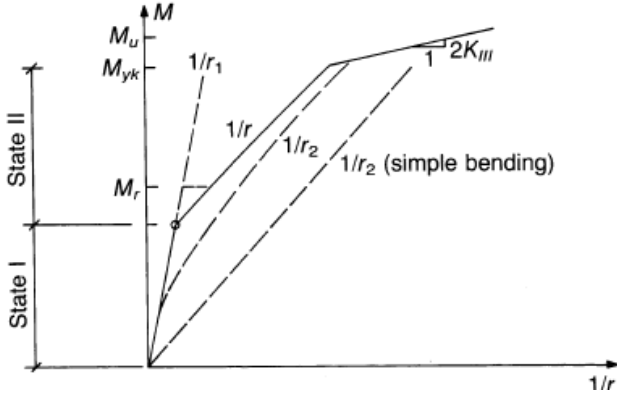


Figure 66. Diagram of mean curvature - bending combined with compression

The difference comparing to the model mentioned before is the effect of tension – stiffening. For taking action due to temperature, shrinkage, and etc. into account, the model gives a definition of hyperbolic law for calculating the tension – stiffening effect which corresponding to the curvature in state 1 and 2, in addition of the ratio of bending moment and a reduction factor β_b .

$$\frac{1}{r_{ts}} = \left(\frac{1}{r_{2r}} - \frac{1}{r_{1r}} \right) \beta_b \left(\frac{M_r}{M} \right) \quad (2.48)$$

Where

$\frac{1}{r_{1r}}$ is the curvature corresponding to the cracking bending moment in state 1.

$\frac{1}{r_{2r}}$ is the curvature corresponding to the cracking bending moment in state 2.

$$\beta_b = \beta_1 \beta_2 \quad (2.49)$$

β_1 is the coefficient characterizing the bond quality of reinforcement.

$\beta_1 = 1$ for high bond bars

$\beta_1 = 0.5$ for smooth bars

β_2 is the coefficient which represents the influence of duration of application or repetition of loading.

$\beta_2 = 0.8$ at first loading

$\beta_2 = 0.5$ for long – term loading or for a large number of load cycles

Therefore, the mean curvature can be defined as:

for state 1

$$\frac{1}{r} = \frac{1}{r_1} \quad (2.50a)$$

for state 2

$$\frac{1}{r} = \frac{1}{r_2} - \frac{1}{r_{ts}} = \frac{1}{r_2} - \left(\frac{1}{r_{2r}} - \frac{1}{r_{1r}} \right) \beta_b \left(\frac{M_{cr}}{M} \right) \quad (2.50b)$$

for $M \geq M_y$

$$\frac{1}{r} = \frac{1}{r_y} - \left(\frac{1}{r_{2r}} - \frac{1}{r_{1r}} \right) \beta_b \left(\frac{M_{cr}}{M_y} \right) + \frac{(M - M_y)}{2K_3} \quad (2.50c)$$

where

$$K_3 = \frac{M_u - M_y}{\left(\frac{1}{r_u} \right) - \left(\frac{1}{r_y} \right)} \quad (2.50d)$$

M_y is the yielding moment

M_u is the ultimate moment

$1/r_y$ is the curvature of yielding moment

$1/r_u$ is the curvature of ultimate moment

Here the case of bending moment greater than yielding moment is not considered, and only the first two steps are entered the analysis.

2.81 Calculation of mean curvature

1. Calculating the curvature which corresponding to the cracking bending moment in state 1 and 2 individually.

$$\frac{1}{r_{1r}} = \frac{M_{cr}}{E_{cm}I_{om,1}} \quad (2.51a)$$

$$\frac{1}{r_{2r}} = \frac{M_{cr}}{E_{cm}I_{om,2}} \quad (2.51b)$$

2. Calculation of the curvature which corresponding to the tension – stiffening effect with the formula (2.48).
3. Calculation of mean curvature with condition

If $M_{tot} < M_{cr}$

$$\frac{1}{r} = \frac{1}{r_1} = \frac{M_{tot}}{E_{cm}I_{om,1}} \quad (2.52a)$$

If $M_{tot} > M_{cr}$

$$\frac{1}{r} = \frac{1}{r_2} - \frac{1}{r_{ts}} = \frac{M_{tot}}{E_{cm}I_{om,2}} - \frac{1}{r_{ts}} \quad (2.52b)$$

4. Pay attention to the self – weight as mentioned before, it should remove the effect of self – weight in the calculation.

$$\left(\frac{1}{r}\right)_b = \frac{1}{r} - \left(\frac{1}{r}\right)_{p,p} \quad (2.53)$$

5. Plotting the diagram of bending moment and mean curvature, and comparing it with experimental data.

The following figures illustrate the comparison of the calculation of mean curvature and experiment. As it can be seen, the model behaves well in the conditions of beam 2, 5 and 6. While for beam1 and 3, the model tends to underestimate the real mean curvature in the experiment, especially the error ups to about 30% when the bending moment of beam 1 reaches 182.5 kNm.

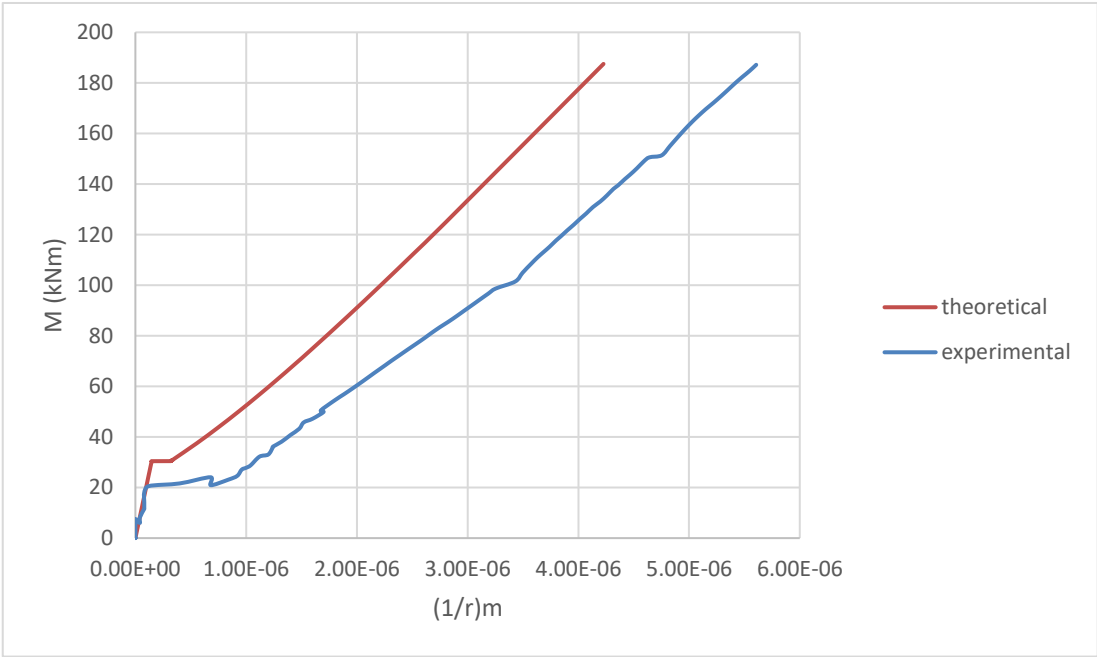


Figure 67. Diagram of the bending moment - mean curvature of beam 1, node C

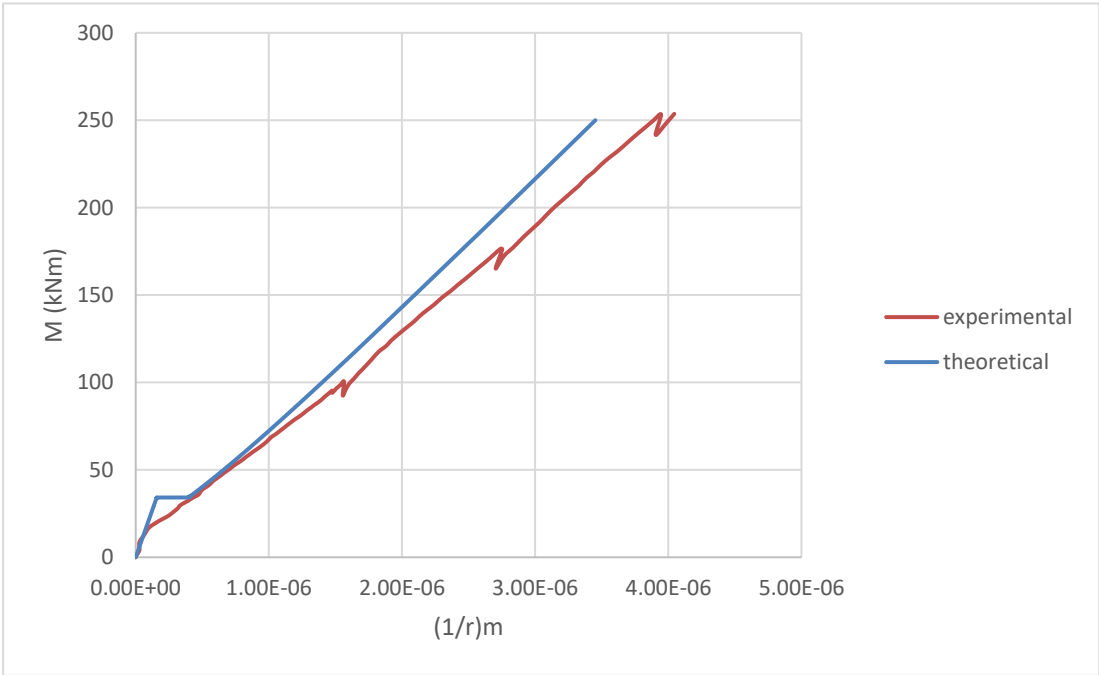


Figure 68. Diagram of the bending moment - mean curvature of beam 2, node C

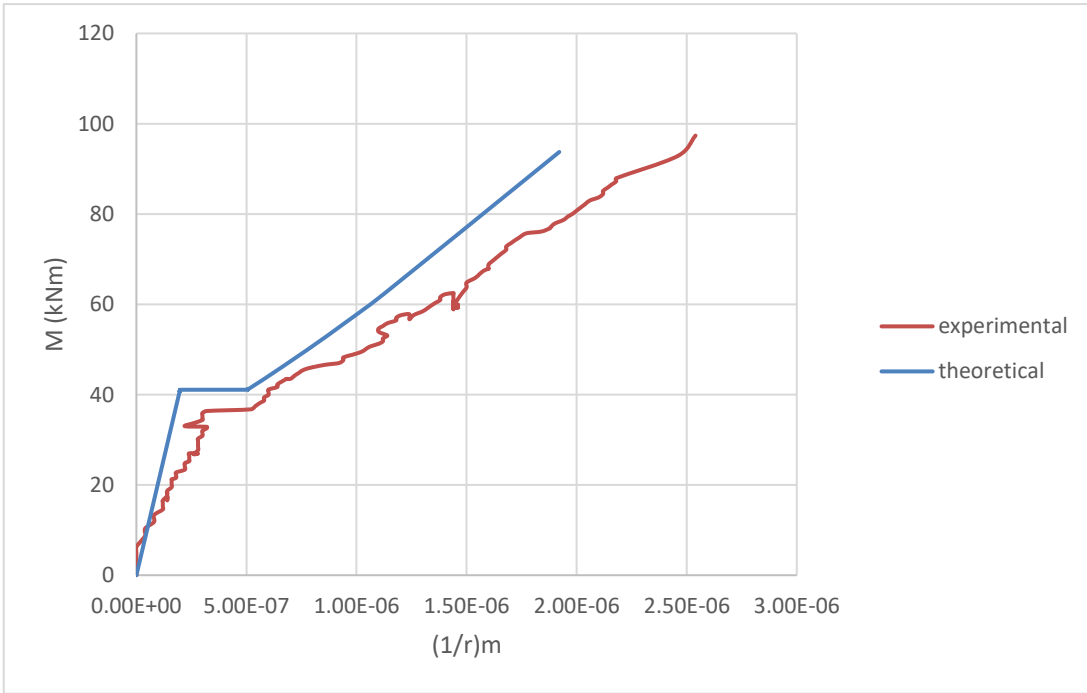


Figure 69. Diagram of the bending moment - mean curvature of beam 3, node A

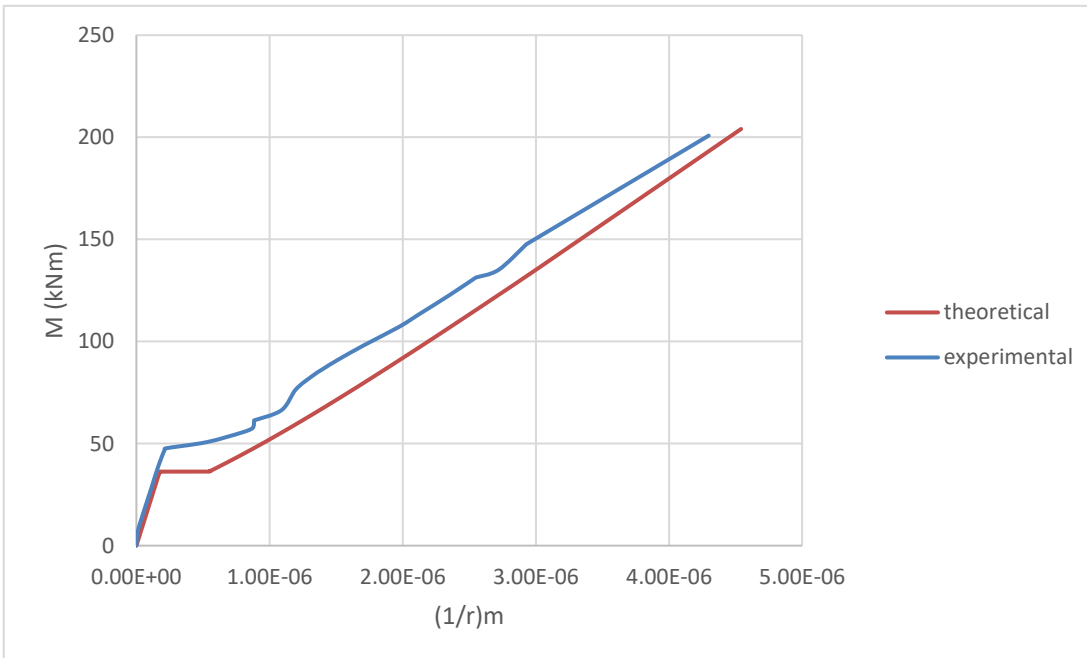


Figure 70. Diagram of the bending moment - mean curvature of beam 5, node C

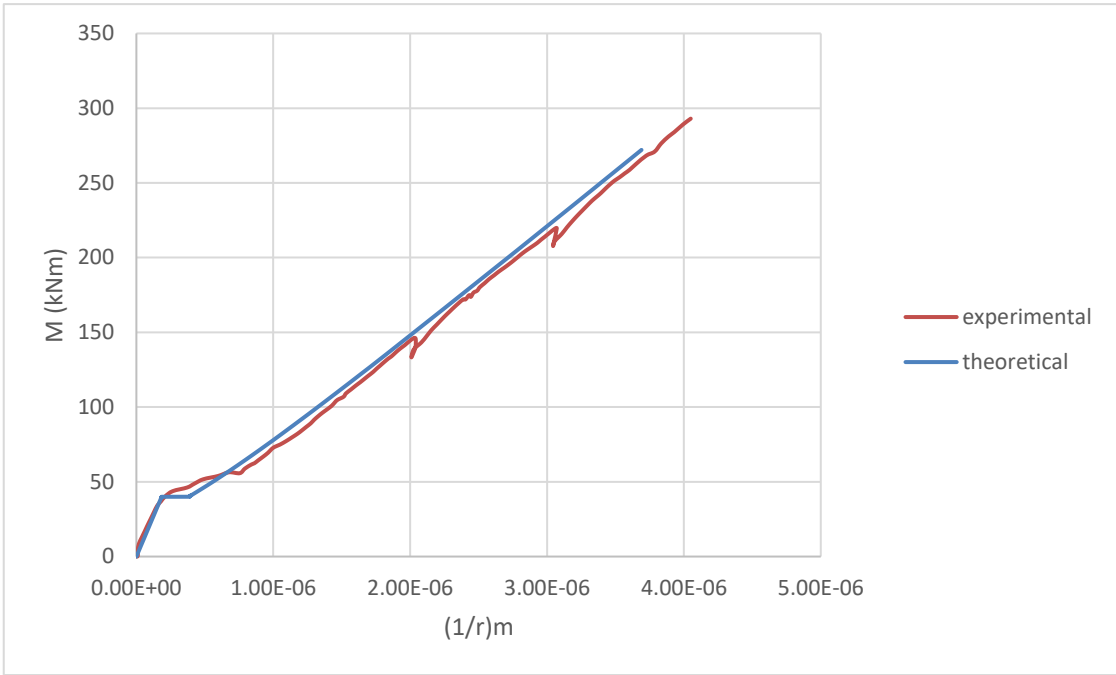


Figure 71. Diagram of the bending moment - mean curvature of beam 6, node C

2.82 Calculation of deflection

The calculation procedure is the same as previously mentioned in chapter 3.52, the difference is only the mean curvature calculated with the theoretical model of CEB – FIP here.

The result of comparison is also similar to others model, which is that the theoretical model behaves well in the condition of low load. As shown in the following figures, the error could be different with the different load condition and number of reinforced bars, but the same point is that the error becomes larger in all cases as the load increases.

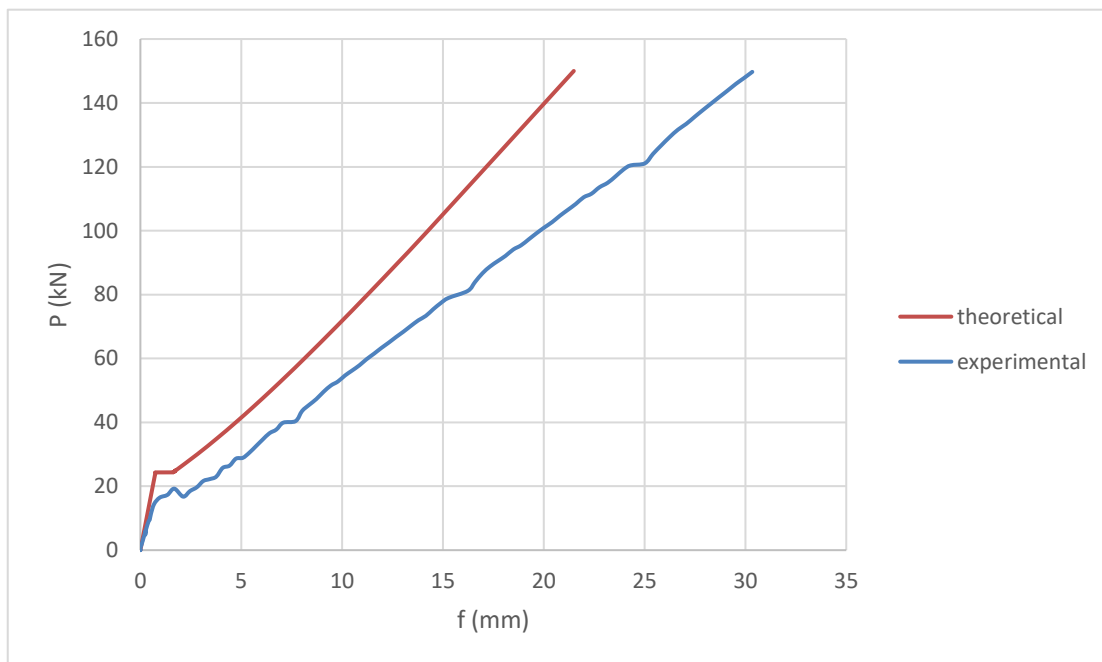


Figure 72. Diagram of load - deflection of beam 1

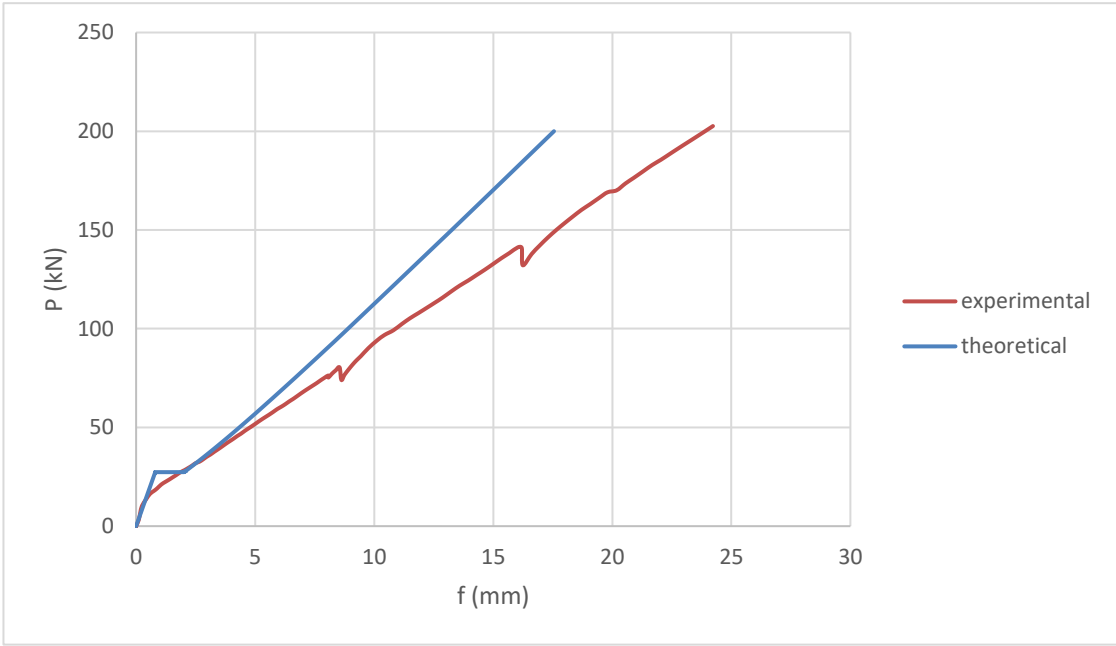


Figure 73. Diagram of load - deflection of beam 2

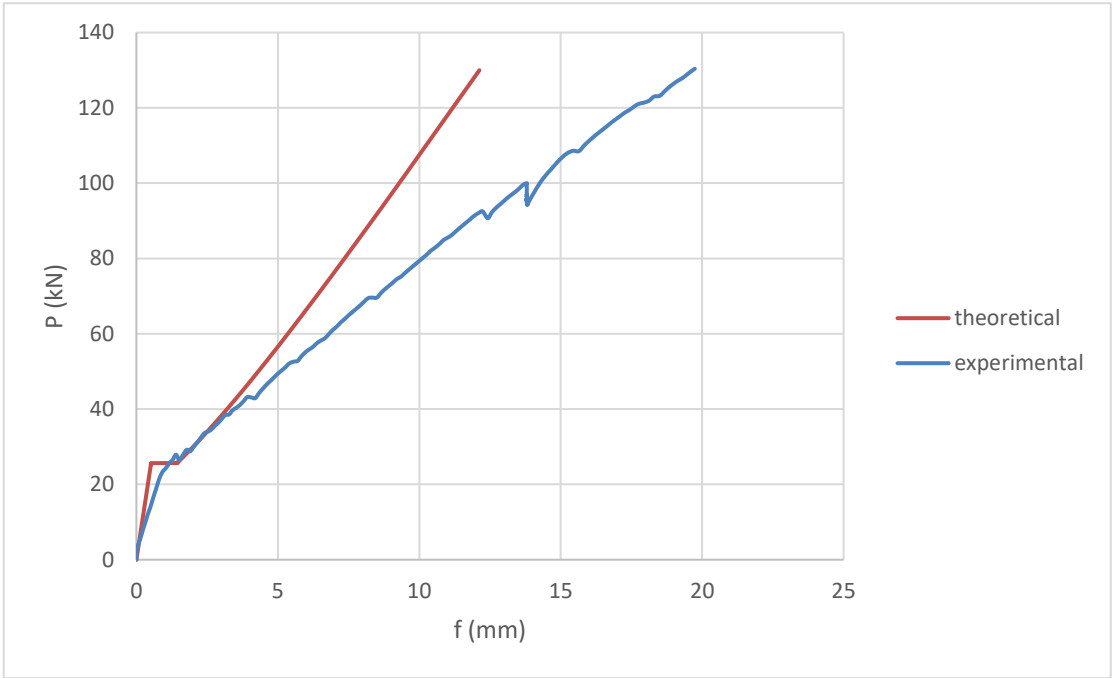


Figure 74. Diagram of load - deflection of beam 3

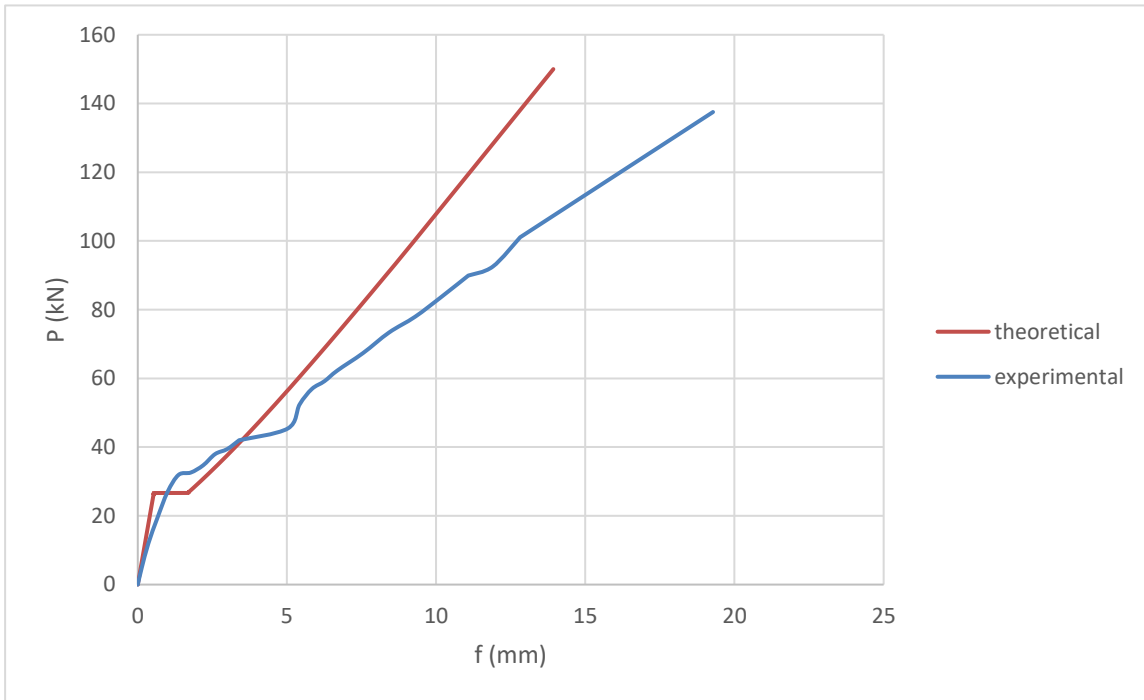


Figure 75. Diagram of load - deflection of beam 5

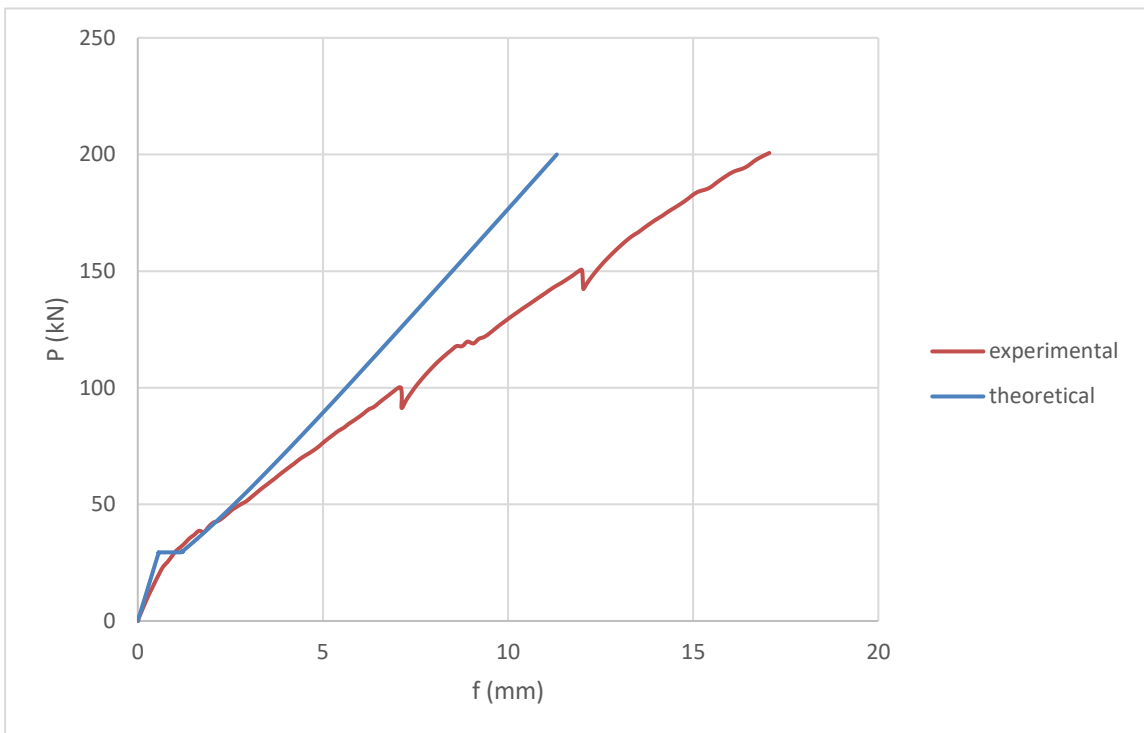


Figure 76. Diagram of load - deflection of beam 6

2.9 Conclusion

In the analysis of mean curvature, the theoretical model of coefficient η and CEB perform well relatively in general. But in the load condition of asymmetric concentrated load, for the beam 5, the two models tend to overestimate the real behavior though the error is not big. But for beam 6, the mean curvature calculated by all models is consistent to the experiment.

While for the deflection, all the results are similar comparing to the experimental data. No matter for different load condition or number of reinforced bars, in state 2, the models are all precise under a certain value of the load. As the load increases, the theoretical values tend to underestimate the behavior of beams, and the gap between the theoretical and experimental data is getting bigger and bigger. One of the important reasons is none of those models above consider the effect of shear. Therefore, in the following chapter discussing the influence of shear is necessary.

3. THEORETICAL MODEL WITH SHEAR EFFECT IN THE DEFORMATION

The shear effect is neglected for many cases while calculating the mean curvature and deflection, as illustrated in the previous chapter. And it is reasonable not only because it is difficult to find a reliable theoretical model, but the complex calculation procedure is also a big barrier. Therefore, many researchers have proposed various theoretical models, all of which have their own advantages and disadvantages. This chapter introduces the simplified model which corresponding to the mixed model proposed by M. Taliano and P.G. Debernardi. The model takes shear effect into consideration and simplifies the calculation procedure of the mixed model.

Mixed model

Traditionally, there are two methods to solve the problem of shear effect, one is the “lattice – like model” proposed by Ritter and Morsch, the other one is “smeared model” offered by Vecchio and Collins.

The lattice – like model assume that the compression truss element is parallel to the crack in the web and the tension truss element which made up of stirrups has an inclination angle of 45 degrees to concrete struts. This model takes some favorable effects into consideration such as aggregate interlock, Dowel effect. Its results are relatively conservative but less precise in the calculation under serviceability condition.

The smeared model is based on the modified compression field theory (MCFT) which considers the average stresses and average strains on equilibrium conditions and compatibility conditions, besides of constitutive laws of concrete. The model treats the cracked concrete with reinforcement as a new material with its own stress – strain characteristics. It can describe the behavior of reinforced concrete beam accurately but with a very complex calculation.

The mixed model is proposed to the basis of experimental results, it can be seen as a modified smeared model. By reference to MCFT, it takes the interaction between the web and chords into account. The model takes the equilibrium scheme based on lattice – like model but with the variability of the inclined angle. In the calculation of concrete contribution, the results obtained are highly consistent with the values provided by the Model Code 1990.

Because there are two iterative procedures corresponding to the mixed model that increased the difficulty of calculation, it is offered the simplified model. Mainly, it is simplified the determinations of inclined angle ϑ and concrete contribution V_c .

Simplified model

In state 1, the behavior of the beam is considered fully keep to the elastic theory, therefore the calculation of curvature is shown as before, and the shear strain calculated by following formula:

$$\gamma = \frac{V}{G * A_{om}} \quad (3.1)$$

Where

G is the shear modulus of concrete.

A_{om} is effective area of the cross section as shown in the following figure.

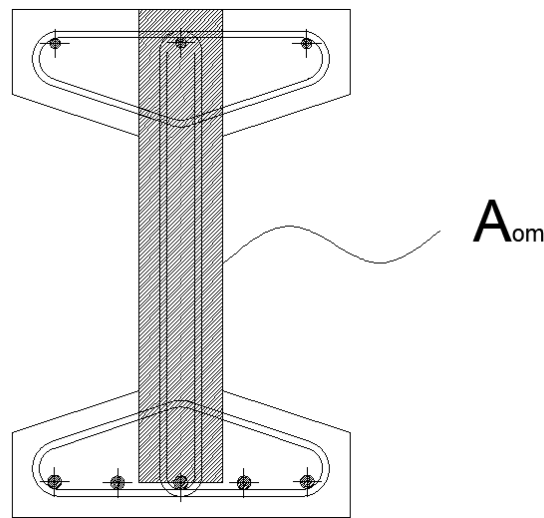


Figure 77. Effective area of the cross section

When the bending moment surpasses its critical value M_{cr} , the cross section cracks because of bending. Under this condition, if the acting shear is smaller than the cracking shear force V_{cr} , it means that the web remains integer and only flange cracks, otherwise, both the web and flange crack.

There is also another situation that needs to pay attention, when the acting shear is greater than V_{cr} with the value of bending moment under M_{cr} , which means the web cracks with an inclined angle but the flange stays intact.

But whenever one of these two conditions is satisfied, it will pass into state 2.

3.1 Mean curvature and shear strain

1. Calculation of concrete contribution V_c .

According to the mixed model, the condition of vertical equilibrium is shown in the following figure.

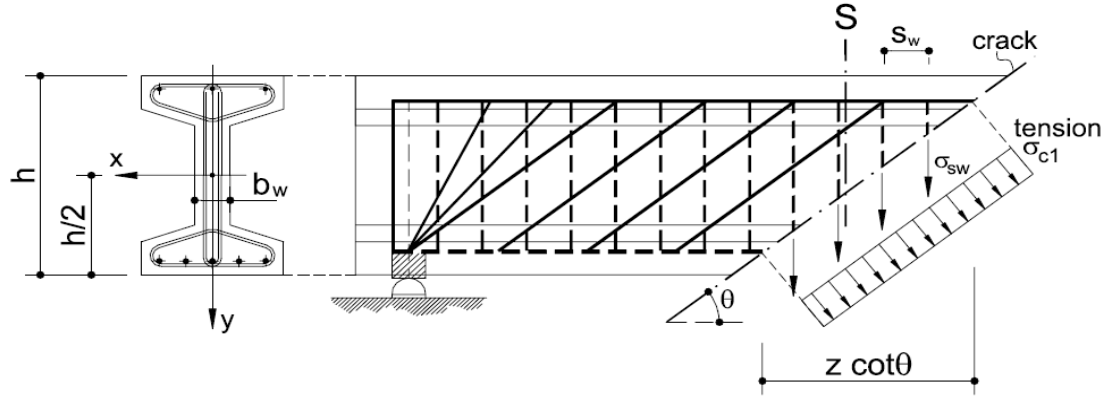


Figure 78. Stress in the cross section inclined θ angle

There are two contributions of resistance in the vertical direction which provided by the concrete and transversal reinforcement respectively.

$$V = V_c + V_{sw} \quad (3.2a)$$

$$V = \frac{A_{sw}}{s_w} * \sigma_{sw} * z * \cot\theta + \sigma_{c1} * b_w * z * \cot\theta \quad (3.2b)$$

In state 1, when there is no crack formed, the concrete contribution offers all shear resistance which means that V_{sw} equals to zero. However, with the load increasing, inclined cracks begin, the concrete contribution remains roughly constant.

Therefore, in the simplified model, it is assumed that the concrete contribution is constant which equals the cracking shear force V_{cr} in state 2. As shown in the following figure, taking beam 6 as an example, comparing the value of V_c calculated by the formula (3.3) and obtained from the mixed model for different shear length.

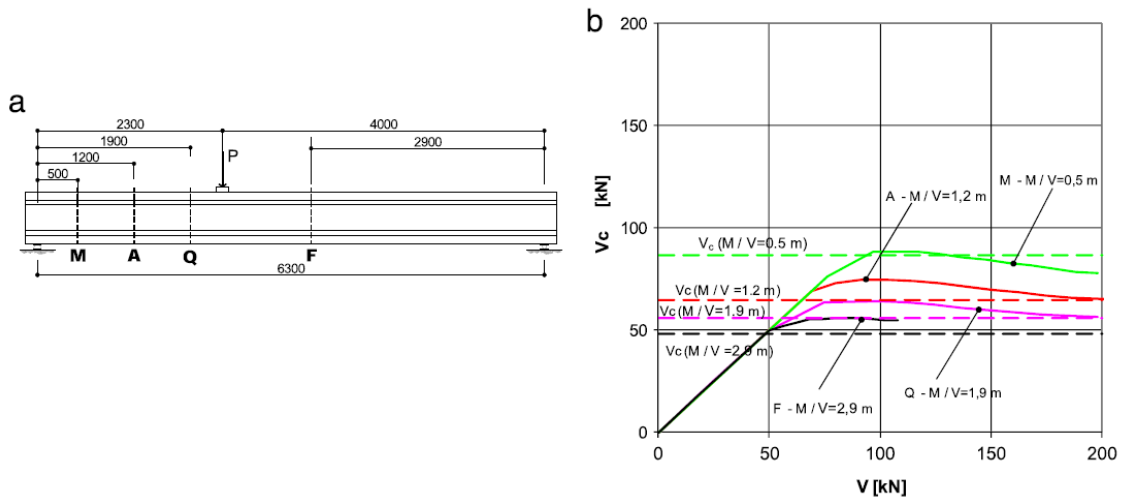


Figure 79. Example of beam 6. (a) geometry. (b) diagram of shear - shear of concrete contribution with various shear lengths

According to the Model Code 1990, the calculation of concrete contribution after web cracking (which takes into account dowel effect, aggregate interlock and the contribution of the compressed concrete zone) is expressed as:

$$V_c \cong C * \left(\frac{3*d}{M/V} \right)^{1/3} * \left(1 + \sqrt{\frac{200}{d}} \right) * \left(\frac{100*A_s}{b_w*d} * |f_{ck}| \right)^{1/3} * \frac{b_w*d}{1000} \leq \frac{J_{x,1}*b_w}{S_x} * f_{ctm} \quad (3.3)$$

Where

C is a coefficient that varies with reference to the mean value of V_c between 0.13 and 0.18 when a_v/d varies from 4 to 8. According to Model Code 1990, it is assumed as 0.15.

d is the depth of the cross section.

A_s is the area of the longitudinal tensile reinforcement.

b_w is the width of the web.

$J_{x,1}$ is the second moment of area in uncracked state.

S_x is the first moment of area above and about the centroidal axis (uncracked section).

a_v is the shear length which corresponding to the distance between load point and support, and it equals M/V .

2. Calculation of normalized shear stress τ/f_{ctm} .

$$\frac{\tau}{f_{ctm}} = \frac{V_{tot} - V_c}{b_w * d * f_{ctm}} \quad (3.4)$$

It is easy to know that the ratio is zero when the cross section of the web is uncracked.

3. The calculation of angle θ .

The angle θ is the second calculation that needs to be simplified. It is related to a lot of parameters in the mixed model such as geometrical properties, loading effect, reinforcement ratios, material, therefore it is carried out a parametric analysis to study the relationship between the angle and these variables. Then finding out that the angle θ is a function of these four variables: ε_{cz} , τ/f_{ctm} , ρ_w , f_{ck} .

1) The approximate relation between normalized shear stress and angle θ_0 .

$$\theta_0 = a * \left(\frac{\tau}{f_{ctm}} \right)^b \quad (3.5)$$

The coefficient a and b are introduced by parameter analysis, and they are a function of transversal reinforcement ratio ρ_w . Where

$$a = 30 + \rho_w * 1150 \quad (3.6a)$$

$$b = 5 * \rho_w - 0.125 \quad (3.6b)$$

2) Calculation of angle θ'_0 , which corresponds to the correction of θ_0 when the concrete compressive strength f_{ck} is different to 25 N/mm².

$$\theta'_0 = \theta_0 * \left[1 + 0.1 * \left(\frac{f_{ck} - 25}{25} \right) \right] \quad (3.7)$$

4. Calculation tensile strain of steel bars in the cracked state.

$$\varepsilon_{s2} = \left\{ M_{tot} + \frac{V_{tot} - V_c}{2} * z * \cot(\theta'_0) \right\} * \frac{d - \chi}{J_{x,2} * E_s} * \alpha_e \quad (3.8)$$

5. Calculation of the mean strain of tensed reinforcement with considering the tension – stiffening effect according to EN1992 1-1.

$$\varepsilon_{sm} = \varepsilon_{s2} - k_t \frac{f_{ctm}}{\rho_{p,eff} E_s} \quad (3.9)$$

6. Calculating the mean strain of compressed chord with assuming the lever arm equals 0.9*d.

$$\varepsilon_{cm} = - \left\{ M_{tot} - \frac{V_{tot} - V_c}{2} * z * \cot(\theta'_0) \right\} * \frac{\chi - 0.1d}{J_{x,2} * E_{cm}} \quad (3.10)$$

7. Calculation of mean axial strain ϵ_{cz} .

$$\epsilon_{cz} = \frac{\epsilon_{sm} + \epsilon_{cm}}{2} \quad (3.11)$$

8. The correction of angle due to possibly varying mean axial strain ϵ_{cz} .

$$\theta = \theta'_0 * \psi \quad (3.12)$$

Where

$$\psi = 0.64 + (960 * \epsilon_{cz}) - (6 * 10^5 * \epsilon_{cz}^2) \quad (3.13)$$

9. Calculation of principal mean compressive strain in the web.

$$\epsilon_{c2} = \frac{\sigma_{c2}}{E_{cm}} = \frac{1}{E_{cm}} * \frac{V_c * \sin^2(\theta) - V}{z * b_w * \cos(\theta)} \quad (3.14)$$

10. Calculation of mean curvature and mean shear strain.

$$\frac{1}{r} = \frac{\epsilon_{sm} - \epsilon_{cm}}{0.9 * d} \quad (3.15)$$

$$\gamma = \frac{2 * (\epsilon_{cz} - \epsilon_{c2})}{\tan(\theta)} \quad (3.16)$$

11. Removing the self – weight effect, and plotting the diagram of bending moment – mean curvature and shear – shear strain.

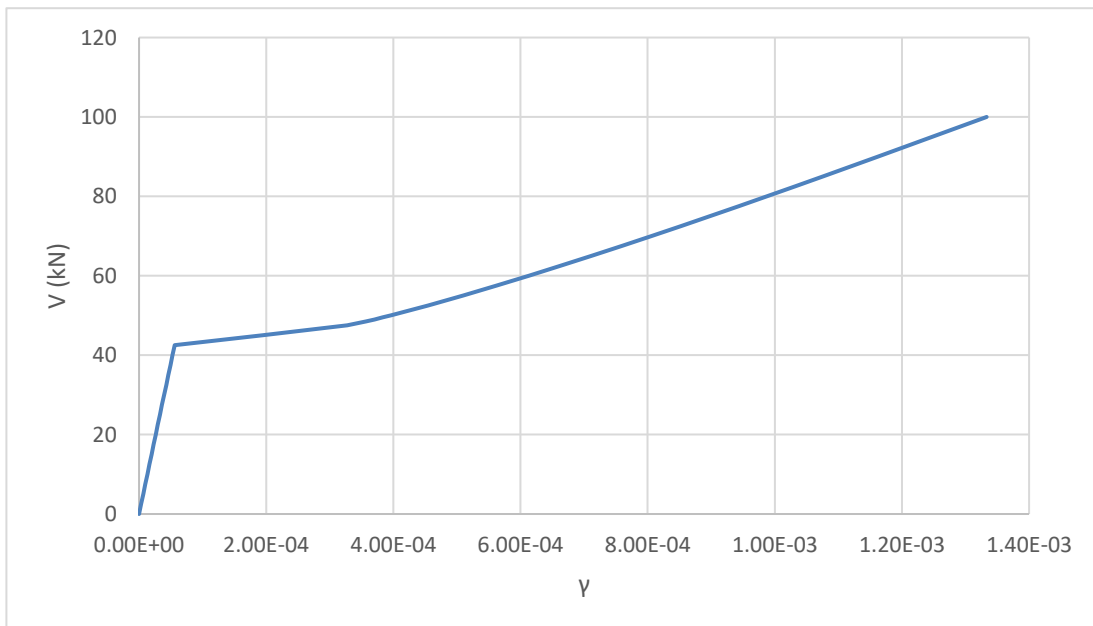


Figure 80. Diagram of shear – shear strain of beam 1,node A

12. Comparison of the calculation of mean curvature with experimental data.

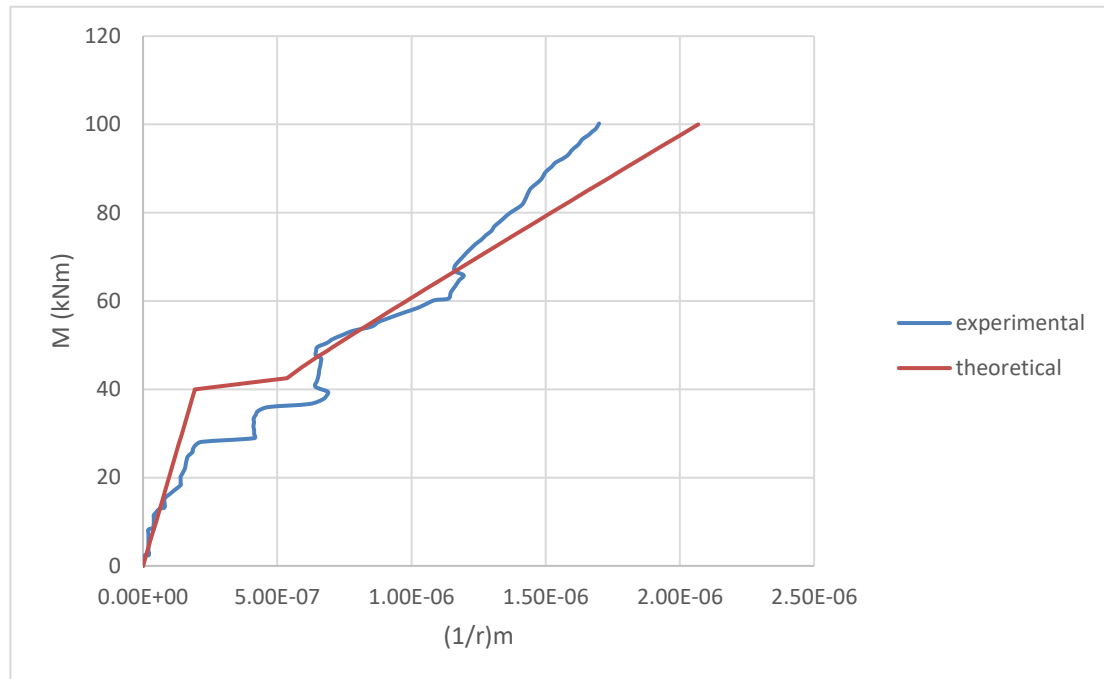


Figure 81. Diagram of bending moment - curvature of beam 1, node A

As shown in the two figures above, figure 80 illustrates the relationship of shear and shear strain of beam 1 in node A, while the figure 81 shows the comparison of theoretical value and experimental value. It is possible to observe that the shear strain is relatively small in the uncracked state, but after the section cracked, the shear strain rises very fast as the shear increases. Moreover, the result of comparison does not verify the accuracy of the theoretical model, it can be seen from figure 81, the theoretical values are much smaller than the experiment at around cracking bending moment, but after that, the theoretical curve rises faster. So that when the bending moment reaches 100kNm, the theoretical mean curvature exceeds 1.2 times the actual value.

If compares the “simplified model” with a classical model mentioned before, the shear contribution can be observed in the calculation of mean curvature as shown in the following figure. Due to the increase of the mean strain of tension chord and decrease of the mean strain of the compression chord by shear, the mean curvature increases.

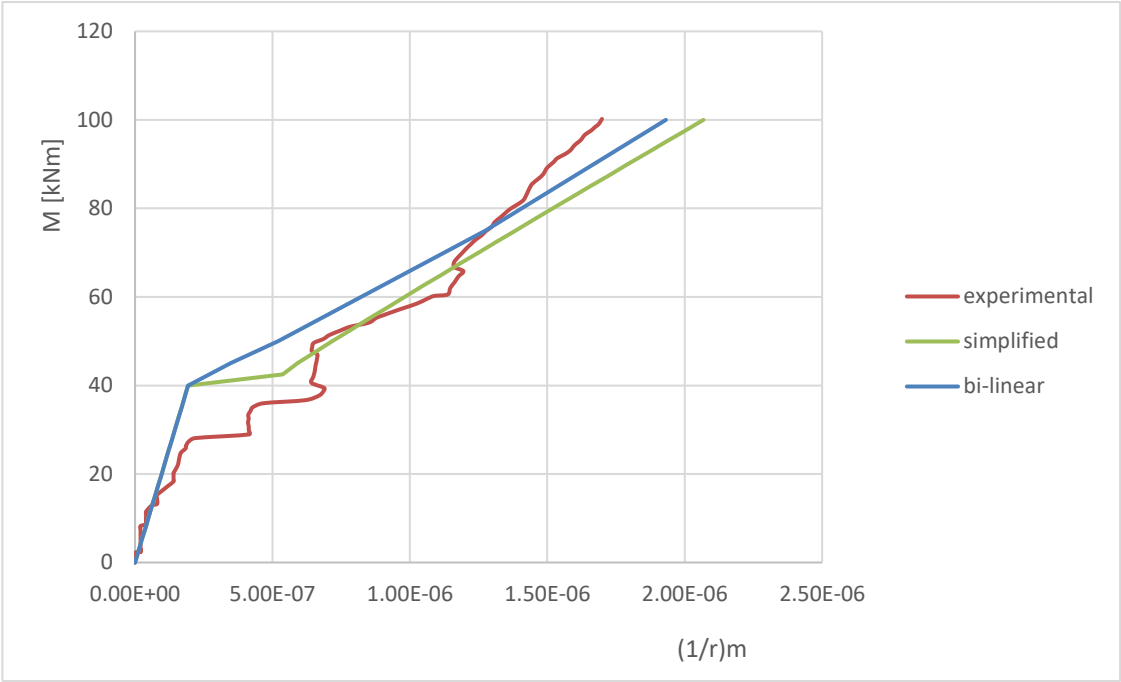


Figure 82. Comparison between simplified model and bi-linear method with experimental curve

The following figures illustrate diagrams of shear and shear strain and comparison of theoretical mean curvature and experimental data of other beams. It can be seen from following figures, as the bending moment increases, the theoretical mean curvature is always smaller than the experimental value, the consideration of shear effect does improve the result of calculation, but not much comparing to the classical model.

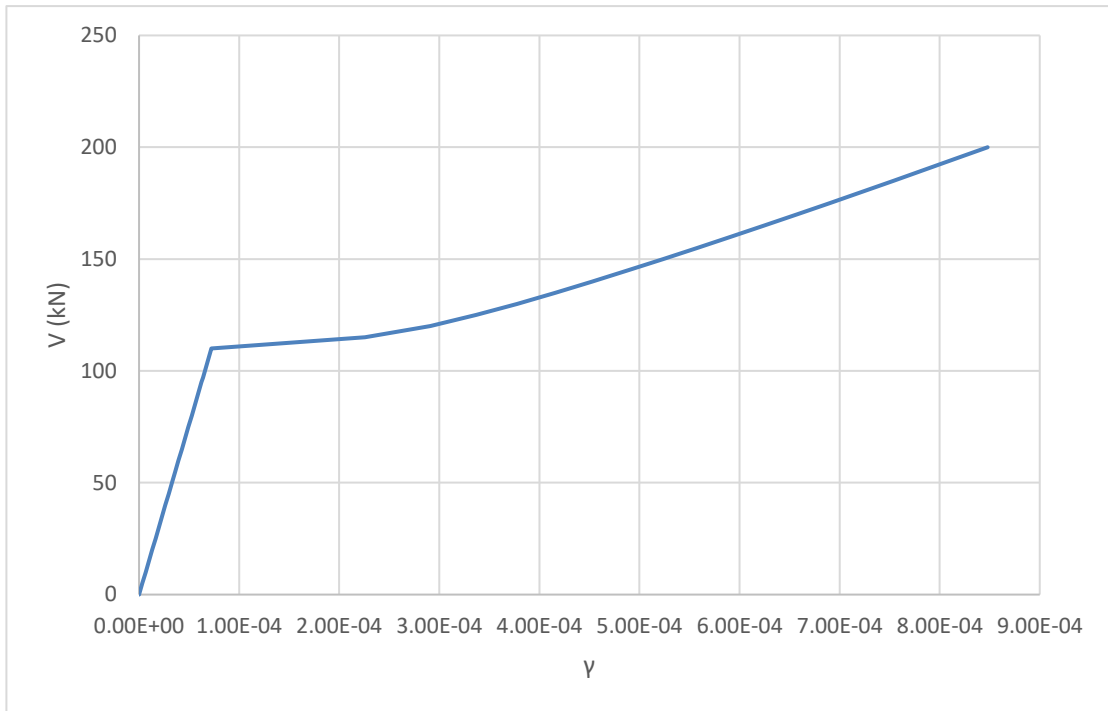


Figure 83. Diagram of shear - shear strain of beam 2, node A

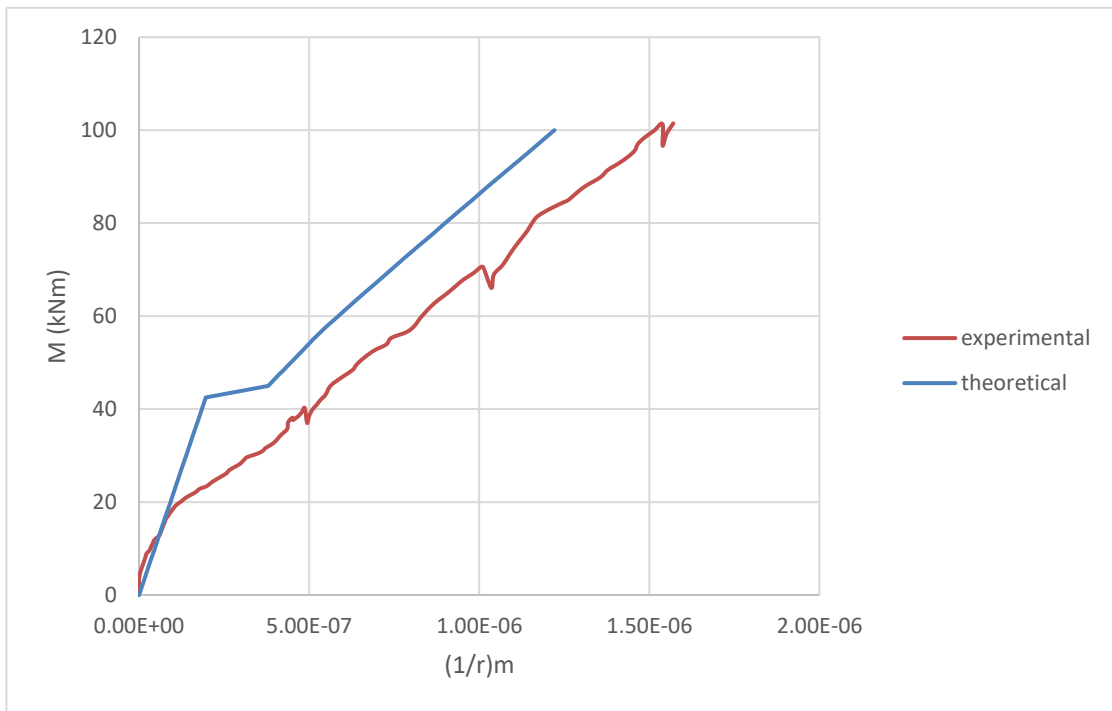


Figure 84. Diagram of bending moment - mean curvature of beam 2, node A

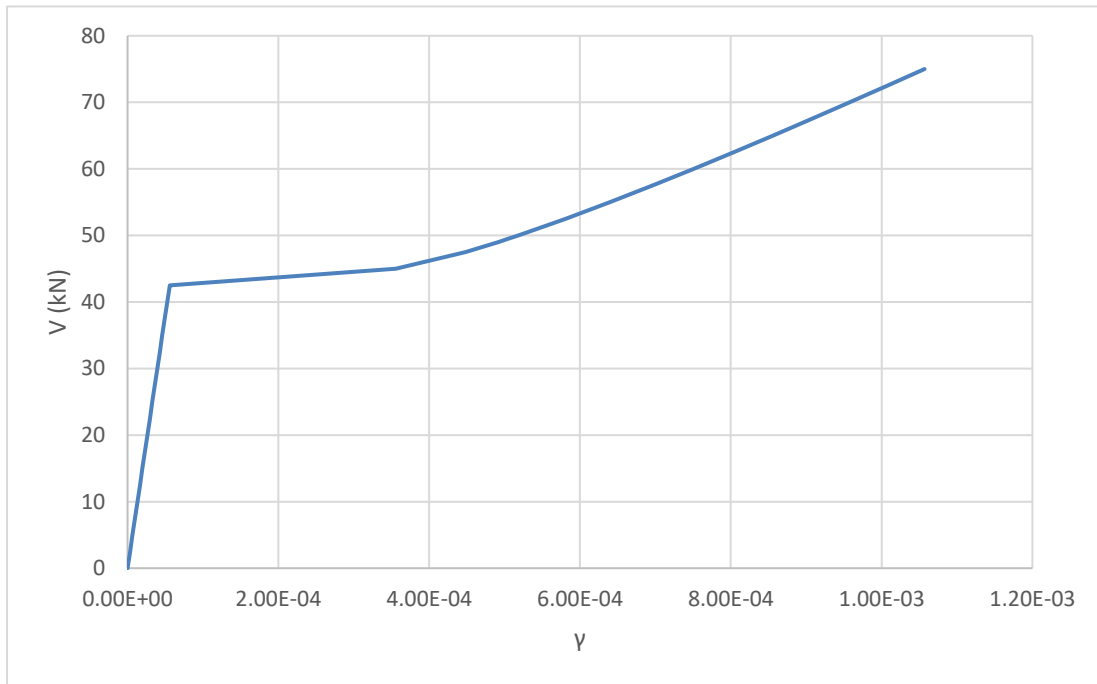


Figure 85. Diagram of shear - shear strain of beam 3, node A

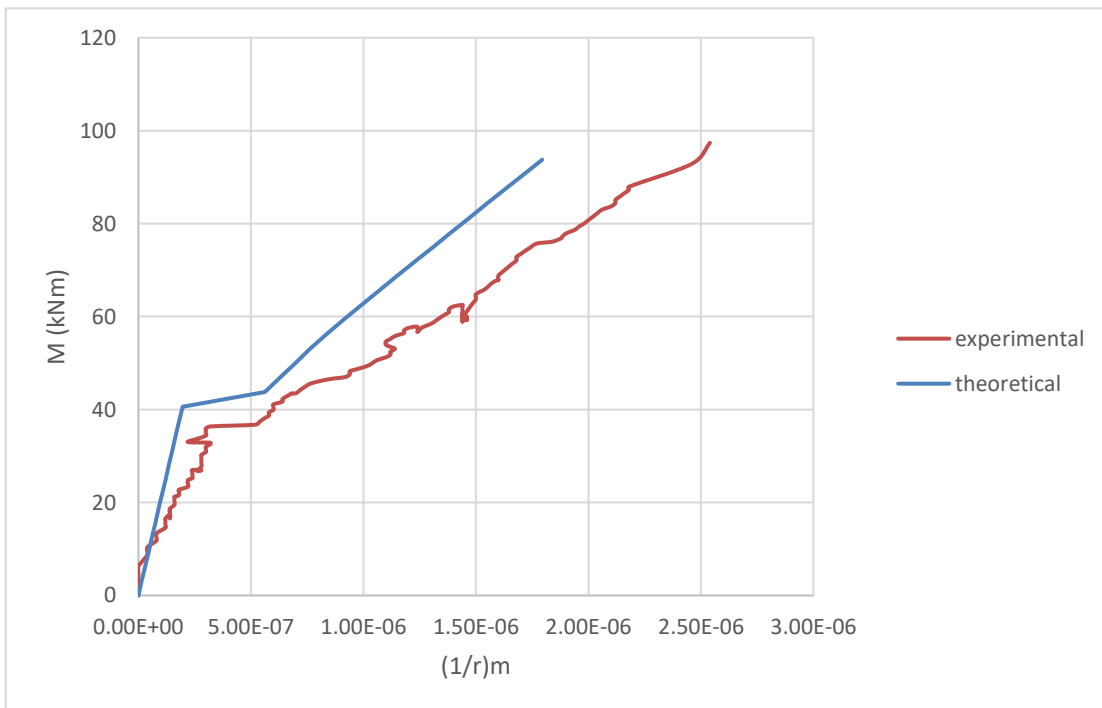


Figure 86. Diagram of bending moment - mean curvature of beam 3, node A

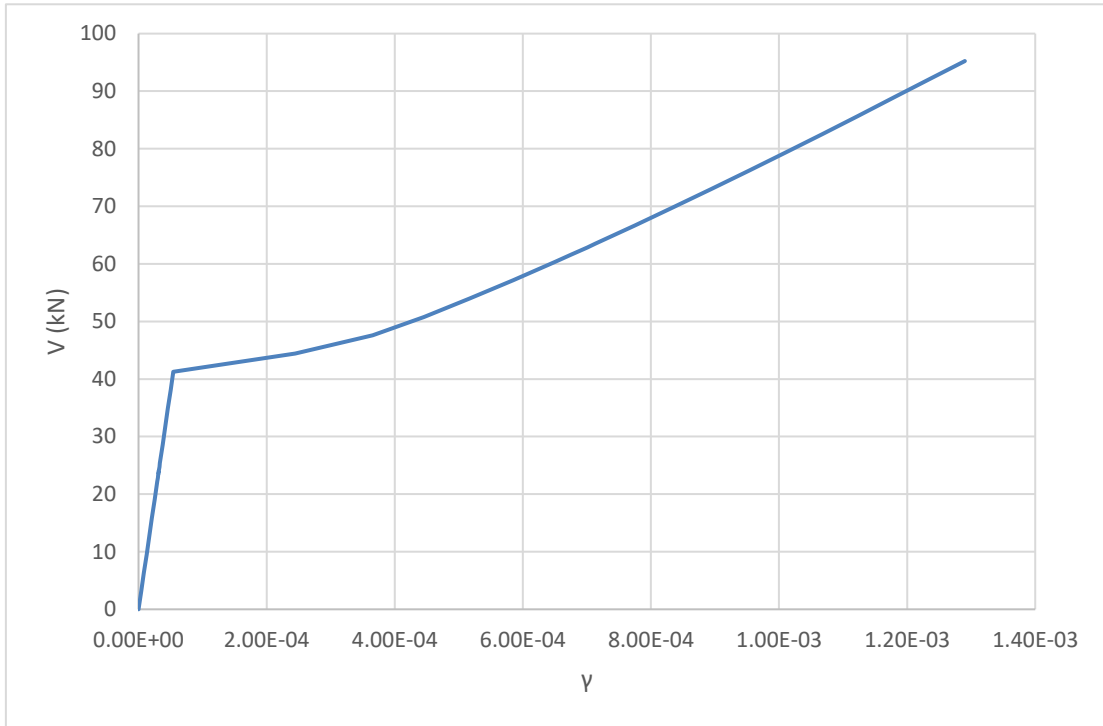


Figure 87. Diagram of shear - shear strain of beam 5, node A

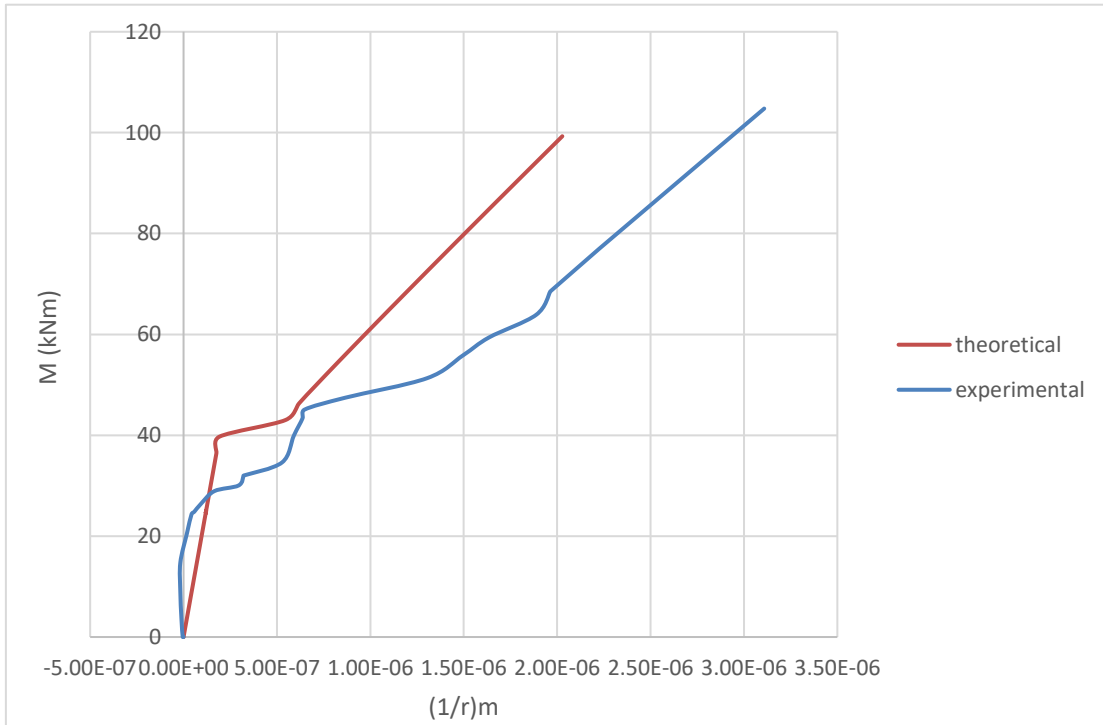


Figure 88. Diagram of bending moment - mean curvature of beam 5, node A

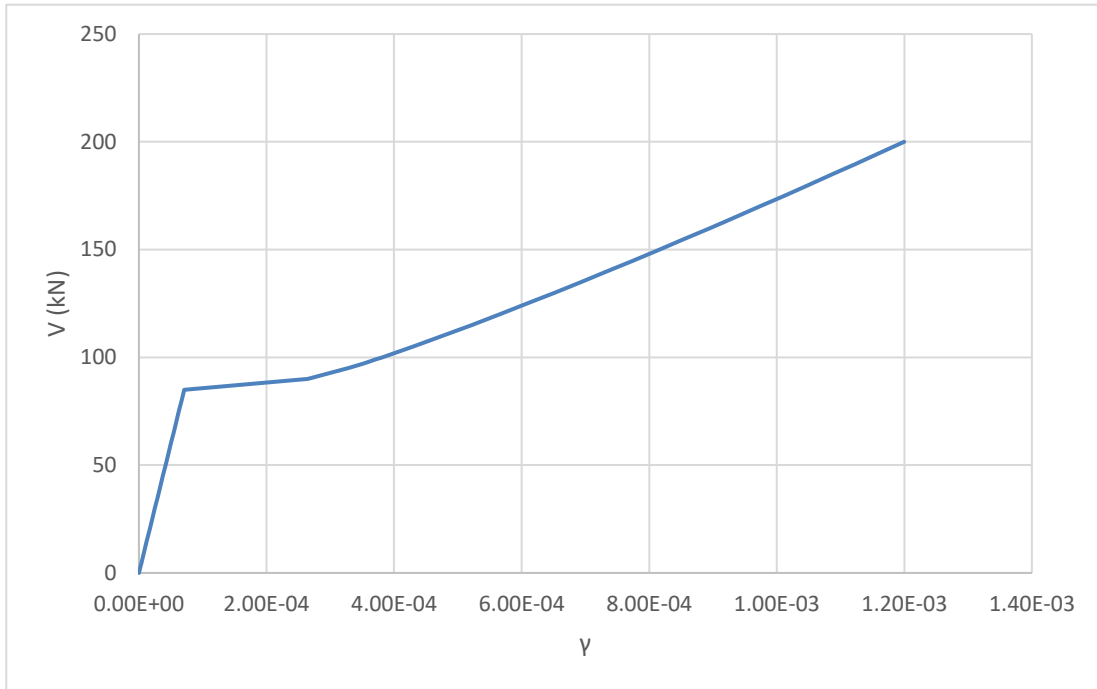


Figure 89. Diagram of shear - shear strain of beam 6, node A

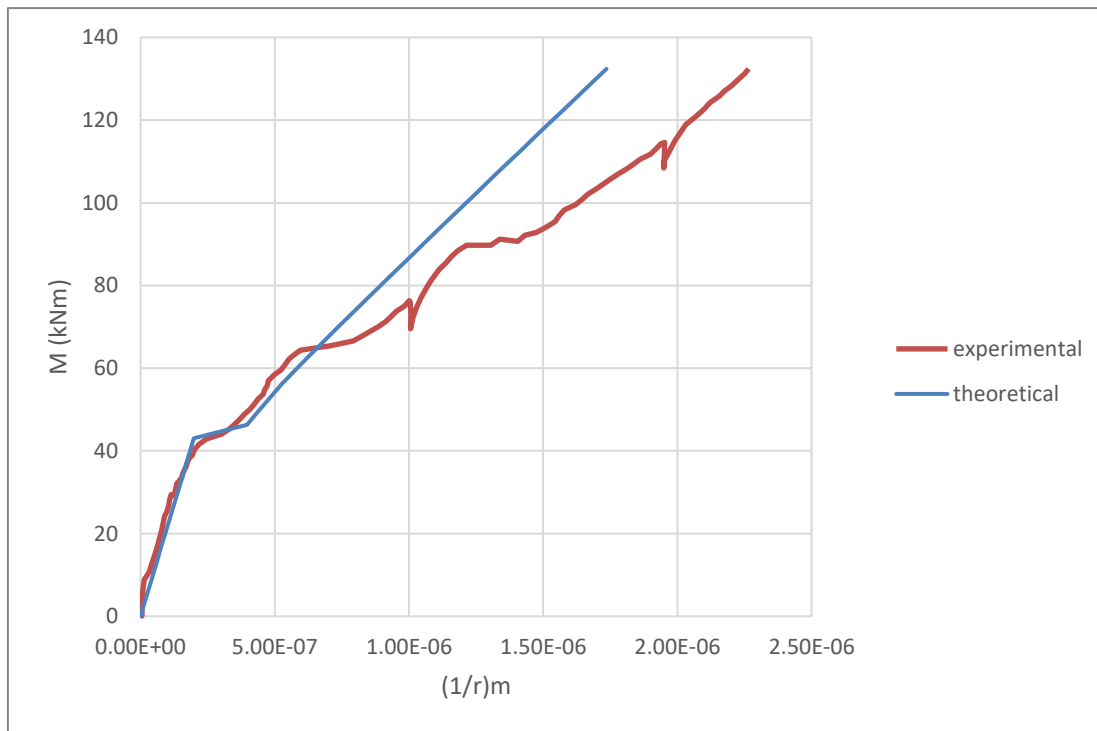


Figure 90. Diagram of bending moment - mean curvature of beam 6, node A

3.2 Calculation of the deflection

As mentioned in the chapter 3, the calculation of deflection is based on the principle of virtual work, here with considering shear effect, there are two contributions in the calculation. Hence the formula becomes:

$$f = \int_0^L M_a * \frac{1}{r_b} dz + \int_0^L t * V_a * \gamma dz \tag{3.17}$$

Where

t is shear factor, in the case of double T beam with thin web t=1.60.

The calculation procedure is similar as before, except the involvement of shear. Therefore, through the previous calculation, calculating the mean curvature and shear strain for every piece of element. Then it can be obtained the contribution of bending moment and shear to the deflection by following formulas:

$$f_M = \sum M_a * \frac{1}{r_b} * L_i \tag{3.18a}$$

$$f_V = \sum t * V_a * \gamma * L_i \tag{3.18b}$$

$$f_{tot} = f_M + f_V \tag{3.18c}$$

For example, the following figures illustrate the bending moment and shear in real system and virtual system of beam 1.

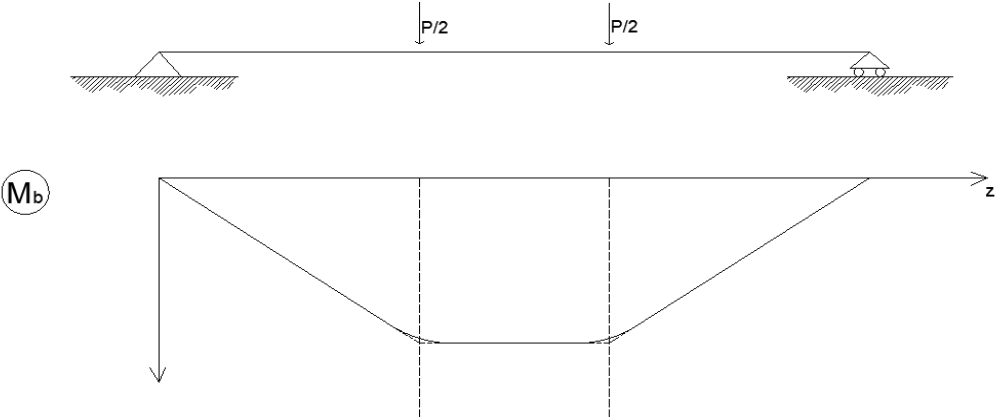


Figure 91. The bending moment of beam 1 in real system

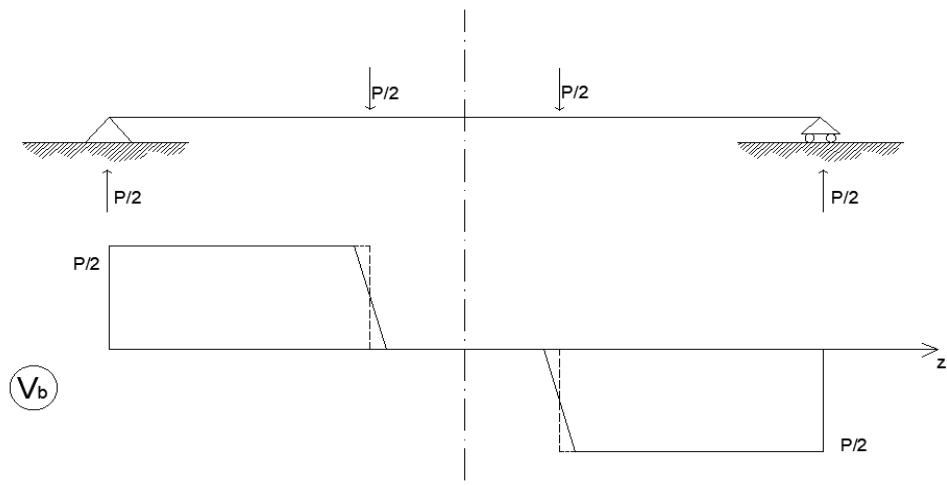


Figure 92. The shear of beam 1 in real system

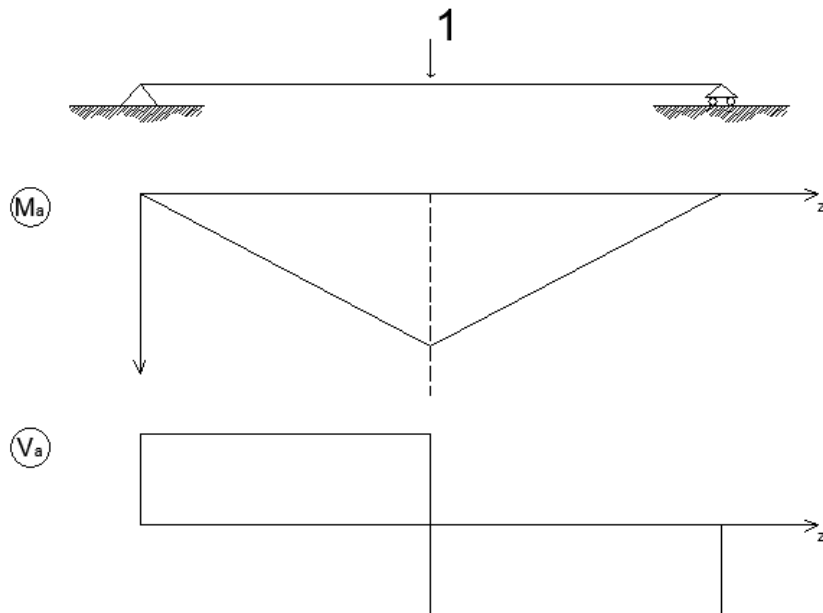


Figure 93. Bending moment and shear of beam 1 in virtual system

In the end, removing the effect of self – weight and plotting the diagram of load and deflection which includes the contribution of bending moment and shear, besides the total deflection.

For other beams, the calculation is exactly the same as above, except for the change of load conditions.

The shear contribution can be considered in two part. One part is the shear strain part, as you can see from the figures. The other part is in the bending deflection, due to the shear increases the mean curvature, which means it increases the bending deflection indirectly. The following two figures show the comparison of theoretical value of total deflection and experimental curve of beam 1 and 2. It is possible to observe that the contribution of shear and bending moment in the total deflection. In the condition of under a certain value of the load, the shear deflection is so small that can be ignored, but as load increases, the shear contribution is getting bigger. For beam 1, the shear contribution takes around 20% when the load reaches 150kN.

Comparing the total deflection with the experimental value, taking the shear effect into consideration significantly improves the accuracy of the description of the behavior of the r.c. beam. When the load ups to 200kN, the addition of shear deflection reduces the error from 27% to 9% for beam 2.

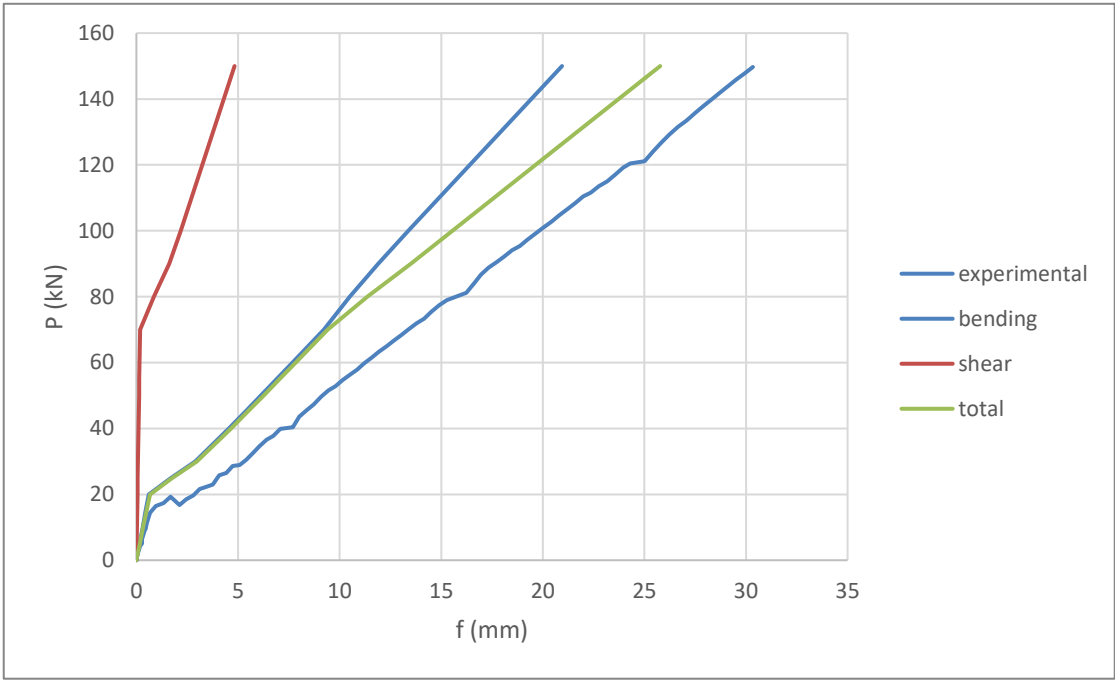


Figure 94. Diagram of load - deflection of beam 1

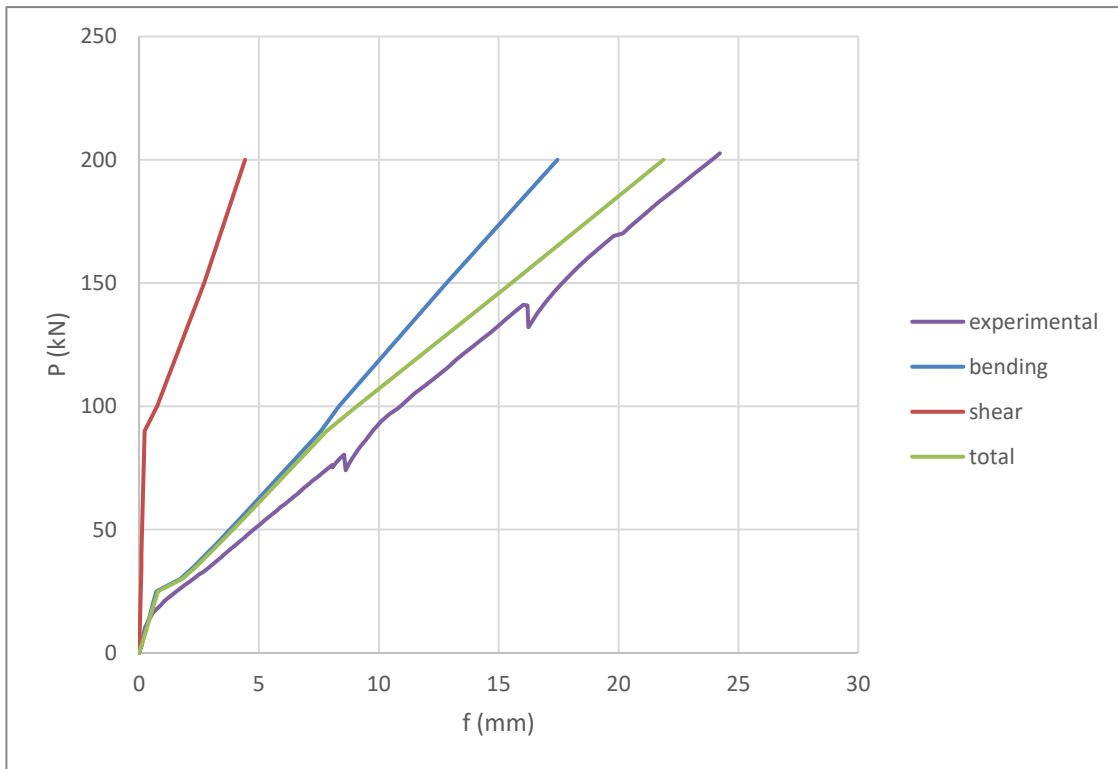


Figure 95. Diagram of load - deflection of beam 2

As shown in the figure 96, for beam 3, the contribution of shear to total deflection is around 30% when the load ups to 130kN.

The figure 97 and 98 illustrate the comparison of the theoretical deflection and experiment data of beam 5 and 6, which also prove the importance of the shear contribution to the total deflection. Especially, the theoretical model of beam 6 is perfectly consistent with its experimental curve.

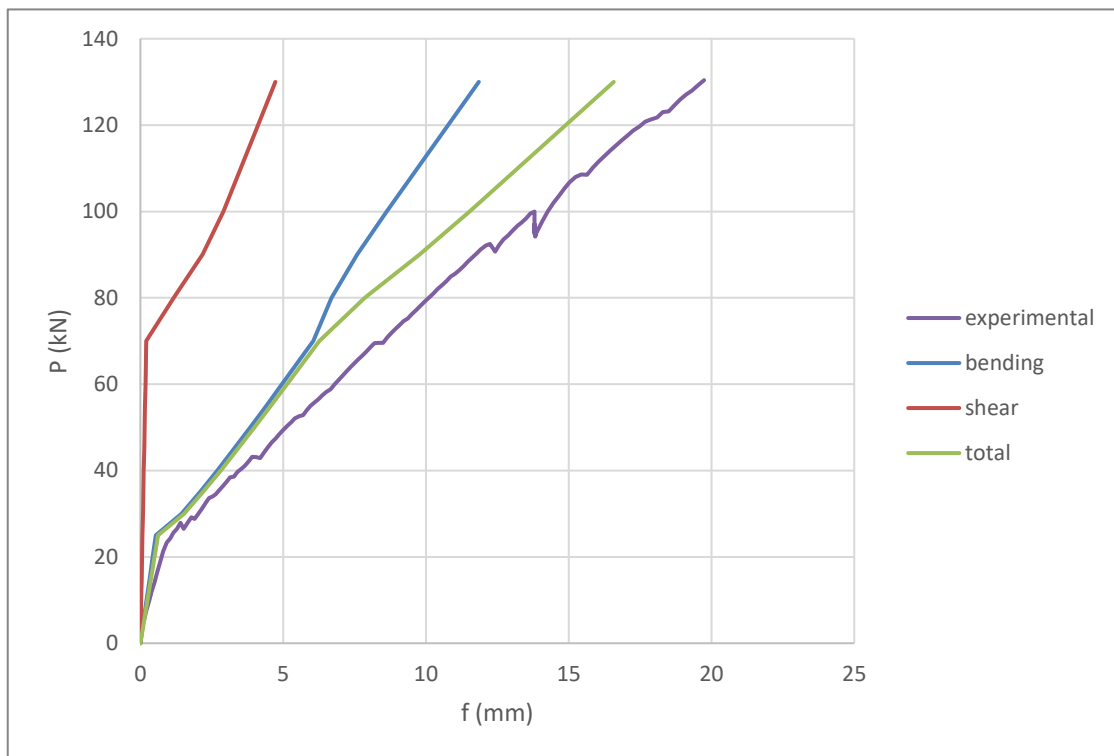


Figure 96. Diagram of load - deflection of beam 3

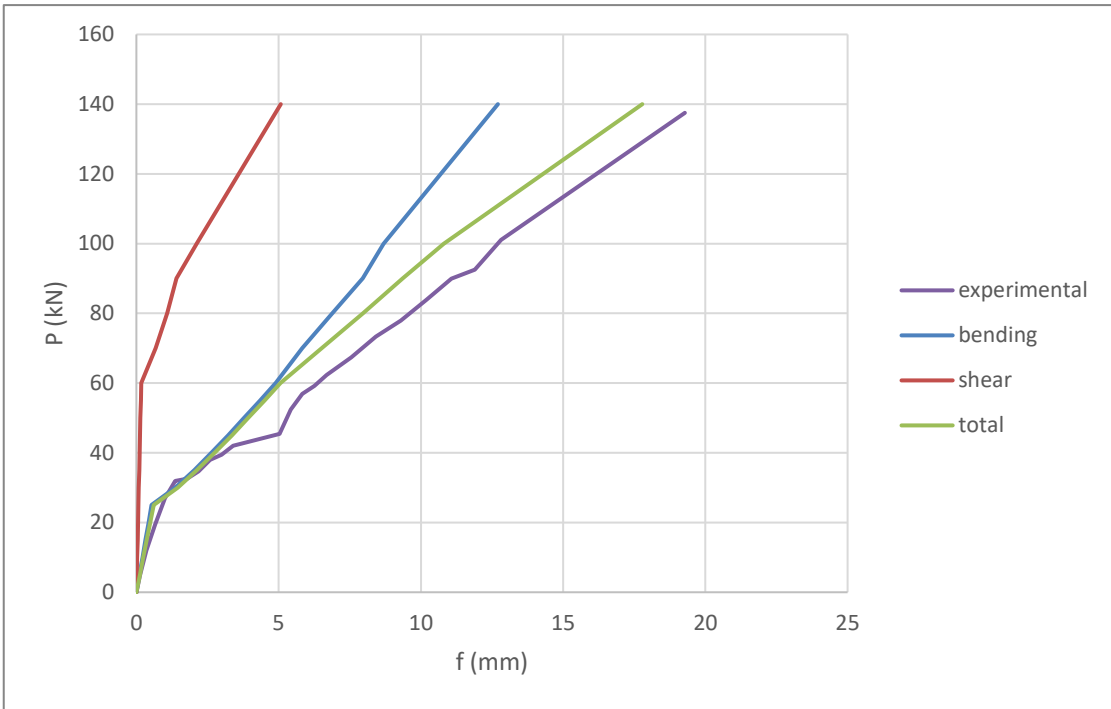


Figure 97. Diagram of load - deflection of beam 5

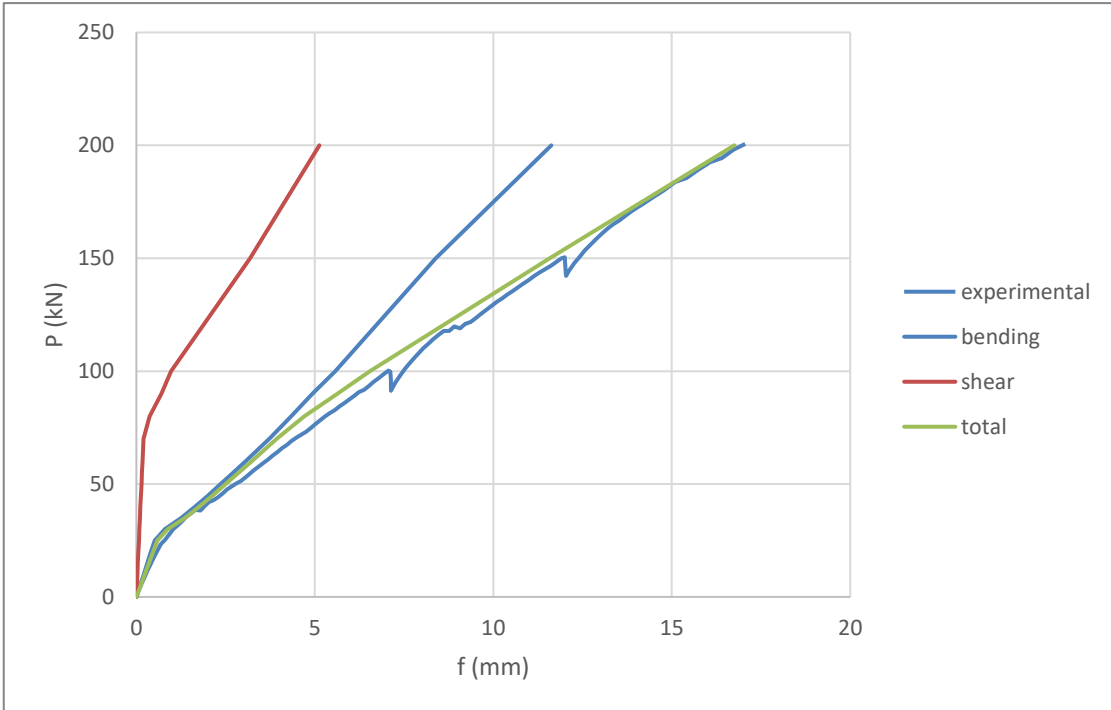


Figure 98. Diagram of load - deflection of beam 6

4. CONCLUSIONS

This thesis mainly evaluates the behavior of reinforced concrete beams with thin web in two aspects, one of which is mean curvature, and the other one is deflection. The load conditions are set up with three types including two symmetric concentrated load, single concentrated load at the central node, and single asymmetric concentrated load. It compares several theoretical models with experimental data to identify the accuracy of the theoretical models and the influence of shear effect.

In the analysis of mean curvature, according to the elastic modulus, two analysis methods are proposed, one is linear analysis method based on the assumption of constant elastic modulus, while the other one is non – linear analysis method, in which removed the assumption. The results of comparison between these two methods with experimental values do not have much difference, although the calculation of non – linear analysis method is more complex than the linear method. Then according to the various tension – stiffening effect, the bi – linear method, method with coefficient η and CEB model are taken into analysis. These methods do improve the calculational accuracy of the mean curvature, but the degree of improvement varies depending on the amount of reinforcement and the position of reference node.

While in the analysis of deflection, for every theoretical model mentioned before, the calculation is on the basis of the virtual work's principle. The results fluctuate slightly due to the variety of values of mean curvature. Compared with experimental values, it is possible to observe that under a certain value of load condition, the calculations are precise relatively. However, when the load exceeds the certain value, the theoretical values are smaller than the experimental values, and the gap between the theoretical curve and experimental curve becomes larger and larger.

Form the previous analysis, it can be seen that the shear effect is not negligible in the considered cases. Therefore, the mixed model has been set up, which is based on the modified compression field theory. However, due to the complexity of its calculation, the simplified model has been proposed to avoid the iterative calculation procedure. The shear effect makes the strain of tension chord increase but decreases the strain of compression chord. Therefore, it increases the value of mean curvature, but comparing with traditional theoretical models to the experimental data, it doesn't have much improvement in calculation results. While for the deflection, through the comparison of theoretical calculation and experimental values, it is

observed that the contribution of shear to total deflection it is obvious that the shear effect has a significant improvement to the description of the real behavior of reinforced concrete beams. In the three mentioned load conditions, the shear contribution is greater than 20% to the total deflection.

NOTATION

| | |
|-------------------|---|
| $(1/r)_m$ | Mean curvature |
| $1/r_1$ | Curvature in state 1 |
| $1/r_{1r}$ | Curvature corresponding to cracking bending moment in state 1 |
| $1/r_2$ | Curvature in state 2 |
| $1/r_{2r}$ | Curvature corresponding to cracking bending moment in state 2 |
| $1/r_{ts}$ | Curvature of tension – stiffening |
| A_{om} | Homogenized area |
| $A_{s,inf}$ | Area of longitudinal tensile reinforcement; |
| $A_{s,sup}$ | Area of longitudinal compressive reinforcement; |
| A_{sw} | Shear reinforcement area |
| a_v | Shear length |
| b_w | Width of the web |
| d | Effective height of cross section |
| E_{cm} | Mean value of elastic modulus of concrete |
| E_s | Elastic modulus of steel bars |
| f | Deflection |
| f_1 | Deflection in state 1 |
| f_2 | Deflection in state 2 |
| $f_{ck,cube}$ | Characteristic compressive cube strength |
| $f_{ck,cylinder}$ | Characteristic compressive cylinder strength |
| f_{cm} | Mean compressive strength of concrete |
| F_{cr} | Cracking force |
| f_{ctm} | Mean value of tensile strength of concrete |
| G | Shear modulus |
| $I_{om,1}$ | Moment of inertia homogenized in state 1 |
| $I_{om,2}$ | Moment of inertia homogenized in state 2 |
| l_{sc} | Length of reduced bond |
| L_s | Transmission length |
| M_b | Bending moment due to load |
| $M_{b,pp}$ | Bending moment due to self – weight |

| | |
|-----------------|---|
| M_{cr} | Cracking bending moment |
| M_u | The ultimate bending moment |
| M_y | The bending moment of yielding of tensed bars |
| M_{yd} | Yielding moment |
| s_w | Spacing of shear reinforcement |
| V_c | Shear of concrete contribution |
| V_{cr} | Cracking shear |
| V_{sw} | Shear of stirrups contribution |
| y | Vertical axis at reference system |
| z | Horizontal axis of the reference system |
| α_e | Ratio of modulus |
| γ | Mean shear strain |
| ϵ_c | Strain in compression chord |
| ϵ_{c1} | The strain at the peak stress |
| ϵ_{c2} | Principal mean compressive strain |
| ϵ_{cm} | Mean strain in compression chord |
| ϵ_{cz} | Mean axial strain |
| ϵ_{s2} | Steel strain in state 2 |
| ϵ_{sm} | Mean strain of tensile chord |
| ϑ | Inclination of the principal compressive strain axis |
| μ_x | Curvature |
| $\rho_{p,eff}$ | Ratio of longitudinal reinforcement in the effective area |
| ρ_w | Transversal reinforcement ratio |
| σ_c | Compressive stress |
| σ_{c1} | Principle tensile stress |
| σ_{s2} | Tensile stress in state 2 |
| σ_{sr2} | Tensile stress corresponding to the cracking bending moment |
| σ_{sw} | Stress in the y-direction acting on the web reinforcement; |
| τ | Mean shear stress |
| ν | Coefficient of Poisson |

LIST OF FIGURES

| | |
|--|----|
| figure 1. General dimension and scheme static in the experiment..... | 1 |
| Figure 2. Detail of the cross section and reinforcement..... | 2 |
| figure 3. Static scheme and struments used in the test..... | 3 |
| Figure 4. Relationship of bending moment and curvature with constant t.s..... | 7 |
| Figure 5. Relationship of bending moment and curvature with linear t.s..... | 7 |
| Figure 6. Relationship of bending moment and curvature in model CEB..... | 8 |
| Figure 7. Dflection due to self – weight..... | 9 |
| figure 8. Linear relationship of stress – strain..... | 10 |
| figure 9. Strain and stress in the cross section for linear analysis..... | 11 |
| Figure 10 Diagram bending moment – curvature of Beam Tr1, Tr3, Tr5. | 12 |
| Figure 11 Diagram bending moment – curvature of Beam Tr2, Tr4, Tr6..... | 12 |
| Figure 12. Diagram of bending moment – mean curvature of beam 1, node C..... | 13 |
| Figure 13. Diagram of bending moment – mean curvature of beam 2, node C..... | 14 |
| Figure 14. Diagram of bending moment – mean curvature of beam 3, node A..... | 14 |
| Figure 15. Diagram of bending moment – mean curvature of beam 5, node C..... | 15 |
| Figure 16. Diagram of bending moment – mean curvature of beam 6, node C..... | 15 |
| figure 17. Schematic representation of the stress-strain relation for structural analysis. From <i>Eurocode 2</i> | 16 |
| figure 18. Strain and stress in the cross section for non-linear analysis..... | 16 |
| figure 19. Strips and referencing point in the cross section..... | 17 |
| Figure 20. Diagram bending moment – curvature of Beam Tr1, Tr3, Tr5. | 19 |
| Figure 21. Diagram bending moment – curvature of Beam Tr2, Tr4, Tr6..... | 19 |
| Figure 22. Diagram of bending moment – mean curvature of Beam 1, node C..... | 20 |
| Figure 23. Diagram of bending moment – mean curvature of Beam 2, node C..... | 20 |
| Figure 24. Diagram of bending moment – mean curvature of Beam 3, node A..... | 21 |
| Figure 25. Diagram of bending moment – mean curvature of Beam 5, node C..... | 21 |
| Figure 26. Diagram of bending moment – mean curvature of Beam 6, node C..... | 22 |
| figure 27. Slices and referencing points in the front view of beam..... | 23 |
| figure 28.a Example of distributing concentrated load of beam 1 and 2..... | 23 |
| Figure 29. Bending moment in real system of beam 1..... | 24 |

| | |
|--|----|
| Figure 30. Bending moment in virtual system of beam 1 | 25 |
| Figure 31. Diagram load – deflection of beam 1..... | 26 |
| Figure 32. Diagram load – deflection with experimental data of beam 1 | 27 |
| Figure 33. Diagram load – deflection with experimental data of beam 2..... | 27 |
| Figure 34. Bending moment in real system of beam 3..... | 28 |
| Figure 35. Bending moment in virtual system of beam 3 | 28 |
| Figure 36. Diagram load – deflection with experimental data of beam 3..... | 28 |
| Figure 37. Bending moment in real system of beam 5..... | 29 |
| Figure 38. Bending moment in virtual system of beam 5 | 29 |
| Figure 39. Diagram load – deflection with experimental data of beam 5..... | 30 |
| Figure 40. Diagram load – deflection with experimental data of beam 6..... | 30 |
| Figure 41. Diagram bending moment – mean curvature of beam 1 node C | 33 |
| Figure 42. Diagram of bending moment – mean curvature of beam 1, node C..... | 34 |
| Figure 43. Diagram of bending moment – mean curvature of beam 1, node A..... | 35 |
| Figure 44. Diagram of bending moment – mean curvature of beam 2, node C..... | 35 |
| Figure 45. Diagram of bending moment – mean curvature of beam 3, node A..... | 36 |
| Figure 46. Diagram of bending moment – mean curvature of beam 5, node C..... | 36 |
| Figure 47. Diagram of bending moment – mean curvature of beam 6, node C..... | 37 |
| Figure 48. The bending moment in real system of beam 1 | 38 |
| Figure 49. The bending moment in virtual system of beam 1..... | 38 |
| Figure 50. Diagram of load – deflection of beam 1 | 39 |
| Figure 51. Diagram of load – deflection of beam 2 | 40 |
| Figure 52. Diagram of load – deflection of beam 3 | 40 |
| Figure 53. Diagram of load – deflection of beam 5 | 41 |
| Figure 54. Diagram of load – deflection of beam 6 | 41 |
| Figure 55. Diagram of bending moment and mean curvature of beam 1, node C..... | 44 |
| Figure 56. Diagram of bending moment and mean curvature of beam 2, node C..... | 45 |
| Figure 57. Diagram of bending moment and mean curvature of beam 3, node A..... | 45 |
| Figure 58. Diagram of bending moment and mean curvature of beam 5, node C..... | 46 |
| Figure 59. Diagram of bending moment and mean curvature of beam 6, node C..... | 46 |
| Figure 60. diagram of load – deflection of beam 1 | 47 |
| Figure 61. Diagram of load - deflection of beam 2..... | 48 |
| Figure 62. Diagram of load - deflection of beam 3..... | 48 |
| Figure 63. Diagram of load - deflection of beam 5..... | 49 |

| | |
|---|----|
| Figure 64. Diagram of load - deflection of beam 6 | 49 |
| Figure 65. Diagram of mean curvature – simple bending..... | 50 |
| Figure 66. Diagram of mean curvature – bending combined with compression | 50 |
| Figure 67. Diagram of the bending moment - mean curvature of beam 1, node C..... | 53 |
| Figure 68. Diagram of the bending moment - mean curvature of beam 2, node C..... | 53 |
| Figure 69. Diagram of the bending moment - mean curvature of beam 3, node A | 54 |
| Figure 70. Diagram of the bending moment - mean curvature of beam 5, node C..... | 54 |
| Figure 71. Diagram of the bending moment - mean curvature of beam 6, node C..... | 55 |
| Figure 72. Diagram of load – deflection of beam 1 | 56 |
| Figure 73. Diagram of load – deflection of beam 2 | 57 |
| Figure 74. Diagram of load – deflection of beam 3 | 57 |
| Figure 75. Diagram of load – deflection of beam 5 | 58 |
| Figure 76. Diagram of load – deflection of beam 6 | 58 |
| Figure 77. Effective area of the cross section | 62 |
| Figure 78. Stress in the cross section inclined ϑ angle..... | 63 |
| Figure 79. Example of beam 6. (a) geometry. (b) diagram of shear – shear of concrete contribution with various shear lengths | 64 |
| Figure 80. Diagram of shear – shear strain of beam 1,node A..... | 66 |
| Figure 81. Diagram of bending moment – curvature of beam 1, node A | 67 |
| Figure 82. Comparison between simplified model and bi-linear method with experimental curve | 68 |
| Figure 83. Diagram of shear – shear strain of beam 2, node A..... | 69 |
| Figure 84. Diagram of bending moment – mean curvature of beam 2, node A..... | 69 |
| Figure 85. Diagram of shear – shear strain of beam 3, node A..... | 70 |
| Figure 86. Diagram of bending moment – mean curvature of beam 3, node A..... | 70 |
| Figure 87. Diagram of shear – shear strain of beam 5, node C..... | 71 |
| Figure 88. Diagram of bending moment – mean curvature of beam 5, node C..... | 71 |
| Figure 89. Diagram of shear – shear strain of beam 6, node C..... | 72 |
| Figure 90. Diagram of bending moment – mean curvature of beam 6, node C..... | 72 |
| Figure 91. The bending moment of beam 1 in real system | 73 |
| Figure 92. The shear of beam 1 in real system..... | 74 |
| Figure 93. Bending moment and shear of beam 1 in virtual sysytem..... | 74 |
| Figure 94. Diagram of load – deflection of beam 1 | 75 |
| Figure 95. Diagram of load – deflection of beam 2 | 76 |

| | |
|---|----|
| Figure 96. Diagram of load – deflection of beam 3 | 77 |
| Figure 97. Diagram of load – deflection of beam 5 | 78 |
| Figure 98. Diagram of load – deflection of beam 6 | 78 |

REFERENCES

- CEB – FIP Model Code 1990. Ed. Thomas Telford.
- CEN. Eurocode 2. Design of concrete structures - Part 1-1: General rules and rules for buildings
- Taliano M. Upper and lower bounds of crack width of r.c. tie -simplified method. Proceedings of the *fib* Symposium in Krakow, Poland, 2019
- Debernardi P.G., Guiglia M., Taliano M. Shear strain in B-regions of beams in service. *Engineering Structures* 33 (2011) 368 – 379
- Debernardi P.G., Taliano M. Shear deformation of r.c. beams. Proceedings of the First *fib* Congress, Osaka, 2002, session 13, pp. 179-188
- Debernardi P.G., Guiglia M., Taliano M. Parametric analysis of the influence of shear on the deflection of RC beams in service. *Magazine of Concrete Research*. 2011, 63(1), 1–16
- Debernardi P.G., Taliano M. Shear deformation in reinforced concrete beams with thin web *Magazine of Concrete Research*, 2006, 58, No. 3, April, 157-171
- Guiglia M. Analisi della deformazione a taglio di travi in calcestruzzo armato ad anima sottile Ph.D. thesis. 2005.
- Cosenza E., Greco C. Il calcolo delle deformazioni nelle strutture in cemento armato. Ed. CUEN 1992
- Frank J.V., Michael P.C. The Modified Compression – Field Theory for Reinforced Concrete Elements Subjected to Shear. *ACI JOURNAL* / March – April (1986) 219 – 231
- Evan C. B., Frank J. V., and Michael P. C. Simplified Modified Compression Field Theory for Calculating Shear Strength of Reinforced Concrete Elements. *ACI Structural Journal*, V. 103, No. 4, July-August 2006. 614 – 624